UNIVERSIDADE FEDERAL DO RIO GRANDE DO SUL
FACULDADE DE ODONTOLOGIA
PROGRAMA DE PÓS- GRADUAÇÃO EM ODONTOLOGIA
NÍVEL DOUTORADO
ÁREA DE CONCENTRAÇÃO PATOLOGIA BUCAL

BIBIANA FRANZEN MATTE

VARIAÇÕES FENOTÍPICAS DO CARCINOMA ESPINOCELULAR ORAL:
EFEITO DAS CARACTERÍSTICAS FÍSICAS DA MATRIZ EXTRACELULAR

Porto Alegre
2019

UNIVERSIDADE FEDERAL DO RIO GRANDE DO SUL

FACULDADE DE ODONTOLOGIA

PROGRAMA DE PÓS- GRADUAÇÃO EM ODONTOLOGIA

NÍVEL DOUTORADO

ÁREA DE CONCENTRAÇÃO PATOLOGIA BUCAL

BIBIANA FRANZEN MATTE

VARIAÇÕES FENOTÍPICAS DO CARCINOMA ESPINOCELULAR ORAL:
EFEITO DAS CARACTERÍSTICAS FÍSICAS DA MATRIZ EXTRACELULAR

Linha de pesquisa: Câncer Bucal

Tese de Doutorado apresentada ao Programa de Pós-Graduação em Odontologia da Universidade Federal do Rio Grande do Sul como requisito à obtenção do título de Doutor em Odontologia.

Área de Concentração: Patologia Bucal

Orientador: Prof. Dr. Marcelo Lazzaron Lamers

Porto Alegre

2019

Dedico este trabalho a todos os pesquisadores com suas mentes inquietas

AGRADECIMENTOS

Tenho muito orgulho da trajetória que estou percorrendo, mas nada seria possível sem o apoio de muitas pessoas especiais. Por isso, preciso deixar registrada minha eterna gratidão às pessoas que fazem essa jornada ter muito mais sentido.

Aos meus pais, Ceci e Carlos, me faltam palavras para expressar o que vocês significam para mim. Obrigada pelo apoio em todos os meus sonhos. Ter vocês do meu lado, sempre com palavras positivas e conselhos, faz toda a diferença. Amo vocês.

Ao meu irmão, Nicholas, por sempre ter cuidado de mim e me incentivado. Sinto muito orgulho de poder dizer que sou tua irmã.

A toda minha família, em especial a minha vó Vera Matte, por sempre estar interessada em entender minhas atividades profissionais. Ao Luis Pedro e família, por ter garantido os percursos com papos animadores e inspiradores.

Ao Alex, pelo apoio incondicional em todos esses anos. Poder dividir essa caminhada contigo, mesmo que às vezes geograficamente distante, tornou tudo mais leve e enriquecedor.

Ao Marcelo Lamers, orientador dessa tese e de toda minha carreira científica. Começamos a trabalhar juntos em julho de 2010 e, após 9 anos de muitos ensinamentos, tenho certeza que minha evolução se deve muito ao teu poder de transmitir conhecimento. Obrigada por me incentivar em todos os projetos que construímos juntos e me mostrar o lado "fora da caixa". Sem teu incentivo, nada disso seria possível.

A Lisiane Bernardi, que esteve junto comigo em todos estes anos científicos. Tua capacidade em ensinar com leveza e ser um ombro amigo tornou tudo mais tranquilo. Thank you for everything!

A Anna Fossati, um grande exemplo de profissional que me mostrou que devemos sempre estar nos atualizando e aprendendo constantemente.

A todo grupo do Laboratório de Migração Celular (LAMOC). Temos um ambiente equilibrado de trabalho, colaboração e descontração e isso é resultado do jeito único de cada integrante. Obrigada Paloma, Leonardo, Luisa Dockhorn, Carlos, Sérgio, Marjoe, Igor, Silene, Luiza Brand, Gabrielle, Luisa Menti, Luise e Julia. Meus agradecimentos especiais para a Paloma, minha dupla de cultura desde 2013, e o Leonardo, que entende de tudo um pouco, desde migração celular a filtros de água. E a Luisa D., que, com muita rapidez, se tornou uma companheira de experimentos.

Dentre os maiores desafios na academia está o de ensinar e guiar a pesquisa de novos alunos. Por isso, preciso agradecer as alunas de iniciação cientifica do LAMOC que se dedicam incansavelmente a aprender todos os dias: Luiza Brand, Gabrielle, Luisa Menti, Luise e Julia. Em especial, a Luiza Brand, que muito além de ter se tornado minha pupila cientifica, se tornou uma amiga para a vida toda e a Gabrielle, por toda dedicação, sempre com uma energia positiva. Tenho certeza que aprendi muito com vocês e ver o desenvolvimento de todas me deixa muito orgulhosa. Podem contar sempre comigo.

Aos membros cativos do LAMOC, apesar de estarem em outras fases de vida, Grasieli Ramos, Alessandro Menna Alves, Natalia Koerich, Natalia Schneider, Alessandra Magnusson e Silvia Barbosa, os ensinamentos de vocês estarão sempre comigo.

A Mariana Menna Barreto, que entrou recentemente ao laboratório, e tive o prazer de poder trabalhar de perto. Obrigada pela cumplicidade e dedicação.

Ao Adam Engler, por ter me dado a oportunidade de fazer pesquisa na University of California San Diego e ainda trabalhar com câncer de boca dentro do seu laboratório, quando essa linha de pesquisa ainda não existia. O aprendizado durante o doutorado-sanduíche foi muito além de novas técnicas de pesquisa.

A todo o grupo do Engler Lab, em especial ao Jesse e Aditya que foram professores incríveis na pesquisa em bioengenharia.

Aos meus amigos de San Diego, Luisa, Renata e Tiago, que trouxeram alegria para os momentos fora do laboratório.

A todos os professores da Patologia Bucal UFRGS, Manoel Sant'anna Filho (*in memoriam*), Pantelis Rados, Márcia Oliveira, Manoela Martins, Marco Martins, Laura Hildebrand, Vinicius Carrard, Fernanda Visioli e Isadora Flores, por todos os ensinamentos sobre diagnóstico histopatológico e docência na nossa Universidade.

Ao Felipe Racchi, bolsista premium do NPBO, pelo auxílio em diversos projetos de pesquisa.

A todos os colegas do PPG-Odontologia, em especial aos colegas da Patologia, por proporcionarem muitas trocas de conhecimentos.

A UFRGS, uma segunda casa, da qual tenho muito orgulho de ter feito parte.

"Sonhar grande e sonhar pequeno dá o mesmo trabalho"
Atribuída a Jorge Paulo Lemann

RESUMO

O carcinoma espinocelular oral (CEC) apresenta variabilidade inter e intratumoral. A doença é formada pelas células tumorais e pelos diversos fatores biológicos, químicos e físicos que compõem o microambiente tumoral com poder de influenciar a progressão tumoral. Neste trabalho, avaliamos as modificações fenotípicas intrínsecas do CEC e a influência de fatores físicos (rigidez) nestas células. Em uma revisão de literatura, foi observado que GAPDH e β-actina são os principais genes de referência utilizados em pesquisas de expressão gênica com CEC. Entretanto, demonstramos experimentalmente a grande variabilidade de 5 genes de referência durante análise comparativa de mais de um subtipo celular de tumor, sendo recomendado o uso de 2 ou mais genes de referência para este tipo de ensaio. Devido à esta variabilidade de expressão gênica, utilizamos a ferramenta transcriptograma em dados de sequenciamento de RNA de amostras de diferentes regiões de carcinoma espinocelular de cabeça e pescoço. Foi constatada que existem diferenças no perfil de expressão gênica entre as diferentes regiões tumorais, mas também entre os tecidos sadios. Esta diferença pode estar associada às diferentes etiopatogenias do câncer de cabeça e pescoço, bem como às diferentes características bioquímicas e biomecânicas a que estão expostos os tecidos desta região. Visto que clinicamente é observado o endurecimento das bordas das lesões de CEC e que observamos que o aumento da organização das fibras colágenas (maior rigidez) está relacionado com pior prognóstico, analisamos a influência da rigidez da matriz extracelular no fenótipo destas células tumorais. Foram utilizadas linhagens de CEC com baixa ($Inv^L/E:N^H$) e alta ($Inv^H/E:N^L$) agressividade expostas a diferentes durezas (0,48 ou 20kPa). Após 24h, observamos que apenas as células $Inv^H/E:N^L$ migraram em maior velocidade em ambiente com alta rigidez (20kPa) quando comparado com baixa rigidez (0,48kPa) ($p<0,01$). Para avaliar o condicionamento mecânico induzido pelo substrato, as células $Inv^L/E:N^H$ foram cultivadas por 5 dias em ambientes com baixa ou alta rigidez e então trocadas de ambiente para avaliar modificações fenotípicas. Observamos que o condicionamento em ambiente rígido tornou as células $Inv^L/E:N^H$ mais agressivas (~2x de aumento na expressão de N-caderina e da velocidade de migração ($p\leq0,05$)), sendo este efeito mediado pelas adesões das células ao substrato ($p<0,01$). Estes dados indicam que a própria resposta fibrosa para contenção do tumor pode modular o comportamento invasivo do CEC, contribuindo tanto para a metástase quanto para a recorrência do tumor. Em virtude dos efeitos das características físicas no comportamento celular, realizamos revisão da literatura em que observamos a diversidade de biomateriais e de estratégias *in vitro* e *in vivo* para reproduzir de maneira fidedigna o microambiente dos tecidos e dos tumores. Nesta tese, demonstramos que existe uma grande heterogeneidade relacionada ao tipo celular do tumor, ao seu local de origem, à resposta celular frente as características físicas do microambiente e às maneiras de reproduzir os aspectos mecânicos *in vitro/in vivo*, o que realça a necessidade de uma visão

holística do processo de tumorigênese para definir novas estratégias de diagnóstico, prognóstico e tratamento de pacientes com CEC.

Palavras-chave: microambiente tumoral; expressão gênica; biomateriais.

ABSTRACT

Oral squamous cell carcinoma (OSCC) has inter and intratumoral variability. The disease is constituted by tumor cells and by the tumor microenvironment different biological, chemical and physical factors, which, altogether, influences tumor progression. In the present work, we evaluated intrinsic phenotype alterations of OSCC and the influence of physical factors (stiffness) in these cells. In a literature review, it was observed that GAPDH and β-actin are the mostly used reference genes in OSCC gene expression studies. However, we demonstrated experimentally, in a comparative analysis of 5 reference genes with more than one tumor cell subtype, that there is an important variability among reference genes and, therefore, it is recommended to use at least 2 reference genes in this experimental setup. Due to the gene expression variability observed, we used the transcriptogram tool in order to analyze RNA sequencing data in different regions of head and neck squamous cell carcinoma. It was observed that there are different gene expression profiles among tumor regions, but also among healthy tissue. This difference might be associated with the different etiopathogenic factors of head and neck squamous cell carcinoma, as well as the different biochemical and biomechanical characteristics present in each tissue region. Since it is clinically observed that CEC lesions have indurated borders and that we observed that increased collagen fibber organization (increased stiffness) is related to a poor prognosis, we analyzed the influence of matrix stiffness on tumor cells phenotype. OSCC cell lines with low ($Inv^L/E:N^H$) and high ($Inv^H/E:N^L$) aggressiveness profile that were exposed to different stiffness substrates (0.48 or 20kPa) were used. After 24h, we observed that only $Inv^H/E:N^L$ migrated with a higher velocity in a stiff substrate (20kPa) when compared to a soft niche (0.48kPa) ($p<0,01$). In order to evaluate mechanical conditioning induced by substrate stiffness, $Inv^L/E:N^H$ cells were cultivated for 5 days in a soft or stiff substrates and then re-plated to different stiffness niches to evaluate phenotype alterations. We observed that stiff niche conditioned $Inv^L/E:N^H$ cells into a more aggressive profile (~2 fold increase in N-cadherin expression and migration velocity ($p≤0,05$)) and these effects were modulated by cell adhesion to the substrate ($p<0,01$). These data indicate that the fibrous response in order to restrain tumor growth can modulate invasive OSCC behavior, contributing to metastasis and tumor recurrence. Since physical characteristics can influence cell behavior, we performed a literature review and observed that there are a diversity of biomaterials and *in vitro* and *in vivo* strategies that can reproduce tissue and tumor microenvironment. In the present thesis, we demonstrated that there is a high heterogeneity among tumor cell types, tumor location, cell response to microenvironment physical characteristics and strategies to reproduce *in vitro/in vivo* mechanical characteristics. This highlights the need of a holistic vision of the tumorigenesis process in order to develop novel strategies for diagnosis, prognosis and treatments for OSCC patients.

Keywords: tumor microenvironment, gene expression, biomaterials

LISTA DE FIGURAS

com todos os tecidos normais (Transcriptogram for normal tissues data present in the HNSCC project in GDC Data Portal and divided by each location site compared to all normal tissues).

Artigo científico 3

Figura 1. Linhagens tumorais invasivas de carcinoma espinocelular oral possuem níveis aumentados de expressão de N-caderina e de marcadores de EMT (Invasive oral squamous cell carcinoma cell lines have increased N-cadherin and EMT markers expression).

Figura 2. Migração das células $Inv^L/E:N^H$ é insensível a rigidez ($Inv^L/E:N^H$ cell migration is stiffness insensitive).

Figura 3. Exposição prolongada a substrato rígido induz as células $Inv^L/E:N^H$ a expressarem marcadores de EMT (Prolonged exposure to stiff substrates induces $Inv^L/E:N^H$ cells to express EMT markers).

Figura 4. Células $Inv^L/E:N^H$ apresentam "memória" após exposição prologada ao substrato rígido ($Inv^L/E:N^H$ cells exhibit "memory" after prolonged exposure to a stiff niche).

Figure 5. Condicionamento prolongado em substrato rígido aumenta a área de adesão da linhagem celular $Inv^L/E:N^H$ (Long-term conditioning in stiff niche increases adhesion area in $Inv^L/E:N^H$ cell line).

Figure 6. Organização do colágeno em espécimes de tumor de pacientes é correlacionado com pior prognóstico (Collagen organization in patient tumors correlates with poor outcomes).

Figura suplementar 1. Células $Inv^L/E:N^H$ migram preferencialmente de maneira coletiva comparado com células $Inv^H/E:N^L$, especialmente em substratos moles ($Inv^L/E:N^H$ cells preferentially exhibit collective, epithelial migration compared to $Inv^H/E:N^L$, especially on soft substrates).

Figura suplementar 2. Análises de migração (Migration analyses).

Artigo científico 4

Figura 1. Modelando o microambiente tumoral (Modelling the tumour microenvironment).

Figura 2. A rigidez da matriz regula a transição epitélio-mesênquima (Matrix stiffness regulates the epithelial-to-mesenchymal transition).

Figura 3. Próxima geração de tecnologias baseadas em materiais para o câncer (Next-generation material-based cancer technologies).

LISTA DE CAIXAS E TABELAS

Artigo científico 1

Tabela 1. Genes de referência avaliados neste estudo, gene ID no NCBI, sequência dos primers, função molecular e temperatura de anelamento (Reference genes evaluated in this study, gene ID NCBI, primers sequence, molecular function and melting temperature).

Artigo científico 2

Tabela 1. Caracterização da amostra de acordo com a localização e o número do CID (Sample characterization according to location site and ICD number).

Artigo científico 3

Tabela suplementar 1. Informação demográfica dos pacientes (Patient demographic information).

Artigo científico 4

Caixa 1. Câncer e metástase (Cancer and metastasis).

Caixa 2. Aspectos fundamentais sobre biomateriais para estudo da biologia do câncer (Key aspects of biomaterials for cancer biology).

Tabela 1. Biomaterias para modelar o microambiente tumoral (Biomaterials for modelling the tumour microenvironment)

LISTA DE ABREVIATURAS E SIGLAS

Antecedentes e justificativa

OMS   Organização Mundial de Saúde

DNA   ácido desoxirribonucleico

CEC   carcinoma espinocelular oral

INCA Instituto Nacional de Câncer José Alencar Gomes da Silva

HPV   papilomavírus humano

UV   ultravioleta

miRNA micro ácido ribonucleico

EMT   transição epitélio-mesênquima/ *epithelial-to-mesenchymal transition*

MET   transição mesênquima-epitélio/ *mesenchymal-to-epithelial transition*

ECM   matriz extracelular/ *extracellular matrix*

MMP metaloproteinase de matriz

TME   microambiente tumoral/ *tumor microenvironment*

CAF   fibroblasto associado ao tumor/ *cancer-associated fibroblasts*

VEGF fator de crescimento vascular endotelial

CAR-T células T com receptor de antígeno quimérico

FDA   *Food and Drug Administration*

IL   interleucina

TNF-α fator de necrose tumoral alfa

TGF-β fator de crescimento transformante beta

HIFα fator indutor de hipóxia alfa

ATP   adenosina trifosfato

GLUT1 transportador de glicose 1

Pa Pascal

YAP *yes-associated protein*

TAZ *WW domain-containing transcription regulator protein 1*

G3BP2 *Ras GTPase-activating protein binding 2*

3D tridimensional

Artigo científico 1

RT-qPCR reverse transcription-quantitative polymerase chain reaction

RG reference gene

OSCC oral squamous cell carcinoma

NCBI National Center of Biotechnology Information

cDNA Complementary DNA

Cq quantification cycle

MIQE Minimum Information for Publication of Quantitative Real-Time PCR
Experiments

Artigo científico 2

GDC Genomic Data Commons

HNSCC Head and Neck Squamous Cell Carcinoma

NGS Next Generation Sequencing

RNA-seq RNA-sequencing

GO Gene Ontology

ICD International Classification of Diseases

Artigo científico 3

OSCC oral squamous cell carcinoma

$Inv^H/E:N^L$ highly invasive OSCC line with low E-cad/N-cad ratio (SCC-25)

$Inv^L/E:N^H$ poorly invasive OSCC line with high E-cad/N-cad ratio (Cal27)

EMT epithelial-to-mesenchymal transition

E-cad E-cadherin

N-cad N-cadherin

TME tumor microenvironment

CAF cancer-associated fibroblast

ECM extracellular matrix

FA focal adhesions

FAK focal adhesion kinase

PA polyacrylamide

TBS-T Tris buffered saline with tween

ANOVA one-way analysis of variance

Artigo científico 4

CAF cancer-associated fibroblasts

ECM extracellular matrix

EHS Engelbreth-Holm-Swarm

MEC mammary epithelial cells

ErbB2 receptor tyrosine-protein kinase

MMP matrix metalloproteinases

RGD arginine-glycine-aspartic acid

GFOGER glycine-phenylalanine-hydroxyproline-glycine-glutamate-arginine

IKVAV isoleucine-lysine-valine-alanine-valine

PEG polyethylene glycol

EMT epithelial-to-mesenchymal transition

ERK extracellular signal–regulated kinase

Rho Rho family of GTPases

G3BP2 Ras GTPase-activating protein-binding protein 2

PDMS polydimethylsiloxane

ROCK Rho-associated protein kinase

YAP yes-associated protein

TNF-α tumour necrosis factor alpha

CXCL5 C-X-C motif chemokine 5

BRCA1 breast cancer marker breast cancer 1

HER2 human epidermal growth factor receptor 2

CTC circulating tumour cells

EpCAM epithelial cell adhesion molecule

FDA Food and Drug Administration

pCBMA Poly(carboxybetaine methacrylate)

PLGA poly(lactide-co-glycolide) acid

PCL Poly(ε-caprolactone)

GO graphene oxide

BMP-2 bone morphogenetic protein-2

MRI magnetic resonance imaging

SPECT single photon emission computed tomography

LOX lysyl oxidases

PET positron emission tomography

PEGDA Polyethylene glycol diacrylate

MeHA Methacrylated hyaluronic acid

DAPI, 4,6-diamidino-2-phenylindole.

SUMÁRIO

1. ANTECEDENTES E JUSTIFICATIVA

O câncer é uma doença em que, devido a mutações genéticas, ocorre descontrole em mecanismos celulares que regulam atividades das células como proliferação e capacidade de invasão em tecidos adjacentes e a distância. A Organização Mundial de Saúde (OMS) estima que, no ano de 2018, aconteceram 18,1 milhões de novos diagnósticos de câncer e que 9,6 milhões de pessoas vieram a falecer no mundo em decorrência da doença. Assim, o câncer é segunda maior causa de morte no mundo, sendo a primeira enfermidades cardiovasculares (WORLD HEALTH ORGANIZATION, 2018). No Brasil, estima-se que, para o ano de 2018, ocorrerão cerca de 420 mil novos casos de câncer (INSTITUTO NACIONAL DE CÂNCER JOSÉ ALENCAR GOMES DA SILVA, 2018).

A doença câncer engloba mais de 100 tipos diferentes de tumores que podem se desenvolver em diferentes regiões do corpo. Apesar dessa grande variabilidade de tipos celulares e localizações, os autores Hanahan e Weinberg, em 2000, estabeleceram 6 alterações essenciais que acontecem na fisiologia celular e que serão determinantes para o desenvolvimento do tumor. Estas alterações foram denominadas como os "*hallmarks of cancer*". As alterações necessárias para o desenvolvimento tumoral incluem capacidade proliferativa ilimitada, manutenção da sinalização para proliferação, escape dos supressores de crescimento, resistência a morte celular, indução de angiogênese e ativação da invasão tecidual e metástase (Hanahan e Weinberg, 2000). Ao revisitar este assunto, em 2011, os autores adicionaram duas potenciais alterações que são a desregulação do sistema energético e fuga da destruição pelo sistema imune. Também foram adicionados duas características promotoras do desenvolvimento tumoral que são as mutações e instabilidade genômica e a promoção de inflamação causada pelo tumor (Hanahan e Weinberg, 2011).

As alterações descritas são consequências de mutações genéticas e alterações epigenéticas celulares. Em condições fisiológicas, durante o ciclo celular, as células passam por fases de checagem da estabilidade do DNA e, ao

ser identificado algum tipo de dano, serão acionados mecanismos de reparo acontecerá a apoptose quando o reparo não for possível (Otto e Sicinski, 2017). Contudo, quando este processo falha, as mutações começam a acontecer. Inicialmente, essas alterações acontecem em proto-ocongenes e genes supressores de tumor. Enquanto que os proto-oncogenes, como o Ras, estimulam a proliferação das células tumorais, mutações em genes supressores de tumor levam à disfunção da regulação do ciclo celular. Entre os genes supressores de tumor mais estudados, estão o pRb e o p53. Com o acúmulo de mutações, ocorre o processo de desenvolvimento da massa tumoral e invasão de tecidos (Wang *et al.*, 2015).

1.1 Carcinoma espinocelular oral

O carcinoma espinocelular oral (CEC) é o tipo de tumor maligno mais frequente na cavidade bucal e tem origem em células epiteliais neoplásicas que atravessam a lâmina basal e invadem o tecido conjuntivo adjacente. Clinicamente, pode ser observado como uma placa branca ou vermelha não removível a raspagem; uma lesão ulcerada que não cicatriza, com mais de duas semanas de evolução, com bordos irregulares e endurecidos, sendo mais frequente em pessoas do sexo masculino, entre a quinta e sexta década de vida (NEVILLE, 2015).

No Brasil, o CEC é o quinto tipo de câncer mais comum em homens e, de acordo com o Instituto Nacional de Câncer (INCA), estima-se que cerca de 14.700 novos casos serão diagnosticados no ano de 2019, sendo 11.200 em pessoas do sexo masculino. Destes, estimam-se que 1.100 casos serão diagnosticados no Rio Grande do Sul (INCA, 2018). De acordo com os dados da Sociedade Americana do Câncer, coletados entre 2008 e 2014, cerca de 67% dos casos de câncer de boca e faringe são diagnosticados com metástase regional e à distância, o que diminui as alternativas de tratamento, assim como as chances de sobrevida após o tratamento. Neste mesmo conjunto de dados, é demonstrado que pacientes com diagnóstico de CEC local possuem 88% de

sobrevida após 5 anos do diagnóstico da doença. Contudo, quando o diagnóstico é feito com metástase à distância, a sobrevida após 5 anos reduz para 39% (Siegel *et al.*, 2019). Portanto, o momento do diagnóstico é essencial para o prognóstico do paciente.

O tratamento do CEC é realizado principalmente através da ressecção total do tumor com área de margem de segurança, podendo ser combinada com quimio e radioterapia (Wise-Draper *et al.*, 2012). Por afetar uma região envolvida em atividades primordiais da vida, como mastigação, gustação e fala, tratamentos agressivos estão relacionados a uma redução significativa da qualidade de vida dos pacientes e impacto psicológicos para os pacientes (Mücke *et al.*, 2015).

Em neoplasias malignas de boca, fatores de risco como o fumo, o álcool, o papilomavírus humano (HPV) e a exposição a radiação UV influenciam o processo de tumorigênese. A presença de diversas substâncias cancerígenas no cigarro levam a mutações e alterações no DNA, como mutações no p53 e aumento da metilação do DNA (Jethwa e Khariwala, 2017). De maneira semelhante, o álcool também atua em alterações da expressão gênica, como a superexpressão de determinados microRNAs (miRNA)(Saad *et al.*, 2015). Existem diversos tipos de HPV, mas estima-se que cerca de 90% dos casos de câncer de boca com infecção por HPV são devido ao HPV tipo 16 (HPV16) (Mork *et al.*, 2001). Estudos indicam que a expressão das oncoproteínas virais E6 e E7 resultam na degradação de proteínas supressoras de tumor das células epiteliais humanas como a p53 e a Rb. Dessa maneira, ocorre a desregulação de pontos de checagem durante o ciclo celular e uma maior instabilidade genética das células (Scheffner *et al.*, 1990; Huh *et al.*, 2007; Verma *et al.*, 2017). A exposição a radiação UV gera danos no DNA por ação direta ou induzida por espécies reativas de oxigênio e, a partir destes danos, ocorrem mutações em proto-oncogenes ou genes supressores de tumor (Rodust *et al.*, 2009; Bota *et al.*, 2017). Alguns fatores de risco estão associados com o desenvolvimento do tumor em regiões especificas. Por exemplo, estima-se que em torno de 30% dos casos de câncer de orofaringe estão relacionados com o

HPV (Plummer *et al.*, 2016) assim como o câncer de lábio também está mais associado a exposição aos raios UV (Biasoli *et al.*, 2016). Portanto, diversos são os fatores identificados como de risco para o desenvolvimento do CEC.

A progressão e o desenvolvimento do tumor dependem das alterações genéticas e epigenéticas apresentadas pelas células malignas. Diversos estudos caracterizam as modificações genéticas apresentadas pelas células e tentam determinar biomarcadores que auxiliem no tratamento e prognóstico da doença (Kang *et al.*, 2015). Dentre as alterações mais estudadas em CEC está a transição epitélio-mesênquima (EMT) em que as células epiteliais alteram sua polaridade e seu fenótipo para uma célula com característica mais mesenquimal. São identificados que, neste processo, ocorre redução da expressão de E-caderina, proteína presente na adesão célula-célula das células epiteliais, para um aumento na expressão de N-caderina e vimentina – proteínas presentes em células mesenquimais. Assim, as células adquirem potencial migratório e de invasão dos tecidos (Smith *et al.*, 2013). Foi observado que baixos níveis de E-caderina e altos níveis de vimentina estão correlacionados com aumento de metástase a distância em pacientes com CEC (Zhou *et al.*, 2015). Os fatores de transcrição Twist, Snail e Zeb estão dentre os fatores reconhecidamente envolvidos na redução de E-caderina e aumento de N-caderina (Lamouille *et al.*, 2014; Nieto *et al.*, 2016). As células apresentam plasticidade no processo de EMT, sendo que é possível a ocorrência do processo inverso – transição mesênquima-epitélio (MET). Assim como em uma mesma massa tumoral, existem grupos de células que podem estar em diferentes estágios da EMT.

A variabilidade dos tumores não é apenas entre os tipos diferentes, mas também existe grande variabilidade entre tumores dos diferentes pacientes além de variabilidade intratumoral. Em um estudo que analisou sequenciamento de RNA em células individuais de carcinoma espinocelular de cabeça a pescoço, foram identificadas que as células tumorais e não-tumorais apresentavam heterogeneidade dentro de uma mesma massa tumoral (Puram *et al.*, 2017). As variabilidades observadas influenciam na resposta ao tratamento e prognóstico dos tumores. Por exemplo, o carcinoma espinocelular de cabeça e pescoço é,

na maioria das vezes, estudado como um grupo de tumores, mas os dados de prognóstico em 5 anos variam entre 25% (hipofaringe) e 60% (laringe) de acordo com a localização do tumor (Gatta *et al.*, 2015). A variabilidade fenotípica repercute na etiopatogenia do tumor como, por exemplo, células que apresentam perfil ativo de EMT terão maior capacidade de invasão e formação de metástase que estão associados as principais causas de insucesso dos tratamentos (Puram *et al.*, 2017).

1.2 *Invasão tecidual*

Para que aconteça a invasão do tecido adjacente ou a distância, as células tumorais precisam migrar pelos tecidos. Este processo é orquestrado por diferentes moléculas e regulado por GTPases da família Rho (Ras-homology), sendo necessário o equilíbrio entre a proteína Rac1 e RhoA. Inicialmente, as células precisam lançar protrusões de membrana, formar e maturar adesões ao substrato, contrair o corpo celular e retrair a parte posterior do corpo da célula (Hanna e El-Sibai, 2013). As células tumorais podem migrar e invadir tecidos como células individuais, de maneira ameboide ou mesenquimal, ou como uma migração coletiva por um grupo de células que mantem a adesão entre as células e cooperam para o sucesso desse movimento. Os diferentes modos de migração possuem plasticidade, ou seja, as células podem alternar entre uma migração coletiva para uma migração de células individuais (Friedl e Alexander, 2011). A migração de células individuais, é observada em neoplasias epiteliais em que as células estão em estágio avançado de EMT e, microscopicamente, estas células apresentam uma morfologia mesenquimal com corpo celular alongado. Enquanto que na migração coletiva das células tumorais, observa-se um grupo de células que mantém adesões célula-célula que são normalmente guiadas por "células líderes", mas que todas as células fazem adesão a matriz extracelular (ECM) e geram força para permitir o movimento. Estas células também liberam metaloproteinases de matriz (MMP) para promover a

degradação da ECM e permitir o movimento do grupo das células (Te Boekhorst e Friedl, 2016).
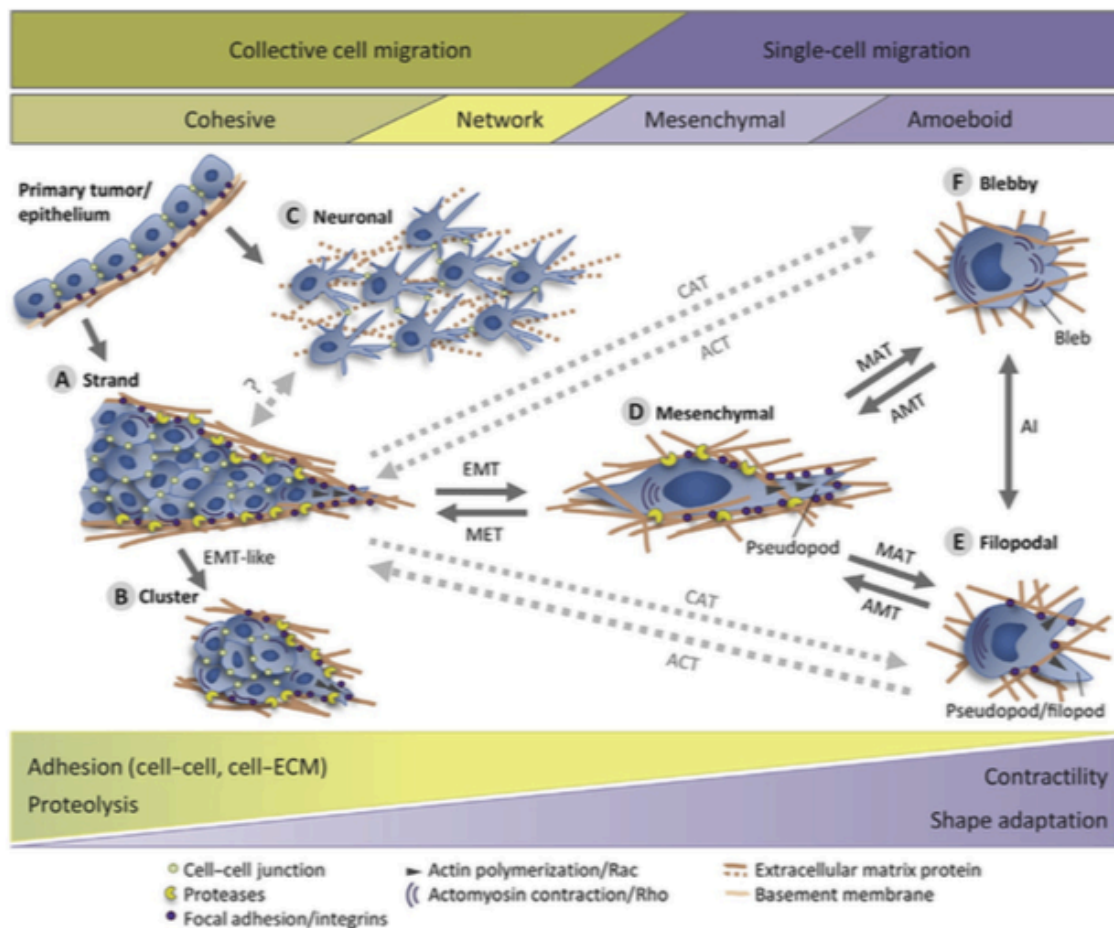
Figura 1. Modelos de migração individual e coletiva, demonstrando que existe plasticidade entre os tipos de migração. As transições entre os tipos de migração depende dos mecanismos de adesão entre as células, adesão com a ECM, dinâmicas de actina além de expressão de genes relacionados ao EMT. Tipos de migração: (A) migração coletiva em cordão com adesão célula-célula forte; (B) migração coletiva coesiva com tração gerada pelo grupo de células; (C) migração coletiva tipo neuronal com grupo de células unidas por adesões transientes; (D) migração individual do tipo mesenquimal com adesão mediada por integrinas com ECM; (E) migração ameboide filopodal mediada por adesão fraca com ECM; (F) migração ameboide do tipo *blebbing* mediada por contração do citoesqueleto e protrusões *bleb-like* sem adesão ao ECM (Te Boekhorst e Friedl, 2016).

A migração das células é influenciada por fatores intrínsecos, como ativação de vias de sinalização pelas células tumorais, mas também por fatores

extrínsecos como a composição da ECM. A influência do ambiente no entorno das células tumorais não é restrita à migração celular, mas também envolve diversas outras etapas da progressão tumoral.

1.3 Microambiente tumoral

Um dos primeiros relatos de interação entre o tumor e outras células do organismo foi em 1863, por Rudolf Virchow, em que ele descreve a infiltração de leucócitos como característica de tumores sólidos (Schmidt e Weber, 2006). Em 1889, Paget, estudando os principais órgãos acometidos por metástase de câncer de mama, descreve que as metástases nestes órgãos não aconteciam ao acaso e assim cria a hipótese conhecida como "*seed and soil hypothesis*". Segundo Paget, as plantas lançam sementes em diversas direções, mas elas crescem e se desenvolvem apenas nos solos favoráveis (Paget, 1989). Assim, alguns órgãos são mais favoráveis para o crescimento de uma segunda massa tumoral do que outros. Apesar destas descrições na literatura, por muitos anos, o estudo em câncer foi centrado nas células tumorais. No entanto, a partir dos anos 1980, estudos demonstraram que os sinais enviados pelo microambiente tumoral (TME) influenciam o fenótipo das células tumorais (Pohl *et al.*, 1988; Weaver *et al.*, 1996). A partir de então, diversos estudos aprofundaram o conceito e as vias biológicas envolvidas entre as células tumorais e o TME.

De acordo com os autores Maman e Witz, o TME pode ser caracterizado como uma arena com interações dinâmicas em que as células tumorais interagem com diversos fatores e que estes também interagem entre si (Maman e Witz, 2018). Por questões didáticas, estes fatores serão divididos em fatores biológicos - células residentes do tecido e recrutadas para o tecido -, fatores químicos – metabólitos e fatores de crescimento – e fatores físicos – constituintes da ECM. O TME evolui e é diferente de acordo com o estágio do tumor assim como é diferente de acordo com o órgão.
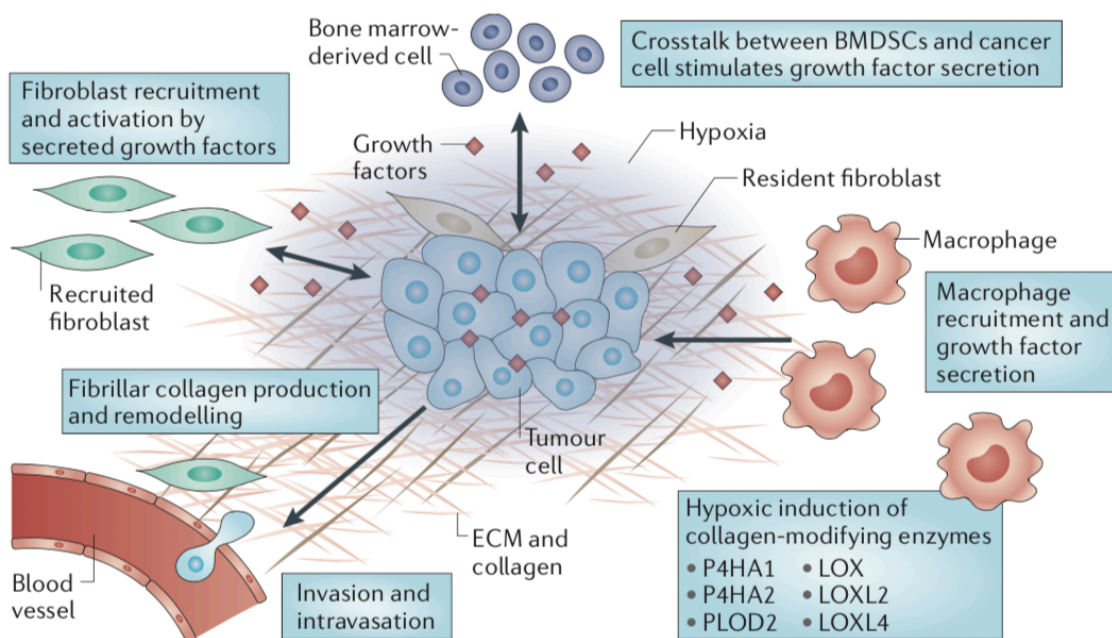
Figura 2. Componentes biológicos, químicos e físicos presentes no TME. Presença de células tumorais, células residentes e recrutadas para o TME e vasos sanguíneos. A interação entre os fatores de crescimento e hipóxia com as células tumorais e não-tumorais e presença dos componentes do estroma deste microambiente também são fatores do TME que influenciam na progressão tumoral (Gilkes *et al.*, 2014).

1.3.1 Fatores biológicos do TME

As células presentes no TME têm capacidade de influenciar a progressão tumoral. Além das células neoplásicas, estão presentes fibroblastos associados ao tumor (CAFs), células endoteliais, pericitos e células inflamatórias, dentre outras. Os diferentes tipos celulares podem ter ação antagonista entre atividades pró e anti-tumorais (Hanahan e Weinberg, 2011).

Os CAFs possuem características diferentes quando comparados com fibroblastos normais residentes do estroma e ainda é discutida a exata origem destas células no TME (Attieh e Vignjevic, 2016). Foi observado que estas células estão em maior número em cortes histológicos de CEC quando comparados com lesões de displasia oral e mucosa normal (Etemad-Moghadam *et al.*, 2009). Os CAFs são caracterizados por apresentarem aumento na

expressão de alfa-miosina de músculo liso e, em estudos *in vitro*, induzirem aumento na proliferação e invasão de células tumorais (Zhou *et al.*, 2014). Os CAFs também atuam sobre as fibras da ECM, produzindo um ambiente com maior rigidez (Pankova *et al.*, 2016), remodelando as fibras e criando "poros" para a passagem das células tumorais (Erdogan *et al.*, 2017; Glentis *et al.*, 2017). Também foi observado que os CAFs criam adesões com as células tumorais e, assim, conduzem a migração das células neoplásicas (Labernadie *et al.*, 2017). Portanto, os CAFs influenciam através de diversos mecanismos como o tumor progride (Attieh e Vignjevic, 2016).

O processo de angiogênese está entre os *hallmarks* do câncer (Hanahan e Weinberg, 2000). A formação de novos vasos na massa tumoral traz maior acesso a nutrientes, oxigênio e excreção de metabólitos, mas também facilita a invasão e disseminação de células tumorais para tecidos à distância (Lee *et al.*, 2009; Zuazo-Gaztelu e Casanovas, 2018). Este processo é ativado em estado de hipóxia quando as células tumorais secretam fator de crescimento vascular endotelial (VEGF) para induzir as células endoteliais a formarem novos vasos no interior do tumor (Potente *et al.*, 2011). Estudos também demonstram que as demais células do TME podem ativar a angiogênese (De Palma *et al.*, 2017), assim como fatores liberados pelas células endoteliais também influenciam as células tumorais (Cao *et al.*, 2014). Desta maneira, existe um *loop*-positivo de interação entre as células tumorais e as células endoteliais, favorecendo a progressão tumoral.

A presença de inflamação no TME constitui o interesse de diversos estudos e alvos terapêuticos. Entende-se que as células tumorais secretam diversas citocinas capazes de atrair células do sistema imune e, concomitantemente, não permitem que sejam "identificadas" por este sistema – um *hallmark* descrito como evasão do sistema imune. Diversas células presentes neste ambiente, como macrófagos, linfócitos T, linfócitos B, linfócitos *natural killer* e neutrófilos são estudadas por terem capacidades pró e anti-tumorais (Elinav *et al.*, 2013; Maman e Witz, 2018). Por exemplo, macrófagos possuem estados flutuantes de polarização entre macrófago M1 e M2, sendo

que o M1 teria atividades anti-tumorais e o M2, atividades pró-tumorais (Biswas *et al.*, 2013). Em uma revisão sistemática com artigos publicados estudados em CEC, foi observado que alta marcação para presença de macrófagos está relacionada a pior sobrevida dos pacientes (Alves *et al.*, 2018). Entre os diversos estudos e novidades neste campo de estudo, terapias que utilizam células T com receptor de antígeno quimérico (CAR-T) foram recentemente aprovadas pelo *Food and Drug Administration* (FDA) e podem representar uma alternativa terapêutica em alguns tipos de câncer (Gauthier e Yakoub-Agha, 2017). Portanto, este é um exemplo de modulação de componentes do TME como terapia.

1.3.2 Fatores químicos do TME

As células presentes no TME realizam a sinalização entre si através de fatores que liberam, como fatores de crescimento, citocinas e vesículas extracelulares. As células tumorais produzem diversas citocinas como IL-6, IL-8, IL-10, IL-4, IL-12, TNF-α, TGF-β (Lippitz, 2013). A liberação destas citocinas é fundamental para atrair diversos tipos celulares para o TME e ativar genes específicos nas células tumorais que contribuem para a progressão tumoral.

Dentre as citocinas, uma das mais estudadas é a IL-6. Existe uma correlação entre os níveis séricos de IL-6 em pacientes com CEC com uma pior sobrevida (Duffy *et al.*, 2008). Nas células tumorais, a IL-6 estimula a via de sinalização de JAK/STAT3 e favorece a EMT, a migração celular e a quimioresistência (Su *et al.*, 2011; Yadav *et al.*, 2011; Stanam *et al.*, 2015). Neste contexto, algumas terapias estão sendo desenvolvidas para atingir esta citocina, mas a presença de efeitos adversos ainda é um desafio (Choudhary *et al.*, 2016).

O rápido crescimento das células tumorais cria regiões dentro do tumor com pouco acesso a oxigênio e nutrientes. Fisiologicamente, estes estados seriam de difícil sobrevivência celular. Contudo, as células tumorais utilizam destas situações a seu favor. A hipóxia é definida como áreas em que acontece

baixa presença de oxigênio em decorrência de limitada difusão de oxigênio (Corbet e Feron, 2017). Como resposta a hipóxia, células tumorais produzem fator indutor de hipóxia 1 alfa (HIF1α), responsável por permitir a sobrevivência das células tumorais em hipóxia, e liberam fatores para aumentar a angiogênese da região para, assim, aumentar a perfusão de nutrientes. (Bertout *et al.*, 2008). A ativação do HIF1α também leva à mudança no metabolismo energético das células – fazendo que com as células deixem de produzir ATP através da fosforilação oxidativa para a execução de glicólise e fermentação lática. Como consequência, as células apresentam aumento de receptores GLUT1 e liberam acido lático para o meio extracelular, tornando este TME ácido (Peppicelli *et al.*, 2014). Contudo, também é observada essa mudança de metabolismo energético em células tumorais em ambientes de normóxia – fenômeno conhecido como efeito Warburg (Vander Heiden *et al.*, 2009).

Em CEC, ao avaliar o pH do TME, foi observado que este variava entre 6,56 e 6,97, enquanto que o pH tecidual normal varia entre 6,77 e 7,49 (Becelli *et al.*, 2007). Este TME ácido traz capacidades favoráveis para as células tumorais como aumento da incidência de metástase, aumento da taxa de mutações e resistência a quimio e radioterapia (Walenta *et al.*, 2000; Peppicelli *et al.*, 2014; Da Silva *et al.*, 2018). Portanto, a complexa presença de diversos fatores relacionados ao TME influenciam o fenótipo e a expressão gênica de células presentes no TME.

1.3.3 Fatores físicos do TME

Os efeitos dos fatores físicos nas células tumorais e em células presentes no TME são uma nova fronteira de pesquisa no câncer, sendo ainda pouco estudados. Dentre os fatores físicos envolvidos na iniciação e progressão tumoral, podemos citar a composição da ECM, a topografia, porosidade e rigidez presente na ECM. Em condições fisiológicas, os diferentes tecidos do corpo humano apresentam composições bioquímicas e biomecânicas diferentes. Por exemplo, órgãos possuem composição de ECM distintas, podendo apresentar

variações entre os tipos de fibras e glicosaminoglicas presentes. Além disso, a membrana basal existente junto a células epiteliais e endoteliais também possui função fundamental na manutenção da polaridade ápico-basal das células. A constituição do estroma é diferente, o que influencia, por consequência, o grau de rigidez. Por exemplo, a rigidez do tecido nervoso cerebral (~50Pa) é menor em comparação com o tecido muscular (~12kPa) (Cox e Erler, 2011; Bonnans *et al.*, 2014). Foi demonstrado que células mesenquimais indiferenciadas quando presentes em matrizes com diferentes graus de rigidez (em nível compatível com dos respectivos órgãos) são capazes de se diferenciar em diferentes linhagens celulares, como neurogênica (1kPa), miogênica (17kPa) e osteogênica (40kPa) (Engler *et al.*, 2006).

As células tumorais transitam entre diferentes tecidos que apresentam composições distintas e estes componentes interferem no arranjo tridimensional da ECM. Assim, as células tumorais precisam se adaptar aos novos ambientes. Por exemplo, células epiteliais neoplásicas de CEC passam de um ambiente com presença de lâmina basal rico em laminina para um tecido conjuntivo rico em colágeno e fibronectina (Kosmehl *et al.*, 1999). Foi demonstrado que células de CEC mais agressivas mudam seu padrão migratório quando comparados a um ambiente com laminina e com fibronectina. Na fibronectina, estas células migram de maneira mais individual e com maior velocidade (Ramos *et al.*, 2016), indicando que a composição da ECM interfere no comportamento das células tumorais. De maneira similar, também foi observado em células epiteliais mamárias que ambientes ricos em fibronectina estimulam o processo de EMT (Park e Schwarzbauer, 2014).

As células tumorais apresentam insensibilidade à topografia do ambiente de acordo com alguns estudos. Foi demonstrado que elas mantêm sua capacidade proliferativa independente da topografia, diferentemente de células não-tumorais (Chaudhuri *et al.*, 2016). Quando as células não-tumorais e tumorais foram desafiadas a migrar em substratos com alterações topográficas de nível semelhantes a degraus em escala micrométrica, foi observado que ambos tipos celulares conseguem migrar neste ambientes. Contudo, as células

tumorais apresentam um comportamento diferente ao "escalar" os degraus além de conseguirem migrar verticalmente em degraus de maior altura (Kushiro *et al.*, 2017). Uma das maneiras das células tumorais migrarem pela ECM é através da liberação de MMPs que são enzimas com capacidade de degradar a ECM (Voura *et al.*, 2013). No CEC, por exemplo, presença de maiores níveis de MMP-2 e MMP-9 estão correlacionados com tumores mais invasivos (Ikebe *et al.*, 1999). Contudo, as células tumorais também conseguem migrar e invadir através de poros realizados na ECM pelos próprios CAFs (Glentis *et al.*, 2017). Ou ainda, já foi demonstrado que, em espaços restritos, as células conseguem forçar o rompimento do envoltório nuclear para poder passar por entre estes poros (Denais *et al.*, 2016). Portanto, existem diferentes mecanismos pelos quais as células tumorais conseguem ativar processo de migração e invasão nos tecidos.

O endurecimento na região do tumor é observado em diversos tipos de tumores de origem epitelial, como no câncer de mama e no CEC. Este endurecimento é resultado de aumento da produção de fibras de colágeno no TME. Em decorrência dessas observações, foi demonstrado que o ambiente rígido leva ao aumento da proliferação celular e favorece o processo de EMT, migração e invasão em células epiteliais de mama (Paszek *et al.*, 2005; Wei *et al.*, 2015) e que é possível estimular uma memória mecânica nestas células (Nasrollahi *et al.*, 2017). O favorecimento da progressão tumoral em ambientes rígidos também já foi observado em câncer hepático, de ovário, pulmão e próstata (Tilghman *et al.*, 2010; Yangben *et al.*, 2013; Moazzem Hossain *et al.*, 2014; Mckenzie *et al.*, 2018). O processo pelo qual as células "sentem" a rigidez da ECM e transformam esta informação em resposta biológica é chamado de mecanotransdução. Este processo acontece de maneira orquestrada pelas adesões focais presentes nas células que fazem a conexão entre integrinas com a ECM e o citoesqueleto da célula.

A via de mecanotransdução mais estudada é a via Hippo em que estão associadas as proteínas *yes-associated protein* (YAP) e a *WW domain-containing transcription regulator protein 1* (TAZ). Foi demonstrado que a quebra

da polarização celular induzida pelo lamelipódio (projeção de membrana envolvida na migração celular) resulta em alteração de ativação de RhoA e inibição de fosforilação de cofilina. Estes eventos induzem a estabilização do citoesqueleto de actina (fibras de estresse), os quais medeiam a ativação do fator de transcrição YAP e sua consequente translocação para o núcleo. No núcleo, YAP promove a transcrição de genes relacionados a formação da adesão focal (Dupont *et al.*, 2011; Nardone *et al.*, 2017), contribuindo para a migração e invasão de câncer de mama devido à maior interação com a ECM (Nardone *et al.*, 2017). O YAP apresenta outras funções importantes para as células tumorais, como para promover a proliferação, EMT e resistência a drogas (Segrelles *et al.*, 2018). Em CEC, altos níveis de expressão de YAP estão correlacionados a um pior prognóstico (Qi *et al.*, 2019). Outra atividade desempenhada por YAP é a de permitir que células epiteliais de mama possuam memoria mecânica, ou seja, as células conseguem "lembrar" da rigidez da matriz anterior enquanto elas migram em direção a substratos com diferentes graus de rigidez (Nasrollahi *et al.*, 2017).
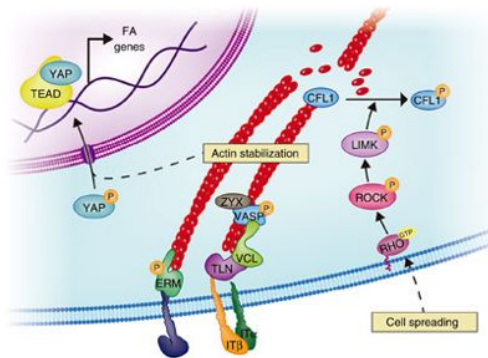
Figura 3. Modelo de mecanismo de ação do YAP. Ao ser ativado por Rho e ROCK, YAP é translocado para o núcleo onde ativa expressão gênica de proteínas relacionadas a adesão da célula a ECM (Nardone *et al.*, 2017).

Outra via envolvida na mecanotransdução é o fator de transcrição Twist com a proteína citoplasmática Ras GTPase-activating protein-binding 2 (G3BP2). Foi demonstrado que Twist e G3BP2 estão conectados no citoplasma e, ao ser estimulada em ambientes rígidos, ocorre a liberação e translocação de

Twist para o núcleo, promovendo EMT (Wei *et al.*, 2015). A relação entre a rigidez da ECM e o comportamento tumoral ainda não foi estudada em CEC.

1.4 Modelos de estudos in vitro do TME

A complexidade dos fatores intrínsecos e extrínsecos que compõem a massa tumoral é um desafio para o estudo desta doença. Modelos animais podem trazer respostas dependendo do contexto, mas ainda é um desafio reproduzir algumas características do TME como o sistema imune e a rigidez (Fenner *et al.*, 2014). Além disso, não é possível isolar variáveis para compreender o estudo de fatores do TME (Mak *et al.*, 2014). Assim, diversas metodologias *in vitro* são desenvolvidas para possibilitar o estudo do TME.

Os primeiros avanços nesta área foram através do grupo da pesquisadora Mina Bissel que demonstrou a importância de utilizar proteínas da ECM para formar um cultivo celular tridimensional (3D) e, assim, tornar os ensaios *in vitro* mais semelhantes com o que é observado *in vivo*. Estes ambientes 3D oportunizavam diferentes expressões de genes e morfologia das células quando comparados com os ambientes 2D (Bissell *et al.*, 1982). A partir de então, foram utilizados proteínas isoladas para fabricação de géis para o estudo do TME em situações fisiológicas e patológicas, como na progressão tumoral. As principais metodologias de estudo utilizavam Matrigel e géis de colágeno para a produção de ambientes 3D. O Matrigel é extraído de sarcoma de Engelbreth-Horm-Swarm de rato e é formado por uma complexa composição de proteínas, como laminina e colágeno tipo IV (Benton *et al.*, 2014). Enquanto que géis de colágeno são normalmente obtidos pela extração de colágeno tipo I de cauda de rato (Timpson *et al.*, 2011). Portanto, de acordo com o objetivo do estudo, pode-se optar por composições de materiais diferentes.

O uso do gel de colágeno permite o estudo da invasão de células tumorais e também a inclusão de outras células presentes no TME para estudo dessa interação (Colley *et al.*, 2011). A diferença na composição das proteínas do Matrigel e do gel de colágeno faz com que as células de câncer de mama

tenham comportamento diferente. Enquanto que no gel de colágeno, as células migram de maneira individual e conseguem se disseminar pelo gel, as células no Matrigel apresentam migração coletiva (Nguyen-Ngoc *et al.,* 2012). Assim, observa-se diferenças em como as proteínas presentes na estrutura dos géis influenciam no fenótipo das células tumorais.

Estes géis são amplamente utilizados para o estudo da ECM em tumores, mas eles demonstram algumas desvantagens por serem de origem natural e, assim, apresentarem variabilidade. Além disso, o estudo isolado de características físicas, como rigidez e porosidade, não é possível. Por exemplo, não é possível aumentar a rigidez de um gel de colágeno sem alterar a adesividade das células a proteínas da matriz devido à maior concentração de colágeno. Assim, foram desenvolvidos géis de origem sintética que permitem o estudo da influência de fatores físicos, como a rigidez, de maneira isolada. Por exemplo, o uso de gel de poliacrilamida. Este tipo de material permite a modulação de diferentes graus de rigidez - desde um substrato mole até um substrato rígido. Sobre esta superfície criada, é adicionado a proteína de adesão de interesse, como colágeno ou fibronectina. Assim, ocorre a manutenção da adesividade de proteínas da matriz, mas com diferentes graus de rigidez que as células conseguem "sentir". Este tipo de substrato permitiu a identificação de vias envolvidas na mecanotransdução de tumores (Paszek *et al.*, 2005; Wei *et al.*, 2015). Portanto, o avanço das metodologias de estudo em câncer permite cada vez mais ampliar nossa compreensão sobre esta doença.

Dentro do exposto, é observado que o CEC é uma doença heterogênea em que diversos fatores influenciam a sua iniciação e progressão. Portanto, com o objetivo de ampliar a compreensão da doença e de alternativas terapêuticas, é necessário estudar a presença das variabilidades presentes nos tumores, além de avaliar o efeito dos fatores do ambiente tumoral sobre a progressão da doença. Portanto, a hipótese da presente tese é que células do CEC apresentam elevada heterogeneidade a qual pode ser modulada por elementos físicos do seu TME.

2. OBJETIVOS

2.1 Objetivo geral

Avaliar modificações fenotípicas que as células tumorais de carcinoma espinocelular oral apresentam e a influência de fatores físicos da matriz extracelular nestas células.

A presente tese será apresentada na forma de quatro artigos científicos, sendo que cada um apresenta objetivos específicos.

2.2 Objetivos específicos do artigo científico 1:

1. Realizar revisão de literatura sobre quais genes de referência são os mais utilizados em estudos envolvendo reação da transcriptase reversa com reação em cadeia da polimerase em tempo real em carcinoma espinocelular oral;

2. Avaliar estabilidade de expressão de genes de referência entre diferentes linhagens celulares de carcinoma espinocelular oral;

2.3 Objetivos específicos do artigo científico 2:

1. Avaliar expressão gênica das diferentes regiões do carcinoma espinocelular de cabeça e pescoço e de tecidos sadios através da ferramenta transcriptograma.

2.4 Objetivos específicos do artigo científico 3:

1. Analisar a influência da rigidez da matriz extracelular sobre as células tumorais de carcinoma espinocelular oral;

2. Correlacionar a organização de colágeno com o prognóstico de pacientes em cortes histológicos de carcinoma espinocelular oral.

2.5 Objetivos específicos do artigo científico 4:

1. Realizar revisão de literatura sobre os biomateriais que são utilizados para o estudo *in vitro* de aspectos do tumor;

2. Realizar revisão de literatura sobre a utilização de estratégias da bioengenharia que permitem diagnóstico e prognóstico das células tumorais.

3. ARTIGOS CIENTÍFICOS

3.1 Artigo científico 1:

Artigo científico submetido no periódico Oral Diseases (ISSN 1601-0825, Fator de Impacto: 2,625)

A variabilidade inter e intratumoral observada nos tumores é um dos grandes desafios terapêuticos e, assim, o estudo da expressão gênica pelos tumores tem grande relevância. Ensaio de reação da transcriptase reversa seguida da reação em cadeia da polimerase em tempo real é uma das principais ferramentas da biologia molecular que permite a análise da expressão de RNA mensageiro nos estudos. Contudo, a análise dos dados precisa ser normalizada por genes de referência e esta deve ser feita de maneira criteriosa. Por ser uma técnica extremamente sensível, dificuldades em termos de normalização estavam sendo encontradas dentro do nosso laboratório na UFRGS. Assim, levantou-se a questão se os genes de referência realmente apresentam níveis de expressão constante entre linhagens celulares diferentes, bem como, quais são os genes de referência mais utilizados nos estudos envolvendo linhagens de carcinoma espinocelular oral. Desta maneira, este artigo científico traz uma revisão de literatura em relação aos genes de referência mais utilizados na literatura e, na sequência, uma análise da estabilidade de cinco genes de referência entre quatro linhagens celulares diferentes. Foi observado que as células apresentam diferenças na expressão de genes de referência utilizados amplamente na literatura e que não existe um gene de referência universal para todos os tipos de amostras biológicas. Assim, evidencia-se a importância de selecionar genes de referência específicos para cada *setup* experimental no intuito de se obter dados confiáveis e reprodutíveis.

Stability of reference genes expression in oral cancer cell lines: a literature review and an *in vitro* evaluation

Running title: Stability of reference genes in oral cancer

Keywords: housekeeping genes; endogenous control; gene expression; oral squamous cell carcinoma; RT-qPCR;

Maurício Tavares Tamborindeguy[1,2], Gabrielle Pedroni[1], Marcelo Lazzaron Lamers[1,3], Bibiana Franzen Matte[1].

[1]Basic Research Center in Dentistry, Dentistry School, Federal University of Rio Grande do Sul, Porto Alegre, Rio Grande do Sul, Brazil,
[2]Center of Biotechnology, Federal University of Rio Grande do Sul, Porto Alegre, RS, Brazil.
[3]Department of Morphological Sciences, Institute of Basic Health Sciences, Federal University of Rio Grande do Sul, Porto Alegre, RS, Brazil.

Corresponding Author:
Bibiana Franzen Matte
Address: Faculdade de Odontologia, Universidade Federal do Rio Grande do Sul, 2492 Ramiro Barcelos Street, 503, ZIP code 90035-003, Porto Alegre, Rio Grande do Sul, Brazil, Phone number +55 51 33085024; Fax +55 51 33085003, e-mail: bfmatte@gmail.com

Abstract

Background: Proper reverse transcription-quantitative polymerase chain reaction (RT-qPCR) assay demands a reliable reference gene (RG), but there is no consensus of a unique RG for all studies. Therefore, the aim of this study is to analyze RG used in oral squamous cell carcinoma (OSCC) literature and also to evaluate RG stability in a cell culture scenario.

Methods: A literature review on OSCC published papers was performed regarding RT-qPCR experiments. It was performed a RT-qPCR experiment with 5 different RG (GAPDH, B-actin, HPRT-1, SDHA and RPLO) in a keratinocyte and in 3 OSCC cell lines with the assistance of specific RT-qPCR computational programs.

Results: Most OSCC papers (~78%) used GAPDH or B-actin as RG. In the RT-qPCR experiment with 4 independent runs, quantification cycles (Cq) of all RG had variability among the cell lines and between the runs. Four software identified B-actin as the most stable RG and that the use of 2 RG would be the optimal number of RG to be used in this experimental condition.

Conclusion: It is observed that there is no unique RG for all biological samples and that the selection of RG can impact in RT-qPCR data analysis.

Introduction

Oral squamous cell carcinoma (OSCC) is an epithelial tumor that invades adjacent tissue and metastasizes to distant sites – which reduces patient overall survival significantly (Siegel *et al.*, 2019). Cancer cells are a result of altered genetic expression that, as a consequence, will have modified phenotypes (Ge *et al.*, 2015). For example, most tumors have altered expression on cell cycle regulation that will promote cell proliferation (Mishra, 2013). Other tumor characteristics as invading adjacent tissue, promoting angiogenesis and resisting cell death are also a consequence of deregulated genetic expression (Hanahan e Weinberg, 2011). Therefore, researches try to elucidate what are these gene expression modifications to understand tumor initiation and progression, but also to develop diagnostic and prognostic biomarkers and treatment practices (Da Silva *et al.*, 2011; Gao *et al.*, 2013; Vincent-Chong *et al.*, 2017). However, tumors are exceedingly heterogeneous among different patients and also within the same tumor mass, which is a challenge to develop ideal diagnostic and prognostic biomarkers (Dagogo-Jack e Shaw, 2018).

A powerful strategy to analyze genetic expression is reverse transcription-quantitative polymerase chain reaction (RT-qPCR) technique, since it is a sensible and reliable method to detect mRNA levels (Ginzinger, 2002; Huggett *et al.*, 2005). This method is used in research laboratories worldwide and was responsible for the identification of many genes associated with OSCC progression and prognosis (Suwanwela e Osathanon, 2017; Zahra *et al.*, 2018). However, since RT-qPCR is highly sensible, there is a need to normalize data to account for inevitable experimental variations (Kuang *et al.*, 2018). The most common way is to normalize data using a reference gene (RG) as an endogenous control. Therefore, it is important to properly choose a good RG for a given experiment (De Jonge *et al.*, 2007). The ideal RG must have stable expression between analyzed samples and no variation under experimental condition. Also, RG levels must be similar to transcript levels of the target gene (Bustin, 2002). Without an appropriate normalization with stable RG, the genetic

expression of the experiment could be inaccurately interpreted, specially when comparing different cell lines or from different patient samples (Tricarico *et al.*, 2002).

Some genes are classically used as RG, such as B-actin, GAPDH and 18S, but it has been demonstrated that the RG varies according to the sample analyzed and the experimental conditions (Jacob *et al.*, 2013; Souza *et al.*, 2013; Liu *et al.*, 2015; Song *et al.*, 2016). Therefore, there is no ideal or unique RG suitable for all tissue types. For OSCC studies, RT-qPCR is widely used to understand the genetic modifications of this disease, but there is not a consensus of the most suitable RG. Therefore, the aim of this study was to review the most commonly used RG in the OSCC literature. Also, it was analyzed 5 common RG (GAPDH, B-actin, HPRT-1, SDHA and RPLO) in 4 different cell lines (HaCat, Cal27, SCC-09 and SCC-25) and the gene stability using 5 different computational programs (NormFinder, Bestkeeper, Delta Ct, GeNorm and Reffinder) was performed. It was observed that most OSCC researchers don't analyze RG stability in theirs qRT-PCR. Also, it was demonstrated that B-actin is the most stable RG for these cell lines studies, but the best approach would be to use at least 2 RG in every qRT-PCR setup. Therefore, it is emphasized the importance to evaluate RG stability in each experimental setup by researchers.

2. Material and methods

2.1 Literature review

In order to analyze most used RG used in RT-qPCR experiments with cell lines broadly available by ATCC and in our laboratory, it was conducted a literature review in National Center of Biotechnology Information (NCBI) / PubMed. The following mesh terms were used: (((((((((((((((head[Title/Abstract] AND neck neoplasms[Title/Abstract])) OR mouth neoplasms[Title/Abstract]) OR oral squamous cell carcinoma[Title/Abstract]) OR (head[Title/Abstract] AND neck cancer[Title/Abstract])) OR oral cancer[Title/Abstract]) AND real time PCR) OR

qRTPCR) AND HaCat) OR SCC25) OR SCC9) OR Cal27) NOT review) NOT systematic review) AND ("2013/01/01"[Date - Publication] : "2017/12/31"[Date - Publication]). Thus, experimental scientific papers that studied gene expression (RT-qPCR) in head and neck cancer with Cal27, SCC-9 and SCC25, and use in someway Hacat cell line in the last five years were analyzed. Scientific papers that were not in English or did not use RT-qPCR in their methodology setup were excluded.

2.2 Materials and reagents

HaCat (human keratinocyte cell line), SCC-9 and SCC-25 (OSCC lineages) cell lines were obtained from Rio de Janeiro Cell Bank (BCRJ, Rio de Janeiro, RJ). Cal27 (OSCC lineage) was obtained from the Tissue Culture Facility at School of Medicine of University of Virginia. HaCat, Cal27 and SCC-9 were cultivated in Dulbecco's modified Eagle's medium (DMEM) with high glucose (Gibco) supplemented with 10% Fetal Bovine Serum (FBS) (Gibco) and 1% penicillin/streptomycin (Gibco). SCC-25 cells were cultivated in DMEM/F12 with 15mM HEPES and 0.5mM sodium pyruvate (Gibco) supplemented with 10%FBS, 1% penicillin/streptomycin (Gibco) and hydrocortisone (400ng/ml, Sigma). All cells were maintained in incubator (37°C, 5% CO_2).

2.3 Total RNA extraction

Total RNA was extracted using Trizol reagent (Invitrogen, Carlsbad, CA, USA) following manufacturer's instructions. Cells were lysed directly in 100mm plates containing 1mL of Trizol. Total RNA was quantified by Spectrophotometer (Thermo Scientific, Wilmington, DE) at 260 and 280nm wavelengths. Only samples with OD (A260/A280) between 1.8 and 2 were used in the following experiments. RNA samples were freezed at -80°C until cDNA conversion.

2.4. Real-time reverse transcription polymerase chain reaction (RT-qPCR)

Complementary DNA (cDNA) was synthesized from 1μg of total RNA with High-capacity cDNA Reverse Transcription Kit (Applied Biosystems, Thermo

Scientific) for RT-PCR, according to the manufacturer's protocol. Real Time PCR was performed using Platinum SYBR Green qPCR (Qiagen). cDNA samples were amplified on Step One Plus Real Time PCR System (Applied Biosystems, USA) in a total volume of 12.5µL (6.25µL of SYBR green, 1µL of Rox dye 1:10, 0.2µL of each primer [1nmol forward and reverse primer], 4.2µL of DEPC water) and 1µL of 1:10 diluted sample. It was used primers for 5 RG listed on Table 1. The cycling conditions was performed accordingly: 10 min at 95ºC, 45 cycles of 15 sec at 95ºC and 1 min at 60ºC followed by a melting curve of 15 sec at 95ºC, 1 min at 60ºC and 15 sec at 95ºC.

2.5 Data analysis

The set of RG selected in the study was evaluated by the following software: BestKeeper(Pfaffl *et al.*, 2004), Delta CT(Silver *et al.*, 2006), Genorm(Vandesompele *et al.*, 2002), NormFinder(Andersen *et al.*, 2004) and RefFinder(Xie *et al.*, 2012). These software use different algorithms to determine the stability and the suitable number of RG that should be used to normalize the relative expression analysis.

Results

Analysis of most used RG in OSCC literature

Since RT-qPCR is a technique that has become widely used in scientific works, a 5-year literature review was conducted looking for OSCC papers that have performed RT-qPCR gene expression studies. MESH terms were used for OSCC, RT-qPCR and for four cell lines (HaCat, Cal27, SCC-9 and SCC-25) that are available by ATCC and are broadly used worldwide. It was analysed 133 papers and data was collected regarding which and how many RG were used in RT-qPCR experiments and which and how many cell lines the papers used. Overall, 10 different types of RG were used (GAPDH, B-actin, 18S, U6, HPRT1, RPLO, LMNB1, TBP, PGK1 and PBGD) (Fig. 1A). More than half of the papers

analysed used GAPDH as the RG (52.9%) and B-actin was the second most used gene (25.4%). Surprisingly, almost 10% of the manuscripts did not refer to use a RG in its analysis. Moreover, most studies used two or more cell lines (79.5%; Fig. 1B) what emphasizes the need to correctly choose an appropriate RG for the analysis. It was also observed that only 3 papers (2.25%) used more than one RG (one of them used two RG and two used three RG) what reflects that authors are not concerned about choosing a stable RG for a RT-qPCR analysis. When it was analysed the specific cell lines that were used in this study with the RG more frequently used, it was observed that Cal27 (52.89% of papers analysed) was the cell line mostly used, followed by SCC-25, SCC-9 and HaCat (Fig. 1C). The most used RG were the same for all cell lines. Therefore, most studies perform RT-qPCR with multiple cell lines, but very few of them were concerned of normalizing data with appropriate RG selection.

RG have variability between experimental setups and cell lines

In order to analyze which RG is more stable to work when comparing 4 different cell lines, RT-qPCR was performed with 5 RG that have different functions inside the cell: GAPDH, B-actin, SDHA, HPRT1 and RPLO (Table 1). It was used a human keratinocyte cell line (Hacat) and three *OSCC cell lines* (Cal27, SCC9 and SCC25) with different aggressiveness profiles. After the reaction was complete, it was analyzed the variance between quantification cycle (Cq) values of the RG. The range, 25th and 75th percentiles, and mean of Cq values for each gene are presented in Fig. 2. All RG genes studied demonstrated variability between the experiments in all cell lines used. Among the RG, the RPLO had the highest variability (e.g. 12.93-25.77 in SCC-25 cell line). The Cq variance was similar in all RG between the cell lines; for example, Cal27 had the lower Cq value in all RG used. Altogether, it was shown that there are variances in the Cq values in all RG studied, which emphasizes the importance to compare and select the most stable RG in each specific experimental setup.

Software analysis indicated the proper use of minimum 2 RG per experiment, including B-actin

Since it was observed variability in all RG used among the 4 cell lines, different RG stability analysis software were used in order to establish which RG would be more accurate in a RT-qPCR experiment. It was used five computational programs: geNorm, NormFinder, BestKeeper, comparative delta Ct and RefFinder - the latter takes into account the value of the other four algorithms. From the five programs used, four identified B-actin as the most stable RG across the four cell lines studied (Fig. 3). Only one algorithm (BestKeeper) identified GAPDH as the most stable RG. In addition, HRPT1 was identified as the second most stable RG by 3 programs and the RPLO gene was shown to be the least stable RG (Fig. 3) independently of the analysis software used. It was also carried out the determination of how many RG are necessary to establish an accurate RT-qPCR experiment with the 4 cell lines used in this study. For this, it was used geNorm to calculate the pairwise variation and a recommended threshold of 0.15 was adopted as a cut-off for reference gene inclusion. It was indicated that, for the four cell lines studied, it is necessary at least 2 RG in order to obtain a reliable result (Fig. 3F). Therefore, RG stability analysis is an important approach in order to increase research quality and reliability of qRT-PCR results.

Discussion

In the last decades, there was an increased access to molecular biology techniques and its application in laboratories all over the world, including RT-qPCR. This technique allows researchers to identify mRNA expression even in very small quantities because it is a sensitive technique. However, due to the high sensitivity, it demands a rigid control of the parameters used to obtain robust results. Due to these difficulties, it was performed the Minimum Information for Publication of Quantitative Real-Time PCR Experiments (MIQE) (Bustin *et al.*,

2009) guideline. The aim of the MIQE guideline is to describe the minimum information necessary that must be described in scientific publications in order to evaluate quality and validity of RT-qPCR experiments. In a literature review performed after MIQE publication, it was observed that the researchers compliance with the guideline was partial (Chapman e Waldenström, 2015). Altogether, it is emphasized that proper analysis and description of publication information in RT-qPCR must be performed in order to guarantee the reliability and reproducibility of the results.

The analysis of gene expression is a common feature in several physiological and pathological studies. For instance, in cancer, it can elucidate biomarkers to improve diagnosis as well as new approaches for patient treatment. However, cancer cells have different mutations that lead to different cell metabolism. Therefore, tumors vary according tissue origin, but even the same type of cancer, as OSCC, also vary between different patients and within the same tumor mass. As a consequence, the use of RT-qPCR technique to examine the expression of target genes demands the selection of stable RG in order to obtain reliable results. Different RG have been identified and selected over the years, but they all have functionalities inside the cells. For example, some RG are related to cell metabolism - like GAPDH, HPRT1 and SDHA - and others are involved in cell cytoskeleton like B-actin. In the literature review performed in this study, it was observed that most OSCC researchers use GAPDH and B-actin. Similarly, another study also performed a literature review with papers that worked with RT-qPCR in vertebrate samples and evidenced that B-actin and GAPDH were also the two mostly used RG (Chapman e Waldenström, 2015). However, recent studies have shown that no gene is stably expressed by all cell lines and that the appropriate reference gene is likely to change according to the sample used, research focus and test conditions used in each analysis (Jacob *et al.*, 2013; Souza *et al.*, 2013; Liu *et al.*, 2015). Therefore, it is emphasized the need to investigate proper RG for each experimental condition.

The majority (80%) of OSCC studies that were analyzed in this study literature review used more than one cell line. The use of multiple cell lines is relevant in order to reinforce the biological phenomenon under study. However, since cell lines are different to one another, it is also extremely important to proper select a stable RG across different cell lines. Only 2.25% of the papers analyzed in the literature review described the use of more than one RG in their studies. In another literature review, the authors found that 13% of papers used multiple RG (Chapman e Waldenström, 2015), what was also considered a low rate. Herein, it was also observed that almost 10% of the papers reviewed did not reference a RG used. All studies reviewed were published after the MIQE guideline what suggests that authors and editors must be more careful when describing and publishing RT-qPCR data.

As it was observed the importance to analyze RG stability, RT-qPCR with 5 different RG was conducted (GAPDH, B-actin, SDHA, HPRT1 and RPLO) in 4 different cell lines (a keratinocyte cell line and 3 OSCC lineages). It was observed that all RG had variances in Cq values between the different runs, what is also observed by other studies that worked with cancer cell lines (Liu *et al.*, 2015; Song *et al.*, 2016). Since in each cycle of RT-qPCR there is an exponential increase of the cDNA copies, even small variances in Cq values are correspondent to large differences in gene expression. Hence, it was necessary to use available software in order to compare RG and choose which one is the most stable and would be the most appropriate to analyze RT-qPCR experiments with these cell lines. The data was analyzed by 5 software - geNorm, NormFinder, BestKeeper, comparative delta Ct and RefFinder – all of them determine RG stability in different ways. B-actin was identified as the most stable RG by four programs – only BestKeeper identified GAPDH as the most stable RG. Also, geNorm showed that, for these analyzed cell lines, it is necessary at least 2 RG for a reliable analysis of RT-qPCR results. It has been observed that RG vary according to the sample analyzed and also the number of RG to be used in an experimental setup. In a study with OSCC patient saliva samples, it was validated 5 RG (MT-ATP6, RPL30, RPL37A, RPLO and RPS17) in oral

cancer salivary gene expression panels – including RPLO that in the present study demonstrated to be the least stable. In a study with head and neck squamous cell carcinoma cell lines treated by different chemotherapy drugs, it was analyzed 12 RG that showed that ALAS1, HMBS and HPRT1 would be the recommended combination (Song *et al.*, 2016). In another study that evaluated stability of RG in an OSCC-model in rats, a combination of Hsp90abl and HPRT1 was recommended for analysis of RT-qPCR data (Peng e Mccormick, 2016). Similar to what it was observed in the current study that HPRT1 also demonstrated a good stability in OSCC samples. However, in the literature review, HPRT1 was used by few researches. Altogether, it is evidenced that there is no universal RG for all samples and researches must identify what are the most stable RG for each specific samples (Jacob *et al.*, 2013; Souza *et al.*, 2013; Liu *et al.*, 2015; Song *et al.*, 2016).

Even though RT-qPCR is already extremely disseminated among laboratories worldwide, there is still need to improve on selection of stable RG used in RT-qPCR analysis. For example, studies must present more complete information and also properly choose RG for analysis. Therefore, it is emphasized the selection of stable RG in order to have reliable analysis.

Author Contribution

M. T. T., G.P. and B. F. M. were involved in study design, acquisition and interpretation of data. M. L. L. was involved in study design and interpretation of data. All authors were involved in manuscript preparation and approved the final version to be published.

Conflict of interest statement

All authors declare no conflicts of interest

REFERENCES

Andersen, C. L., Jensen, J. L., & Ørntoft, T. F. (2004). Normalization of real-time quantitative reverse transcription-PCR data: a model-based variance estimation approach to identify genes suited for normalization, applied to bladder and colon cancer data sets. *Cancer Res, 64*(15), 5245-5250. doi:10.1158/0008-5472.CAN-04-0496

Bustin, S. A. (2002). Quantification of mRNA using real-time reverse transcription PCR (RT-PCR): trends and problems. *J Mol Endocrinol, 29*(1), 23-39.

Bustin, S. A., Benes, V., Garson, J. A., Hellemans, J., Huggett, J., Kubista, M., . . . Wittwer, C. T. (2009). The MIQE guidelines: minimum information for publication of quantitative real-time PCR experiments. *Clin Chem, 55*(4), 611-622. doi:10.1373/clinchem.2008.112797

Chapman, J. R., & Waldenström, J. (2015). With Reference to Reference Genes: A Systematic Review of Endogenous Controls in Gene Expression Studies. *PLoS One, 10*(11), e0141853. doi:10.1371/journal.pone.0141853

da Silva, S. D., Ferlito, A., Takes, R. P., Brakenhoff, R. H., Valentin, M. D., Woolgar, J. A., . . . Kowalski, L. P. (2011). Advances and applications of oral cancer basic research. *Oral Oncol, 47*(9), 783-791. doi:10.1016/j.oraloncology.2011.07.004

Dagogo-Jack, I., & Shaw, A. T. (2018). Tumour heterogeneity and resistance to cancer therapies. *Nat Rev Clin Oncol, 15*(2), 81-94. doi:10.1038/nrclinonc.2017.166

de Jonge, H. J., Fehrmann, R. S., de Bont, E. S., Hofstra, R. M., Gerbens, F., Kamps, W. A., . . . ter Elst, A. (2007). Evidence based selection of housekeeping genes. *PLoS One, 2*(9), e898. doi:10.1371/journal.pone.0000898

Gao, G., Chernock, R. D., Gay, H. A., Thorstad, W. L., Zhang, T. R., Wang, H., . . . Wang, X. (2013). A novel RT-PCR method for quantification of human papillomavirus transcripts in archived tissues and its application in oropharyngeal cancer prognosis. *Int J Cancer, 132*(4), 882-890. doi:10.1002/ijc.27739

Ge, L., Liu, S., Xie, L., Sang, L., Ma, C., & Li, H. (2015). Differential mRNA expression profiling of oral squamous cell carcinoma by high-throughput RNA sequencing. *J Biomed Res, 29*. doi:10.7555/JBR.29.20140088

Ginzinger, D. G. (2002). Gene quantification using real-time quantitative PCR: an emerging technology hits the mainstream. *Exp Hematol, 30*(6), 503-512.

Hanahan, D., & Weinberg, R. A. (2011). Hallmarks of cancer: the next generation. *Cell, 144*(5), 646-674. doi:10.1016/j.cell.2011.02.013

Huggett, J., Dheda, K., Bustin, S., & Zumla, A. (2005). Real-time RT-PCR normalisation; strategies and considerations. *Genes Immun, 6*(4), 279-284. doi:10.1038/sj.gene.6364190

Jacob, F., Guertler, R., Naim, S., Nixdorf, S., Fedier, A., Hacker, N. F., & Heinzelmann-Schwarz, V. (2013). Careful selection of reference genes is required for reliable performance of RT-qPCR in human normal and cancer cell lines. *PLoS One, 8*(3), e59180. doi:10.1371/journal.pone.0059180

Kuang, J., Yan, X., Genders, A. J., Granata, C., & Bishop, D. J. (2018). An overview of technical considerations when using quantitative real-time PCR analysis of gene expression in human exercise research. *PLoS One, 13*(5), e0196438. doi:10.1371/journal.pone.0196438

Liu, L. L., Zhao, H., Ma, T. F., Ge, F., Chen, C. S., & Zhang, Y. P. (2015). Identification of valid reference genes for the normalization of RT-qPCR

expression studies in human breast cancer cell lines treated with and without transient transfection. *PLoS One, 10*(1), e0117058. doi:10.1371/journal.pone.0117058

Mishra, R. (2013). Cell cycle-regulatory cyclins and their deregulation in oral cancer. *Oral Oncol, 49*(6), 475-481. doi:10.1016/j.oraloncology.2013.01.008

Peng, X., & McCormick, D. L. (2016). Identification of reliable reference genes for quantitative gene expression studies in oral squamous cell carcinomas compared to adjacent normal tissues in the F344 rat model. *Oncol Rep, 36*(2), 1076-1084. doi:10.3892/or.2016.4883

Pfaffl, M. W., Tichopad, A., Prgomet, C., & Neuvians, T. P. (2004). Determination of stable housekeeping genes, differentially regulated target genes and sample integrity: BestKeeper--Excel-based tool using pair-wise correlations. *Biotechnol Lett, 26*(6), 509-515.

Siegel, R. L., Miller, K. D., & Jemal, A. (2019). Cancer statistics, 2019. *CA Cancer J Clin, 69*(1), 7-34. doi:10.3322/caac.21551

Silver, N., Best, S., Jiang, J., & Thein, S. L. (2006). Selection of housekeeping genes for gene expression studies in human reticulocytes using real-time PCR. *BMC Mol Biol, 7*, 33. doi:10.1186/1471-2199-7-33

Song, W., Zhang, W. H., Zhang, H., Li, Y., Zhang, Y., Yin, W., & Yang, Q. (2016). Validation of housekeeping genes for the normalization of RT-qPCR expression studies in oral squamous cell carcinoma cell line treated by 5 kinds of chemotherapy drugs. *Cell Mol Biol (Noisy-le-grand), 62*(13), 29-34. doi:10.14715/cmb/2016.62.13.6

Souza, A. F., Brum, I. S., Neto, B. S., Berger, M., & Branchini, G. (2013). Reference gene for primary culture of prostate cancer cells. *Mol Biol Rep, 40*(4), 2955-2962. doi:10.1007/s11033-012-2366-5

Suwanwela, J., & Osathanon, T. (2017). Inflammation related genes are upregulated in surgical margins of advanced stage oral squamous cell carcinoma. *J Oral Biol Craniofac Res,* 7(3), 193-197. doi:10.1016/j.jobcr.2017.05.003

Tricarico, C., Pinzani, P., Bianchi, S., Paglierani, M., Distante, V., Pazzagli, M., . . . Orlando, C. (2002). Quantitative real-time reverse transcription polymerase chain reaction: normalization to rRNA or single housekeeping genes is inappropriate for human tissue biopsies. *Anal Biochem, 309*(2), 293-300.

Vandesompele, J., De Preter, K., Pattyn, F., Poppe, B., Van Roy, N., De Paepe, A., & Speleman, F. (2002). Accurate normalization of real-time quantitative RT-PCR data by geometric averaging of multiple internal control genes. *Genome Biol, 3*(7), RESEARCH0034.

Vincent-Chong, V. K., Salahshourifar, I., Woo, K. M., Anwar, A., Razali, R., Gudimella, R., . . . Zain, R. B. (2017). Genome wide profiling in oral squamous cell carcinoma identifies a four genetic marker signature of prognostic significance. *PLoS One, 12*(4), e0174865. doi:10.1371/journal.pone.0174865

Xie, F., Xiao, P., Chen, D., Xu, L., & Zhang, B. (2012). miRDeepFinder: a miRNA analysis tool for deep sequencing of plant small RNAs. *Plant Mol Biol*. doi:10.1007/s11103-012-9885-2

Zahra, A., Rubab, I., Malik, S., Khan, A., Khan, M. J., & Fatmi, M. Q. (2018). Meta-Analysis of miRNAs and Their Involvement as Biomarkers in Oral Cancers. *Biomed Res Int, 2018*, 8439820. doi:10.1155/2018/8439820

Table 1. Reference genes evaluated in this study, gene ID NCBI, primers sequence, molecular function and melting temperature.

Gene symbol	Gene ID NCBI	Primer sequence (5'→3')	Molecular function	Melting temperature (ºC)
GAPDH	ID: 2597	**Forward** CTTTGTCAAGCTCATTTCCTGG **Reverse** TCTTCCTCTTGTGCTCTTGC	Glycolytic enzyme	F: 57 R: 57
HPRT-1	ID:3251	**Forward** AGATGGTCAAGGTCGCAAG **Reverse** GTATTCATTATAGTCAAGGGCATATCC	Metabolic salvage of purines	F: 57 R: 57
B-Actin	ID: 60	**Forward** CCAACCGCGAGAAGATGA **Reverse** CCAGAGGCGTAGAGGGATAG	Cytoskeletal structural protein	F: 57 R: 58
RPLO	ID: 6175	**Forward** CTCTGCATTCTCGCTTCCTGGAG **Reverse** CAGATGGATCAGCCAAGAAGG	Structural component of the large ribosomal subunit	F: 63 R: 58
SDHA	ID: 6389	**Forward** TGGTTGTCTTTGGTCGGG **Reverse** GCGTTTGGTTTAATTGGAGGG	Electron transporter in TCA cycle and respiratory chain	F: 57 R: 58

Figures

Figure 1
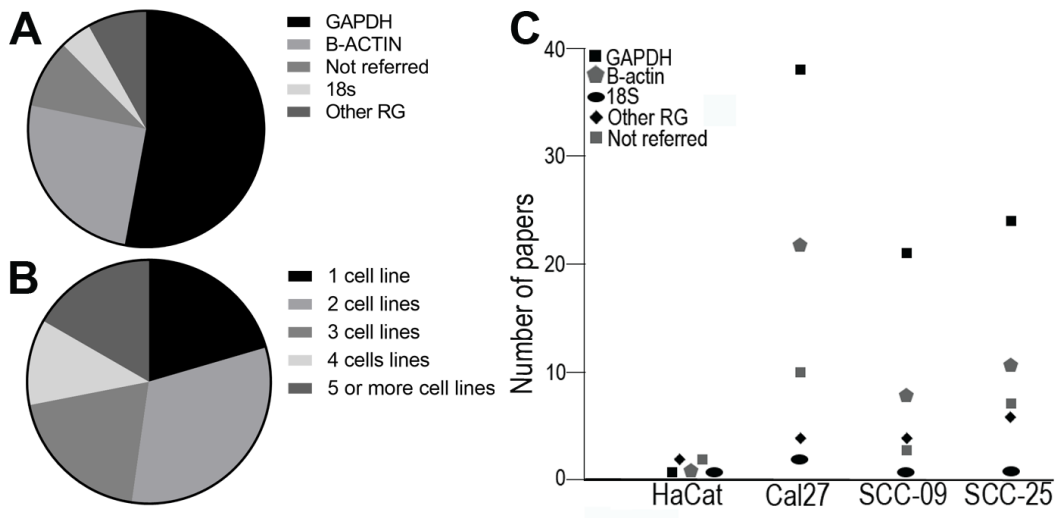
Figure 1. 5-year literature review of OSCC papers that performed RT-qPCR gene expression studies. (A) Most used reference genes in OSCC literature. **(B)** Analysis of how many cell lines the papers used in their experiments. **(C)** Number of papers that used specific cell lines of this study (Cal27, SCC-25, SCC-9 and HaCat) with the RG genes most frequently used.

Figure 2
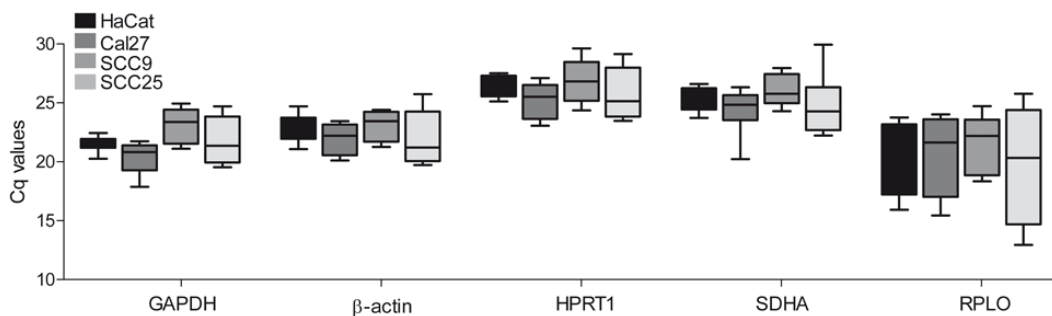
Figure 2. Cq values of the different reference genes analyzed in 4 different cell lines. Cq values of each reference gene in four human cell lines (n=4). The range, 25th and 75th percentiles, and mean of Cq values for each gene is indicated and horizontal line in the middle of the bars indicates average expression level. The lower the Cq value, the higher is the expression of the gene.

Figure 3
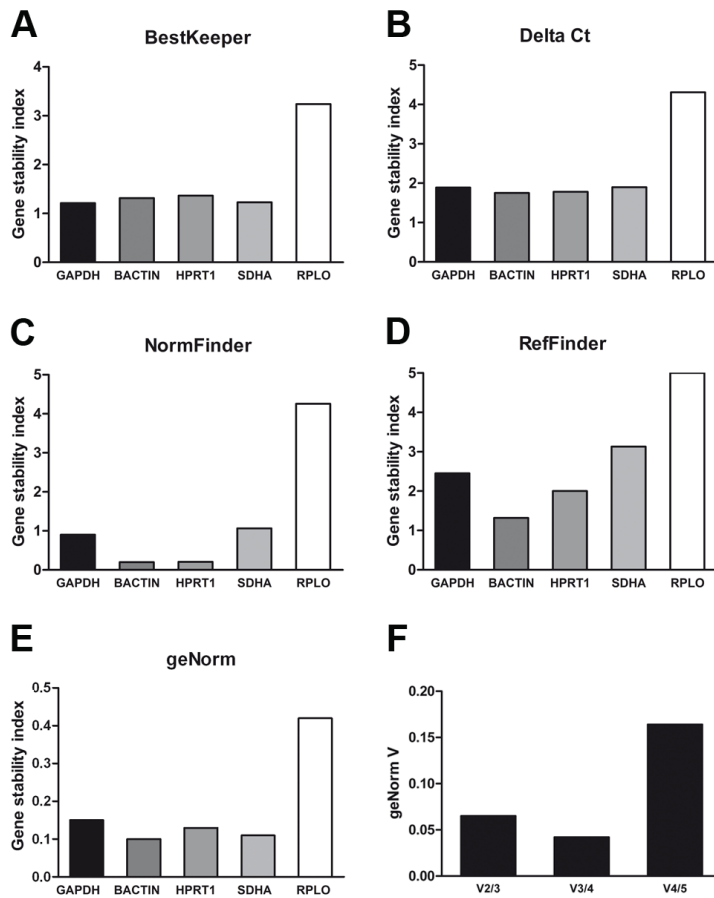
Figure 3. Stability analysis of RG by five different computational programs (BestKeeper, deltaCt, Normfinder, RefFinder and geNorm) and determination of the optimal number of reference gene. **(A) (B) (C) (D) (E)** Gene stability index of five reference genes by each computation program indicated. The lower the stability index value, the higher is the stability of the RG and lower is its variation. **(F)** Determination of the optimal number of RG for normalization by geNorm software. Pair-wise variation value was generated by geNorm and a recommended threshold of 0.15 was adopted as a cut-off for reference gene inclusion.

3.2 Artigo científico 2:

Artigo científico submetido como *short communication* no periódico Otolaryngology-Head and Neck Surgery (ISSN 0194-5998, Fator de Impacto: 2,310)

Diversos fatores influenciam a etiopatogenia do carcinoma espinocelular de cabeça e pescoço e, conforme observado no artigo científico 1, as células tumorais apresentam grande variabilidade em relação a expressão de genes considerados como genes de referências. Assim, levantou-se o questionamento de como é a variabilidade de um conjunto de transcritos nas diferentes regiões do tumor. Com o desenvolvimento de sequenciamento de nova geração, houve um avanço em relação à quantidade de dados disponíveis para avaliação do código genético humano. Dentro de estudos em câncer, estão disponíveis conjuntos de dados que podem ser avaliados para detecção de informações relevantes em um grande número de amostras. Assim, este artigo tem como objetivo analisar a expressão gênica de dados disponíveis no *Genomics Data Commons Data Portal* (*GDC Data Portal*) de carcinoma espinocelular de cabeça e pescoço através da ferramenta do transcriptograma em colaboração com professores do Instituto de Física da UFRGS. O transcriptograma é uma forma de normalizar e visualizar um grande número de dados. Os dados disponíveis no *GDC Data Portal* foram divididos entre as regiões de ocorrência do tumor em comparação com os respectivos tecidos sadios. Observou-se que o perfil de expressão evidenciado no transcriptograma é diferente de acordo com a região de localização do tumor. Quando o perfil de expressão gênica foi analisado apenas nas amostras de tecidos sadios, as diferentes regiões dos tecidos também apresentaram variação no seu perfil. Assim, é possível entender que a própria região de origem do tumor tem influência no comportamento das células no microambiente tumoral e na progressão do tumor. Portanto, as regiões de desenvolvimento do carcinoma espinocelular de cabeça e pescoço devem ser

levadas em consideração no momento de executar pesquisas, decidir tratamentos e prognósticos para estes pacientes.

Gene expression profile variability among Head and Neck Squamous Cell Carcinoma location sites

Bibiana F. Matte[1], Gilberto L. Thomas[2], Rita M. C. de Almeida[2], Marcelo L. Lamers[1,3]

[1] Department of Oral Pathology, Dental School, Federal University of Rio Grande do Sul, Porto Alegre, RS, Brazil.
[2] Physics Institute, Federal University of Rio Grande do Sul, Porto Alegre, RS, Brazil.
[3] Department of Morphological Sciences, Institute of Basic Health Sciences, Federal University of Rio Grande do Sul, Porto Alegre, RS, Brazil.

Corresponding Author:
Marcelo Lazzaron Lamers
Address: Faculdade de Odontologia, Universidade Federal do Rio Grande do Sul, Rua Ramiro Barcelos, 2492, sala 503, CEP 90035-003, Porto Alegre, Rio Grande do Sul, Brasil, Telefone +55 51 33085011; Fax +55 51 33085003, e-mail: marcelo.lamers@ufrgs.br

Abstract

Next Generation Sequencing data available in the Genomic Data Commons (GDC) Data Portal granted an opportunity to researchers worldwide analyze a large amount of data. Here, we used the transcriptogram method to analyze gene expression variability on Head and Neck Squamous Cell Carcinoma (HNSCC) data available in the GDC. The profile of whole-genome gene expression of all tumors available in the GDC was compared with the normal tissue data and then stratified according to the different regions of neoplastic and healthy tissue. It was observed that different location sites of HNSCC have different gene expression profile. Meanwhile, it was also observed that healthy tissue from different head and neck regions present gene expression profile variability. Therefore, tumor development and progression is influenced not only by key mutations, but also by different gene expression due to characteristics of the tissue region.

Introduction

Head and Neck Squamous Cell Carcinoma (HNSCC) accounts for over 90% of all cancer types in the head and neck region and is the sixth most common cancer type worldwide (Siegel *et al.*, 2019). The tumor occurrence location site appears to have an impact on tumor prognosis, since the 5-year survival rate varies according to tumor region, ranging from 25% (hypopharynx) to 60% (larynx)(Cooper *et al.*, 2009; Gatta *et al.*, 2015). This range might be related to differential gene expression induced by etiopathogenic factors and understanding this relation might contribute to more effective personalized treatment.

The Next Generation Sequencing (NGS) HNSCC project, available in the Genomic Data Commons (GDC) Data Portal has 500 available cases with RNA-sequencing (RNA-seq) data. We analyzed this data with de Almeida laboratory transcriptogram method (Rybarczyk-Filho *et al.*, 2011) in order to identify altered molecular pathways. We observed that genetic expression of both healthy tissue and tumors from different sites on the head and neck vary significantly. Therefore, researches regarding HNSCC molecular pathways must consider tumor location site since gene expression diversity is expected to influence tumor progression and patient prognosis.

Methods

RNA-seq data from the HNSCC Project was extracted from the GDC Data Portal. The transcriptome of all collected data was analyzed with the Transcriptogramer- software available online (lief.if.ufrgs.br/pub/biosoftwares/transcriptogramer)(Rybarczyk-Filho *et al.*, 2011). Normal tissue samples were used as controls to compare with tumor samples. Transcriptograms are obtained by first ordering a list of genes using protein-protein association information such that the probability that any two genes on the list are associated exponentially decays with the distance between the genes positions on the list. The ordering method minimizes a cost function using Monte

Carlo prescription and different intervals of the gene list are enriched with different Gene Ontology (GO) terms or KEGG pathways. Here we used the ordering for humans as published previously (De Almeida *et al.*, 2016). There were 500 HNSCC tumor RNA-seq data available and 43 normal tissue. According to available metadata, it was used the International Classification of Diseases (ICD) from the data collected to separate the data by tumor location sites (Table 1). Mean transcriptograms for each tumor location site was compared to: 1- their correspondent healthy tissue when normal data was available and 2- the normal tissue was compared in the specific region with all normal tissue data available. The significance of differences between two transcriptogram classes was estimated using a two-tailed Welch's *t* test on the class average to obtain a *P* value for each list position.

Results

The transcriptograms comparing all HNSCC tumor location sites with all normal available tissue samples demonstrated important differences in the gene expression analysis. Differences within cell cycle genes and cell adhesion were evidenced. When we separated the data sample according to tumor region, striking differences between the regions were observed (Fig. 1). For example, tumors located in the tongue (n=149) showed reduced expression of genes related to extracellular matrix adhesion while tumors located in larynx (n=112) demonstrated overexpression when comparing to their correspondent normal tissue. In order to understand what could drive differences between tumor locations, we also produced transcriptograms comparing exclusively the normal tissue data (e.g. normal tongue tissue compared to all normal tissues) (Fig. 2). Interestingly, transcriptogram profiles vary between each region, demonstrating that each region of the head and neck has a unique gene expression. Altogether, it is evidenced that tumor region have different gene expression profile and this may be due, in part, to the original differential expression from the normal tissue itself.

Discussion

Due to the large scale of genetic sequencing and data availability, our current challenge is to properly analyze enormous amounts of data and extract from it relevant information that can help in cancer diagnosis and prognosis. For HNSCC, it has been demonstrated, with NGS studies, six most frequently mutated genes - TP53, NOTCH1, CDKN2A, PIK3CA, HRAS and PTEN genes. Also, tobacco users, HPV negative and positive have distinct genetic profiles (Stransky *et al.*, 2011; Network, 2015). In a single-cell transcriptomic analysis in HNSCC patients, it was demonstrated the heterogeneous composition of malignant and non-malignant cells inside a tumor mass (Puram *et al.*, 2017). Therefore, large sequencing cohorts elucidate relevant biological alteration in HNSCC. Herein, we have shown that tumors from different sites have distinct genetic alterations. These alterations can be explained not only by the mutation within the neoplastic cells, but also by surrounding tissue of the tumor (e.g. extracellular matrix) since healthy tissue gene expression profile also varies between regions. The differences observed in the normal tissue gene expression among locations in the head and neck also raises questions about the multiple factors that can influence cell behavior in other diseases. Altogether, expanding our knowledge with NGS can have profound effects in the health area.

The identification of intratumoral heterogeneous expression in HNSCC emphasizes that personalized treatment is an interesting option for these patients. In order to develop personalized treatments, it is necessary to analyze large amounts of biological and clinical data. The implementation of big data analysis and machine learning technologies in the cancer field will allow advances in the identification of biological patterns in each tumor region and key mutations of each tumor. As a consequence, clinical treatments could be based on those patterns identification in order to achieve better patient prognosis. Interdisciplinary work is therefore required in order to develop biological analysis for the large amount of data available.

Here we demonstrated that regions of the head and neck have different genetic expression and that reflects on tumor expression profiles. Unraveling HNSCC heterogeneity is an important step in order to improve diagnosis and treatment practices.

Conflict of interest statement
All authors declare no conflicts of interest

REFERENCES

Siegel RL, Miller KD, Jemal A. Cancer statistics, 2019. *CA Cancer J Clin.* 2019;69(1):7-34.

Gatta G, Botta L, Sánchez MJ, et al. Prognoses and improvement for head and neck cancers diagnosed in Europe in early 2000s: The EUROCARE-5 population-based study. *Eur J Cancer.* 2015;51(15):2130-2143.

Cooper JS, Porter K, Mallin K, et al. National Cancer Database report on cancer of the head and neck: 10-year update. *Head Neck.* 2009;31(6):748-758.

Rybarczyk-Filho JL, Castro MA, Dalmolin RJ, Moreira JC, Brunnet LG, de Almeida RM. Towards a genome-wide transcriptogram: the Saccharomyces cerevisiae case. *Nucleic Acids Res.* 2011;39(8):3005-3016.

de Almeida RM, Clendenon SG, Richards WG, et al. Transcriptome analysis reveals manifold mechanisms of cyst development in ADPKD. *Hum Genomics.* 2016;10(1):37.

Network CGA. Comprehensive genomic characterization of head and neck squamous cell carcinomas. *Nature.* 2015;517(7536):576-582.

Stransky N, Egloff AM, Tward AD, et al. The mutational landscape of head and neck squamous cell carcinoma. *Science.* 2011;333(6046):1157-1160.

Puram SV, Tirosh I, Parikh AS, et al. Single-Cell Transcriptomic Analysis of Primary and Metastatic Tumor Ecosystems in Head and Neck Cancer. *Cell.* 2017;171(7):1611-1624.e1624.

Table

Table 1. Sample characterization according to location site and ICD number.

Location site	Tumor	Normal tissue	ICD 10
All	500	43	C00-14; C32; C41
Lips	3	-	C00.9
Tongue	149	15	C01-C02
Mouth	109	4	C03-06
Amygdala	36	-	C09.9
Pharynx	20	-	C10-13
Overlapping tumors of mouth, pharynx, lips	69	13	C14.8
Supraglottic region	1	-	C32.1
Larynx	112	11	C32.9
Jaw	1	-	C41.8

Figure 1
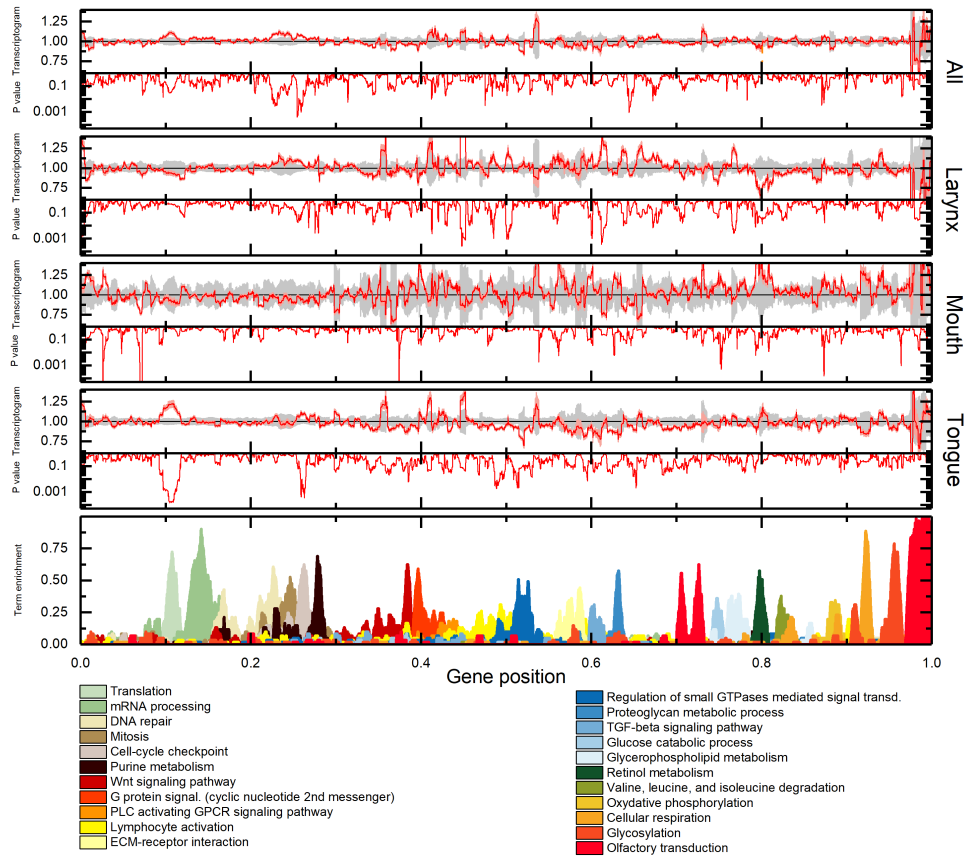
Figure 1. Transcriptogram for all tumor present in the HNSCC project in GDC Data Portal and divided by each tumor site compared to respective normal tissue. The x-axis indicates the relative position in the ordered list of 9684 genes. The transcriptogram part of each panel are presented as mean± s.e.m. of tumor samples (red line ± pink region) and normal samples (black line ± gray region). The P value panels are from a two-tailed Weyl's t test for each point of the transcriptogram. There are a transcriptogram panel and a p value panel for each site: all tumors (n= 500), larynx (n= 112), mouth (n=109) and tongue (n= 149). Last panel is the term enrichment map showing the correspondence between the ordered gene list and major biological terms and pathways. The colored profiles correspond to the density distribution within the list of specific Gene Ontology (GO) term or KEGG pathway. A term enrichment value of 1 on the y-axis indicates that all genes in an interval of radius r=30 participate in a given GO term or KEGG pathway. Peaks mark regions enriched with genes related to the term or pathway indicated in the legend.

Figure 2
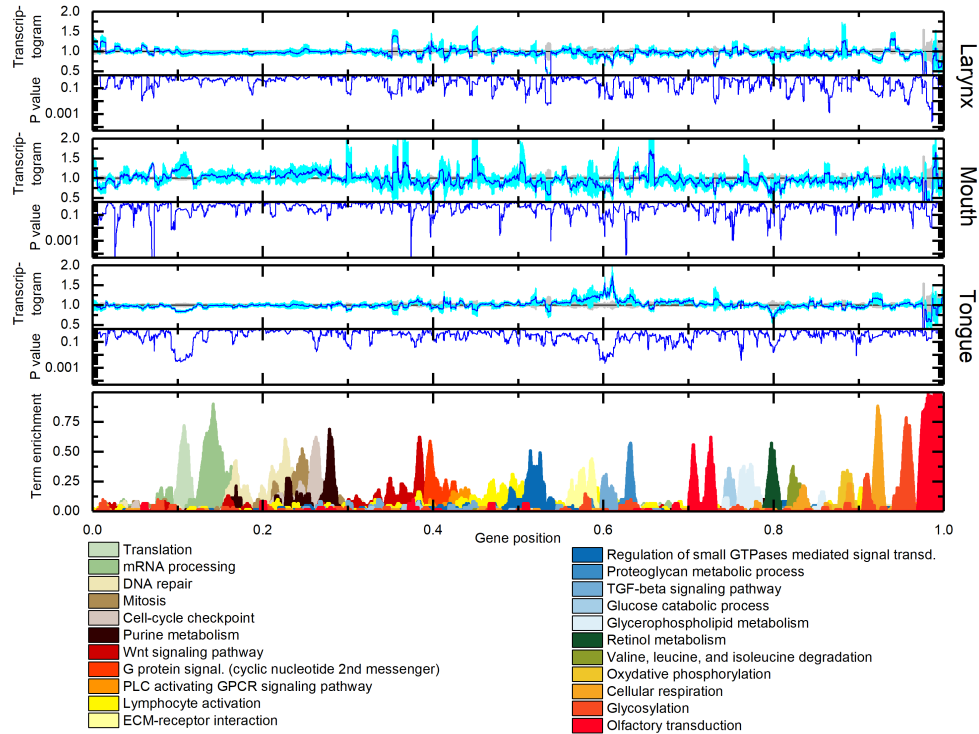
Figure 2. Transcriptogram for normal tissues data present in the HNSCC project in GDC Data Portal and divided by each location site compared to all normal tissues. The x-axis indicates the relative position in the ordered list of 9684 genes. The transcriptogram part of each panel are presented as mean± s.e.m. of normal tissue region samples (dark blue line ± light blue region) and normal samples (black line ± gray region). The P value panels are from a two-tailed Weyl's t test for each point of the transcriptogram. There are a transcriptogram panel and a p value panel for each site: larynx (n= 11), mouth (n= 4) and tongue (n=15). Last panel is the term enrichment map showing the correspondence between the ordered gene list and major biological terms and pathways. The colored profiles correspond to the density distribution within the list of specific Gene Ontology (GO) term or KEGG pathway. A term enrichment value of 1 on the y-axis indicates that all genes in an interval of radius r=30 participate in a given GO term or KEGG pathway. Peaks mark regions enriched with genes related to the term or pathway indicated in the legend.

3.3 Artigo científico 3:

Artigo científico publicado no periódico Journal of Cell Science (ISSN 0021-9533, Fator de Impacto: 4,401:, DOI: 10.1242/jcs.224360).

Dentre as alterações observadas de que a região do tumor influencia na progressão tumoral e de que as lesões de carcinoma espinocelular oral, clinicamente, apresentam bordos endurecidos, o próximo objetivo foi analisar se diferentes durezas do ambiente poderiam modular o comportamento da células tumorais. A influência da rigidez da matriz já havia sido observada em outros tipos de tumores, como no câncer de mama, o que reforçava a nossa hipótese. Um dos principais laboratórios que estuda mecanotransdução é conduzido pelo Prof. Adam Engler na University of San Diego California onde uma parte deste estudo foi realizada com o apoio do Programa Doutorado Sanduíche da CAPES. Neste estudo, foi possível analisar que células tumorais de carcinoma espinocelular oral mais invasivas apresentam maior capacidade de migração em substratos rígidos e que células com menor agressividade podem ser mecanicamente moduladas a terem modificações fenotípicas indicativas de maior agressividade tumoral. Com o intuito de correlacionar com dados clínicos, foi observado que pacientes com tumores com maior organização de colágeno apresentam pior prognóstico. Portanto, a rigidez da matriz extracelular em carcinoma espinocelular oral influencia na progressão deste tumor.

The Company of
Biologists

RESEARCH ARTICLE

Matrix stiffness mechanically conditions EMT and migratory behavior of oral squamous cell carcinoma

Bibiana F. Matte[1,2], Aditya Kumar[2,3], Jesse K. Placone[2,3], Virgílio G. Zanella[1,4], Manoela D. Martins[1], Adam J. Engler[2,3,*] and Marcelo L. Lamers[1,5,*]

ABSTRACT

Tumors are composed of heterogeneous phenotypes, each having different sensitivities to the microenvironment. One microenvironment characteristic – matrix stiffness – helps to regulate malignant transformation and invasion in mammary tumors, but its influence on oral squamous cell carcinoma (OSCC) is unclear. We observed that, on stiff matrices, a highly invasive OSCC cell line (SCC25) comprising a low E-cad to N-cad ratio (Inv^H/E:N^L; SCC25) had increased migration velocity and decreased adhesion strength compared to a less invasive OSCC cell line (Cal27) with high E-cad to N-cad ratio (Inv^L/E:N^H; Cal27). However, Inv^L/E:N^H cells acquire a mesenchymal signature and begin to migrate faster when exposed to prolonged time on a stiff niche, suggesting that cells can be mechanically conditioned. Owing to increased focal adhesion assembly, Inv^L/E:N^H cells migrated faster, which could be reduced when increasing integrin affinity with high divalent cation concentrations. Mirroring these data in human patients, we observed that collagen organization, an indicator of matrix stiffness, was increased with advanced disease and correlated with early recurrence. Consistent with epithelial tumors, our data suggest that OSCC cells are mechanically sensitive and that their contribution to tumor progression is mediated in part by this sensitivity.

This article has an associated First Person interview with the first author of the paper.

KEY WORDS: Cancer, Extracellular matrix, Elasticity, Collagen, Hydrogel

INTRODUCTION

Oral squamous cell carcinoma (OSCC) is the most common oral cancer in the USA (Markopoulos, 2012) and originates from epithelial cells, whose genetic mutations induce them to lose polarity, invade adjacent connective tissue and even metastasize to distant tissues (Leemans et al., 2018). With the loss of polarity, cells undergo an epithelial-to-mesenchymal transition (EMT) and acquire a migratory phenotype (Smith et al., 2013; Nieto et al., 2016; Lamouille et al., 2014). EMT is orchestrated by the expression

and/or nuclear localization of several families of transcriptional factors (Yao et al., 2017; Kong et al., 2015; Fan et al., 2013), including TWIST, SNAIL and ZEB. One change accompanying EMT in OSCC cells is a switch from epithelial to mesenchymal adhesion proteins, i.e. E-cadherin (E-cad) to N-cadherin (N-cad) (Angadi et al., 2016). However, EMT is a dynamic, transitional process and cells at different stages of the process can co-exist within the same tumor. In addition to tumor heterogeneity, the tumor microenvironment (TME) is often involved in this process and can even modulate cancer progression. Tumors, cancer-associated fibroblasts (CAFs), the immune system and the extracellular matrix (ECM) often interact in reciprocal ways that promote subpopulations to grow, become aggressive and spread (Hanahan and Coussens, 2012; Bissell and Hines, 2011). Although many TME properties have been studied extensively in a variety of tumor types, the influence of TME on OSCC remains relatively understudied, despite its prevalence and, especially, in the context of how TME physical properties regulate OSCC cell behavior.

OSCC is clinically observed as an ulcer with irregular, elevated and indurated margins (Scully and Porter, 2001). As with mammary (Leventhal et al., 2009), ovarian (McKenzie et al., 2018), head and neck, esophageal, and colorectal cancer (Conklin et al., 2011; Hanley et al., 2016), OSCC tumors present clinically as a region that is stiffer than normal counterpart tissue (Scully and Porter, 2001). As such, stiff matrix *in vitro* triggers an invasive phenotype in mammary epithelial cells and increases migration in an epithelial ovarian cancer cell line (McKenzie et al., 2018; Wei et al., 2015; Paszek et al., 2005). Similar stiffness sensitivities and tumor stromal changes have been found in 2D cell culture for lung (Tilghman et al., 2010), prostate (Moazzem Hossain et al., 2014) and hepatocellular (Yangben et al., 2013) carcinomas. The ubiquitous nature of stiffness-mediated cell behavior changes begs the question of how cells sense ECM properties, such as stiffness. Mechano-sensing often occurs through a complex series of structures, beginning with focal adhesions (FAs) that directly connect cells to the ECM through integrins and, ultimately, to the cytoskeleton and nucleus (Holle and Engler, 2011). Positive feedback between these structures promotes FA formation and maturation, force generation, migration or invasion, and the expression and translocation of EMT and YAP/TAZ transcription factors to the nucleus (Nardone et al., 2017). These factors often have co-regulators that control localization, such as with TWIST1 whose cytoplasmic partner G3BP2 regulates its translocation to the nucleus and induction of an invasive phenotype (Wei et al., 2015). Yet, all of these signals are transient, as cancer cells often transition back and forth between epithelial and mesenchymal states, raising the question of whether OSCCs have mechanical memory. After being exposed to a stiff niche, mammary epithelial cells migrated faster and showed YAP-dependent increases in actomyosin expression, even when the second niche was softer (Nasrollahi et al., 2017). Studies also often focus on cell–matrix

[1]Department of Oral Pathology, Universidade Federal do Rio Grande do Sul, Porto Alegre, RS, Brazil. [2]Department of Bioengineering, University of California, San Diego; La Jolla, CA 92093, USA. [3]Sanford Consortium for Regenerative Medicine, La Jolla, CA 92037, USA. [4]Head and Neck Surgery Department, Santa Rita Hospital, Santa Casa de Misericórdia de Porto Alegre, Porto Alegre, RS, Brazil. [5]Department of Morphological Sciences, Institute of Basic Health Sciences, Universidade Federal do Rio Grande do Sul, Porto Alegre, RS, Brazil.

*Authors for correspondence (aengler@ucsd.edu; marcelo.lamers@ufrgs.br)

J.K.P., 0000-0002-3464-8177; A.J.E., 0000-0003-1642-5380; M.L.L., 0000-0001-5296-5662

Journal of Cell Science

1

interactions in the absence of cell–cell connections. Recent work both in normal (Sunyer et al., 2016; Xi et al., 2017) and transformed epithelia (Lintz et al., 2017), suggests that cell sheets sense a combination of matrix and cell stiffness to direct migration; but whether OSCC cells respond individually or collectively to stiffness differences, or whether they have a mechanical memory is unclear.

Thus, to better understand stiffness responses in OSCC, we examined stiffness-mediated responses in four OSCC cell lines with a range of epithelial and invasive phenotypes, as well as tumor-recurrence-free survival time of OSCC patients, assessed by collagen organization as a surrogate for stiffness (Conklin et al., 2011; Hanley et al., 2016; Wei et al., 2015). We found that the epithelial phenotype appears plastic when cells conditioned within a stiff niche present EMT-like responses; focal adhesions; moreover, specifically, integrin activation, appears to be crucial in the regulation of this response. At the clinical level, increases in stiffness, as measured by enhanced collagen organization, appears to correlate with advanced disease and shorter recurrence-free survival time. Together, this suggest that the progression of oral cancers, as with other epithelial tumors, is mechanically sensitive.

RESULTS

Increased EMT marker expression and invasion correlate in oral squamous cell carcinomas

Oral cancer cells – which have epithelial origins – exhibit a spectrum of EMT marker expression and the ability to localize those markers to the nucleus. To illustrate this, protein and mRNA expression from four OSCC cell lines were analyzed; SCC9 and SCC25 cell lines had higher N-cadherin (N-cad) to E-cadherin (E-cad) ratios compared to those in Cal27 and FaDu cell lines (Fig. 1A), indicating that SCC cell lines have a more mesenchymal-like phenotype. Accordingly, mRNA analyses of EMT transcription factors, e.g. Zeb1, Zeb2, Snail1, Snail2 and Twist, also showed that SCCs cell lines have higher expression of all EMT markers analyzed (Fig. 1B). Cal27 and SCC25 cells are also morphologically distinct from each other (Fig. 1C). Thus, to correlate EMT marker expression and morphological differences with the level of invasiveness of the cell lines, we carried out organotypic cultures, for which cells were cultivated on top of a fibroblast-embedded collagen matrix for 21 days in an air–liquid interface. Cells with more E-cad than N-cad, e.g. Cal27, did not invade the collagen matrix compared to SCC9 – a line with more N-cad than E-cad, which invades the collagen matrix by day 21 (Fig. 1D). The latter resembles histopathological specimens of patients diagnosed with OSCC, where there is significant stromal invasion (Angadi et al., 2016; Colley et al., 2011). On the basis of these differences, we subsequently divided cell lines according to invasiveness and EMT protein expression, e.g. less invasive with high E-cad to N-cad ratio (Inv^L/E:N^H; Cal27) and highly invasive with low E-cad to N-cad ratio (Inv^H/E:N^L; SCC25).

Inv^L/E:N^H cell migration is initially stiffness insensitive

Although well-studied mammary and ovarian cancer cell lines exhibit EMT, and become invasive at increased stiffness (McKenzie et al., 2018; Wei et al., 2015; Paszek et al., 2005), such correlation is not yet clear for oral cancer. Thus, we analyzed the migration profile of Inv^L/E:N^H and Inv^H/E:N^L cells after they had been plated on collagen-coated hydrogels for 12 h with two different stiffness – a soft (0.48 kPa) matrix, close to healthy tongue stiffness (Brown et al., 2015; Cheng et al., 2011), and a stiff (20 kPa) matrix that represents the degree of stiffening and stromal remodeling present in other cancers (McKenzie et al., 2018; Wei et al., 2015; Paszek et al., 2005).
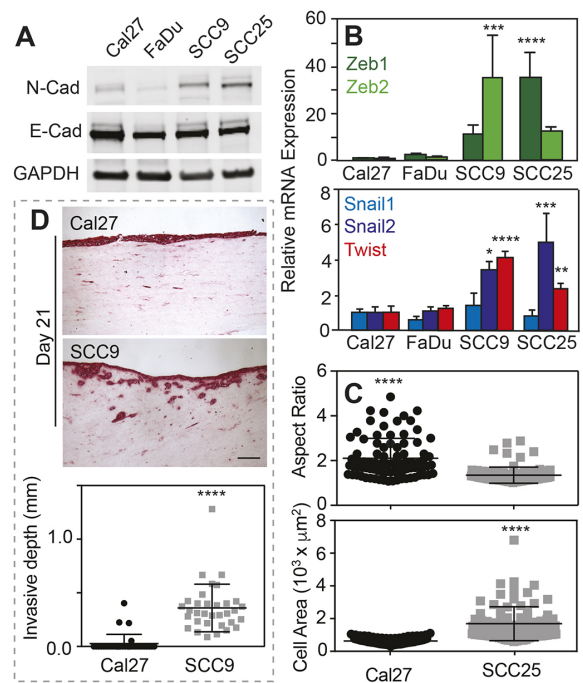
Fig. 1. Invasive oral squamous cell carcinoma cell lines have increased N-cadherin and EMT marker expression. (A) Western blot of indicated cell lines (Cal27, FaDu, SCC9, SCC25) and proteins (N-Cad, E-cad, GADPH). (B) Relative mRNA expression of the indicated EMT transcription factors for the indicated cell lines. n=4 samples for each plot. *, **, *** and **** represent P<0.05, 0.01, 0.001 and 0.0001, respectively, for one-way ANOVA and Tukey's multiple comparison test. (C) Plot of aspect ratio (major to minor cell axes) and cell area for the indicated cell lines. ****P<0.001 for two-tailed Welch's t-test. n=86 and 87 for Cal27 and SCC25, respectively, from triplicate experiments. (D) Histological sections (top) of a collagen gel invasion assay stained using PicroSirius Red, of cells cultured at an air-liquid interface. The indicated cell lines were cultured on the collagen gels for 21 days prior to staining. Plot showing the invasion depth (bottom). n=3 samples and ****P<0.001 for two-tailed Welch's t-test. Scale bar is 50 μm.

We observed that Inv^L/E:N^H cells tended to migrate in cell clusters, especially on the soft substrate, and Inv^H/E:N^L cells tended to migrate individually, which resembles epithelial and mesenchymal cell behavior, respectively (Fig. S1) (Friedl and Alexander, 2011). This behavior also appeared to be independent of substrate stiffness. Although morphology or mode of migration did not differ with respect to stiffness, we found that Inv^H/E:N^L cells had significantly increased collective and individual migration velocity (Fig. 2A,B), and were more processive on stiff substrates relative to Inv^L/E:N^H cells (Fig. 2C,D). Interestingly, Inv^L/E:N^H cells appeared to be stiffness insensitive with respect to migration velocity and directionality, whereas Inv^H/E:N^L cells were fastest on stiff substrates when migrating collectively (P<0.01 between collective and single migration on 20 kPa substrates). In all cases, migration appeared to occur through random walk, based on a lack of difference in either the angle between migration steps (i.e. orientation correlation coefficient; Engler et al., 2004) or the persistence index (i.e. path length divided by total displacement; Fig. S2).

To determine what underlying functional differences drive these observations, we assessed how strongly cells pulled on their surroundings when migrating and how well cells adhered to their

2
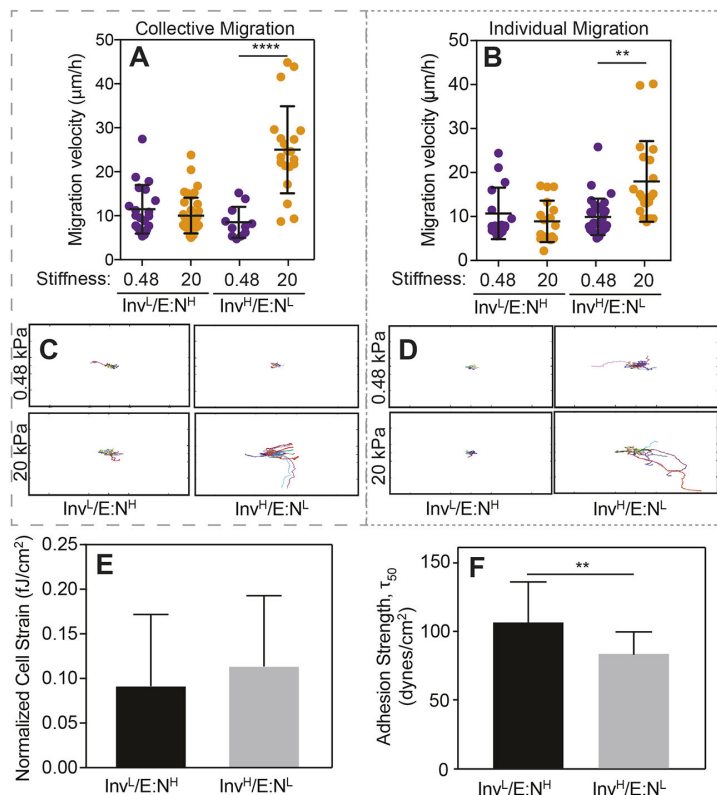
Fig. 2. Inv^L/E:N^H cell migration is stiffness insensitive. (A,B) Collective (A) and individual (B) cell migration for the indicated cell lines on soft (purple) and stiff (orange) substrates. Each point represents the average velocity of an individual cell. For panel A, n=20, 40, 20 and 20 cells for the groups from triplicate experiments. For panel B, n=16, 17, 31, and 20 cells for the groups from triplicate experiments. **P<0.01 and ****P<0.0001 for Welch's t-test comparisons of velocities as a function of stiffness for each cell line. (C,D) Rose plots of collective (C) and individual (D) cell migration pathways for the indicated cell lines on soft (top) and stiff (bottom) substrates over a 24 h period. n=4 for each plot. Plot size is 1 mm^2. (E) Average cell strain normalized to cell area for the indicated cell line. n=42 (Inv^L/E:N^H) or 17 (Inv^H/E:N^L) cells from triplicate experiments. fJ, femtojoules. (F) Average adhesion strength for the indicated cell lines exposed to shear stress that caused 50% of the population to detach, i.e. τ_{50}. n=9 for both groups. **P<0.01 for Welch's t-test.

surroundings, by using traction force microscopy (Munevar et al., 2001) and spinning disk assays (Fuhrmann et al., 2017), respectively. We found no difference between the contractile forces between these lines (Fig. 2E). However, we did observe lower adhesion strength for Inv^H/E:N^L cells relative to their Inv^L/E:N^H counterparts (Fig. 2F), consistent with previous reports that metastatic cell lines have lower adhesion strength (Fuhrmann et al., 2017). Together, these data suggest that the lower adhesion strength of Inv^H/E:N^L cells can produce labile adhesions primed to create faster migrating cells. Furthermore, our data further suggest two questions: (1) how stable is each population and (2) are focal adhesion differences driving this phenomenon?

Inv^L/E:N^H cells exhibit increased EMT and migration after prolonged exposure to a stiff niche

Although Inv^L/E:N^H cells were initially stiffness insensitive, we next asked whether they remain insensitive to stiffness and EMT when cultivated for a prolonged period of time in a stiff niche. After 5 days in a stiff niche, absolute mRNA expressions of five EMT transcription factors were generally higher in Inv^L/E:N^H cells. However, although higher, none were statistically similar to those in Inv^H/E:N^L cells, which appeared stiffness insensitive, albeit at significantly higher expression (Fig. 3A). In addition to marker expression, we assessed E-cad and N-cad protein expression after 5 days, finding that culturing Inv^L/E:N^H cells in a stiff niche for 5 days was sufficient to induce a 2.5-fold increase in N-cad expression, consistent with Twist-mediated activation of N-cadherin expression (Hao et al., 2012). Again, Inv^H/E:N^L cells expressed significant levels of N-cad but did not exhibit a trend with stiffness (Fig. 3B). Since EMT marker expression changed, we next

determined whether that change impacted cell migration. After cultivation for 5 days in a soft or stiff niche, Inv^L/E:N^H cells were re-plated onto either soft or stiff niches and migration velocity was analyzed (Fig. 4A). When challenged with combinations of soft and stiff, neither combination exhibited a significant change in migration. However, whereas all groups migrated faster when re-plated on stiff matrix, independently of mode of migration or initial stiffness conditions, single-cell migration for cells initially on stiff matrix was significantly faster compared to cells initially cultured on soft matrix (Fig. 4B). This behavior was not observed for collective migration, as the initial seeding conditions did not affect migration speed after re-plating on stiff gels. This is unlike other epithelial lineages that collectively migrate faster (Sunyer et al., 2016; Xi et al., 2017). Together these data suggest that Inv^L/E:N^H cells can be induced by stiffness, much like mammary epithelial cells (Wei et al., 2015), in order to begin to express EMT markers and exhibit behaviors consistent with a stable mesenchymal state. However, while mammary cells initially cultured on stiff matrix maintain their phenotype independent of their secondary matrix (Nasrollahi et al., 2017), Inv^L/E:N^H cells exhibited a dual phenotype: cells initially cultured on stiff and re-plated on soft matrix did not appear to exhibit memory, whereas those re-plated on stiff matrix did appear to be primed for migration. Furthermore, this behavior is only exhibited when cells migrate in a single, mesenchymal manner.

Adhesion of Inv^L/E:N^H cells is modulated by prolonged exposure to a stiff niche

To understand whether focal adhesion differences drive the gradual conversion of Inv^L/E:N^H cells from epithelial to mesenchymal behaviors, e.g. low to high migration, we assessed the extent to which
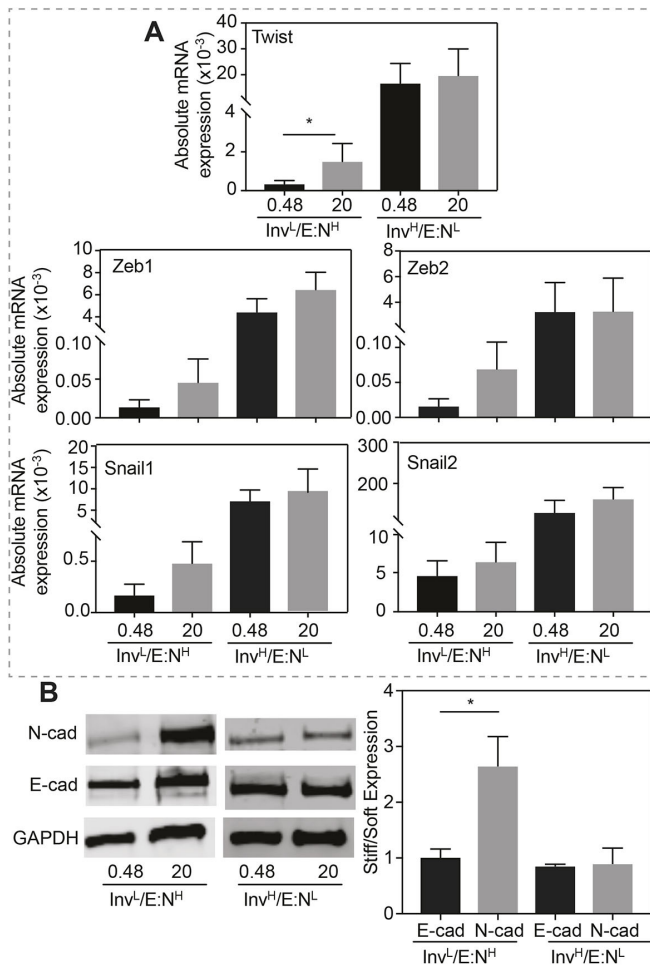
Fig. 3. Prolonged exposure to stiff substrates induces Inv^L/E:N^H cells to express EMT markers. (A) Absolute mRNA expression for the indicated transcription factors, normalized to GAPDH, is plotted for the indicated cells cultured on soft or stiff substrates. n=5, 5, 9 and 8 samples for each condition from triplicate experiments. *$P<0.05$ for Welch's t-test. (B) Western blots (left panel) and average expression ratio (in kPa, right panel) of N-cadherin, E-cadherin and GAPDH for the indicated cell lines. For each protein, the average expression ratio on stiff to soft substrate is plotted. n=4 for each protein. *$P<0.05$ for Welch's t-test relative to the other stiffness or cadherin.

the substrate can imprint on the focal adhesion assembly of a cell. As previously, Inv^L/E:N^H cells were cultured on soft or stiff substrates, replated, and focal adhesion assembly was assessed by paxillin staining on stiff substrates (Fig. 5A). Individual cells cultured initially on soft substrate – which migrate less than their counterparts continuously cultured on stiff substrate, had less adhesive areas

(Fig. 5B). These data suggest that, regarding oral carcinomas, larger adhesions can enable cells to migrate faster, which is unlike their mammary counterparts (Fuhrmann et al., 2017) perhaps due to faster single-cell migration (Fig. 4). To normalize substrate-induced adhesive differences in Inv^L/E:N^H cells (Fig. 2F), we cultured cells on continuously stiff and mixed stiffness substrates in high-cation
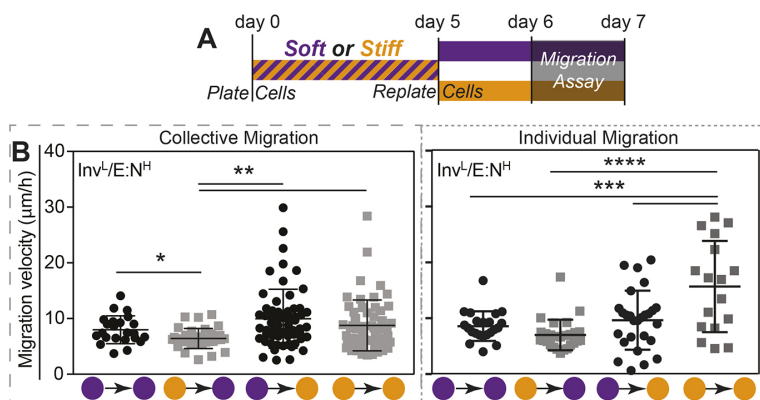
Fig. 4. Inv^L/E:N^H cells exhibit 'memory' after prolonged exposure to a stiff niche. (A) Schematic of experimental design for cell commitment and migration assay. (B) Collective (left) and individual (right) migration was monitored for Inv^L/E:N^H cells on soft–stiff substrate combinations as indicated (soft=purple; stiff=orange). All data were analyzed using one-way ANOVA with Tukey's multiple comparisons test with *$P<0.05$, **$P<0.01$. n=23, 35, 61 and 58 cells for collective migration, and n=22, 27, 27 and 17 cells for individual migration from triplicate experiments.
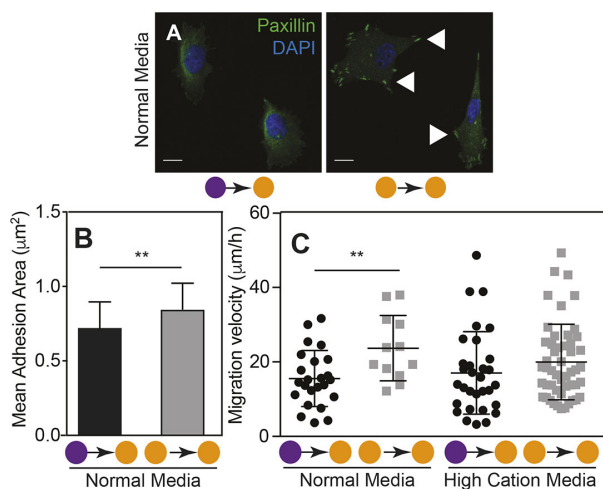
Fig. 5. Long-term conditioning in a stiff niche increases the adhesion area in Inv^L/E:N^H cells. (A) Images of Inv^L/E:N^H cells on soft-to-stiff substrate (left) and stiff-to-stiff substrate (right) stained for paxillin (green) and nuclei (blue). Arrowheads indicate assembled focal adhesions. Scale bars: 10 µm. (B) Plot of the mean adhesive area of Inv^L/E:N^H cells cultured in normal medium on soft-to-stiff or stiff-to-stiff substrate (n=39 or 51, respectively). **P<0.01 for Welch's t-test comparisons. (C) Individual cell migration velocity is plotted for cells as outlined in Fig. 4A. Each point represents the average velocity of an individual cell. Cells were cultured on soft-to-stiff or stiff-to-stiff substrate in normal or high-cation medium as indicated. n=24, 12, 31 and 50 cells for each condition. **P<0.01 for Welch's t-test comparisons of velocities as a function of stiffness for each line. Soft=purple; stiff=orange.

media (cell-specific DMEM plus 2.5 mM MgCl$_2$, see Materials and Methods), which has previously been shown to activate integrins and modulate adhesion independent of adhesion area (Fuhrmann et al., 2017); a high concentration of cations is also present in tumors relative to stroma (Seltzer et al., 1970, 1970). Whereas cells on continuously stiff substrate migrated faster in media containing normal cation levels (see Materials and Methods) compared with cells on mixed substrates (soft-to-stiff), high-cation media reduced migration differences for Inv^L/E:N^H cells on continuously stiff and mixed substrates (Fig. 5C). These data suggest that Inv^L/E:N^H cell migration after EMT requires larger but labile adhesions to adequately bind the stiffer ECM in the tumor and stroma.

Increasing collagen organization predicts poor outcome in OSCC patients

Collagen organization has previously been used as a surrogate for *in vivo* tumor rigidity (Wei et al., 2015) and correlates with poor outcome regarding a variety of tumors (Conklin et al., 2011; Hanley et al., 2016). Thus, we examined tumor sections of 29 OSCC patients (Table S1) by polarized PicroSirius Red staining to determine whether the margins that surrounded oral carcinomas had aligned collagen (Fig. 6A, arrowheads), which is indicative of stiffer tissue (Acerbi et al., 2015). We found that organized collagen surrounding tumor margins was associated with higher clinical TN stage (Fig. 6B), as well as more collagen present within OSCCs and tumor stroma (Fig. 6C). When using both tumor severity and collagen amount within the tumor to stratify patient outcomes, recurrence within the first 2-year period was most prevalent in patients having a higher TN stage, with organized and densely packed collagen surrounding tumor margins (Fig. 6D), and was below average patient outcomes (Liu et al., 2013). Concordant Inv^L/E:N^H cell behavior on stiff matrix that shows phenotype conversion and enhanced migration agree with these results, and demonstrate that large, mesenchymal-like tumors are supported by highly organized collagen that facilitates stromal invasion. Moreover when TN stage III/IV tumors are stained for intracellular proteins that would respond to more densely packed collagen, we found that an adhesion-associated protein, e.g. focal adhesion kinase (FAK), exhibited asymmetric distribution compared to stromal regions (Fig. 6E), which is also consistent with activated adhesive complexes that result in differential migration of tumor cells in culture (Fig. 5).

DISCUSSION

Cancer cells are exceedingly diverse within a tumor, having different phenotypes and, sometimes, even expressing different oncogenes (Navin et al., 2011; Greaves and Maley, 2012). As a consequence, subsets of cancer cells can be exceedingly influenced by the tumor microenvironment, inducing a change in phenotype and migration away from the primary mass. By contrast, stromal cells can be influenced by the tumor, i.e. cancerized, to help remodel the niche (Curtius et al., 2018). What results is a tumor-adjacent stroma composed of many new biological, chemical and physical signals (Quail and Joyce, 2013) that support metastasis. As we described earlier, this dynamic, reciprocal interaction has been well-studied *in vitro*, specifically for the influence that niche stiffness has on mammary (Levental et al., 2009; Wei et al., 2015; Paszek et al., 2005), ovarian (McKenzie et al., 2018), lung (Tilghman et al., 2010), prostate (Moazzem Hossain et al., 2014) and hepatocellular (Yangben et al., 2013) carcinomas but not for OSCCs. Our data demonstrated that cells comprising different levels of invasiveness respond differently to matrix stiffness. Whereas Inv^L/E:N^H cells remain surprisingly plastic, and able to increase migration and EMT marker expression gradually over time as directly by matrix stiffness, while their counterpart Inv^H/E:N^L cells appear more mesenchymal and adopt migratory phenotypes rapidly when the substrate permits. These observations are consistent with OSCC progression observed in patients, where advanced stages of disease have more organized collagen around keratin pearls, which can trigger a more-invasive phenotype and increased disease recurrence.

Tumor stiffness is correlated with increased EMT and invasion in breast cancer (Wei et al., 2015). As observed clinically for OSCC, lesions have a stiffened margin (Scully and Porter, 2001). Thus, we hypothesized that this exerts influence in cancer progression, although tumor stiffness was not explicitly measured from OSCC patient samples. Consistent with the concept that different tumor subset can exhibit different stiffness responses, we found that two OSCC cell lines comprising different E-cad expression – indicating that they are at different stages of EMT – were initially more (Inv^H/E:N^L) or less (Inv^L/E:N^H) migratory on a stiff 20 kPa substrate. Migration speed is inversely correlated to adhesion strength in mammary cancer cells (Fuhrmann et al., 2017) and, consistent with this, we found that the more migratory Inv^H/E:N^L cells also exhibited lower adhesion strength. Once chronically exposed to stiff

5
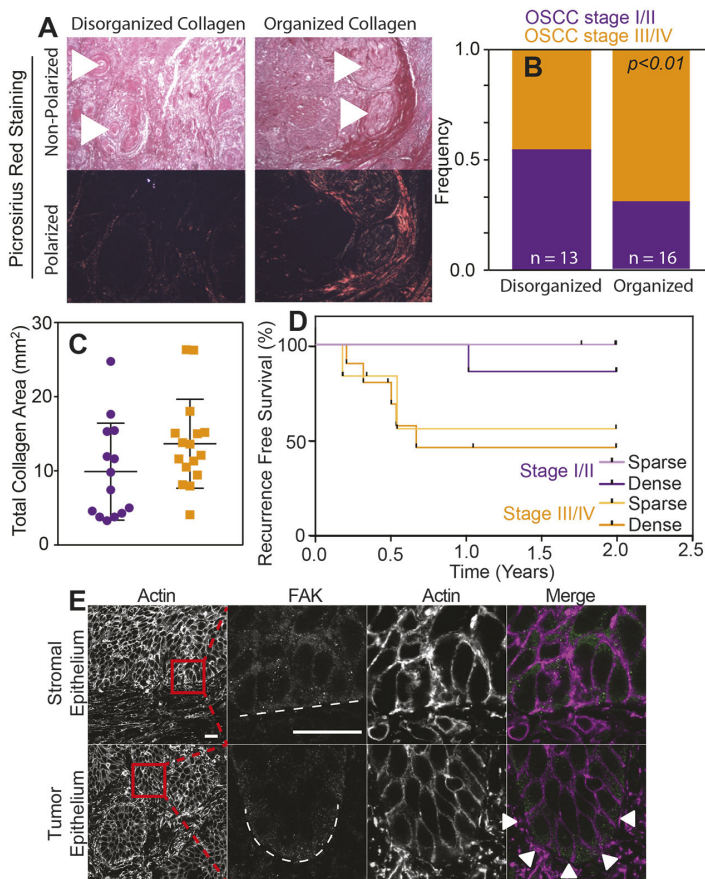
Fig. 6. Higher collagen organization of tumor correlates with poorer outcome for OSCC patients. (A) PicroSirius Red staining of histological sections of tumors with the indicated collagen organization. The same image was taken under polarized and non-polarized (brightfield) light (bottom and top images, respectively). Arrowheads indicate the location of selected keratin pearls. (B) Frequency of clinical TN stages I/II (purple) vs III/IV (orange) for OSCC relative to collagen organization within the tumor. Number of patients in each group were $n=13$ and $n=16$. $P<0.05$ for Welch's t-test comparing collagen organization and tumor stages. (C) Plotted collagen area of PicroSirius Red-stained tumor tissue of clinical TN stages I/II (purple) vs III/IV (orange) observed under polarized light. (D) Survival rate without tumor recurrence in percent of OSCC patients. Data of patients with tumors of the same TN stage but with above (dense) or below (sparse) average total collagen area were pooled. Kaplan–Meier plot of recurrence of recurrence-free survival for patients in the indicated categories on the basis of histological assessment. By using a log-rank (Mantel–Cox) test, $P<0.05$ was assessed and compared between dense stage III/IV and sparse stage I/II tumor tissue. $n=6, 7, 6$ and 10 for sparse stage I/II, dense stage I/II, sparse stage III/IV and dense stage III/IV tumor tissue, respectively. (E) Histological staining for actin and focal adhesion kinase (FAK) of representative stomal and OSCC tumor epithelium. The last three panels in each row show the magnification of the boxed area in the first panel. Dashed lines indicate the edge of each indicated feature; arrowheads indicate FAK polarization to the tumor edge. Scale bars: 20 µm.

substrates, $Inv^L/E{:}N^H$ cells did acquire a more-mesenchymal state, with increased EMT marker expression and migration speed but increased mean adhesion area (Fuhrmann et al., 2017). This is in contrast to invasive mammary cancer cells, which have smaller, labile adhesions relative to their non-malignant counterparts (Fuhrmann et al., 2017). Artificially enhancing integrin affinity reduced migration speed of stiffness-conditioned $Inv^L/E{:}N^H$ cells, suggesting that, despite their size, they can still be distributed in a manner labile enough to facilitate higher migration speed. Despite their trends regarding stiffness, these OSCC cell lines in particular exhibit smaller adhesions than other SCC cell lines (Hoshino et al., 2012) and metastatic mammary lines (Fuhrmann et al., 2017), which may still enable adhesion to be labile and migration to be effective. Intracellular connections to the molecular clutch and cytoskeleton proteins (Case and Waterman, 2015; Elosegui-Artola et al., 2018) might also be more dynamic in OSCC cells and help facilitate their invasion. Matrix stiffness can assemble (Levental et al., 2009; Paszek et al., 2005; Provenzano et al., 2009) and polarize them in stiff 3D matrix (Mekhdjian et al., 2017) so, even if $Inv^H/E{:}N^L$ cells assembled robust adhesions, they may be primed for migration based on their directionality. Interestingly, OSCC patients with a poor prognosis had an increase in FAK expression within the invasive front of tumors (Flores et al., 2018), further suggesting that polarity of the adhesive machinery and not just its amount in a cell contributes to tumor invasion. Thus, it would appear that tumor stiffness modulates EMT and prime cells

based on the environment and cell state to trigger an increase in migratory behavior.

Cancer invasion, similar to that of neoplastic cells, requires a reciprocal relationship between cells and ECM that helps to dictate whether cells adopt collective or individual migration modes (Friedl and Alexander, 2011), which each allows migration at varying speeds. In a niche that resembles a basement membrane, malignant epithelia grow collectively, without protrusions; but in stromal gels containing type I collagen, faster single-cell migration is preferred (Nguyen-Ngoc et al., 2012). We found that, whereas invasive OSCCs are faster compared with their non-invasive counterparts that were, initially, substrate insensitive, collective migration of $Inv^H/E{:}N^L$ cells was faster than single-cell migration. Epithelial sheets can efficiently use durotaxis (Sunyer et al., 2016; Xi et al., 2017), i.e. migration guided by rigidity gradients, but it would appear that for OSCC cells, a collective mode of migration is more effective, as they are more mesenchymal-like. A stiffer niche enhances nuclear translocation of YAP (Taubenberger et al., 2016) and signals (Calvo et al., 2013) that promote focal adhesion assembly (Nardone et al., 2017), but weaker $Inv^H/E{:}N^L$ cell-matrix adhesion might indicate that invasive OSCC cells migrate together and slower than cells of other tumors, whose preferred mode of migration is as single cells (Nguyen-Ngoc et al., 2012). However, unlike Nguyen-Ngoc and co-workers, we have only explored OSCC migration on type I collagen substrates, but ECM composition directly modulates migration (Ramos Gde al., 2016) and how processive cells can be (Montenegro et al., 2017). Thus, our

observation of faster collective migration could be limited by ECM ligand, which – although type I collagen is the dominant ligand in tumor-adjacent stroma (Pickup et al., 2014) – could nonetheless alter the ratio of cells that migrate individually compared with those migrating collectively.

Stiff tissue observed by collagen organization has already been associated with poor survival in breast, head and neck, esophageal, and colorectal cancer (Conklin et al., 2011; Hanley et al., 2016), so one possible means of assessing the impact of stiffness, migration mode and mechanism on oral carcinomas is to directly examine them. By using PicroSirius Red staining (Drifka et al., 2016), we found that collagen organization correlated with the advanced stages of disease and resulted in early recurrence of the disease. An important caveat about most *in vitro* systems, including ours, is that it lacks in supporting stromal cells, such as cancer-associated fibroblasts (CAFs). CAFs can modify tumor ECM by increased collagen deposition and alignment that, as a consequence, turns the niche into a stiffer microenvironment (Pankova et al., 2016). With CAFs being present in the indurated tumor margins and capable of remodeling the niche, we suggest that our model, in which $Inv^L/E:N^H$ cells are mechanically conditioned by their niche to undergo EMT and increase their migration, occurs in patients. While these patient observations will benefit from additional studies, it is safe to conclude that $Inv^L/E:N^H$ cells can be mechanically conditioned with a stiff matrix, and that this drives EMT, increases migratory velocity and affects focal adhesion assembly in a manner that, at least partially, reflects the advanced stages of OSCC lesions *in vivo*.

MATERIALS AND METHODS

Cell culture
OSCC cell lines were a kind gift from Akihiro Sakai, University of California San Diego (UCSD). Mycoplasma testing was performed at the UCSD Stem Cell Core Facility using PCR in November 2017. Cal-27 cells were cultivated in DMEM high glucose (Gibco) supplemented with 10% fetal bovine serum (FBS) (Gemni Bio) and 1% penicillin/streptomycin (Gibco); FaDu, SCC-9 and SCC-25 cells were maintained in DMEM/F12 with 15 mM HEPES (Teknova) supplemented with 10% FBS, 1% penicillin/streptomycin, and 400 ng/ml of hydrocortisone (Sigma). Cells were maintained in incubator at 37°C with 5% CO_2. For cell culture in high-cation medium, 2.5 mM of $MgCl_2$ was added to the above-described media.

Real-time PCR
RNA was extracted from cells using Trizol and total RNA quantity and quality was checked using absorbance (A280/A260). cDNA was generated by adding random hexamer primers and Super Script III reverse transcriptase (Thermo) to 2 µg of RNA. Quantitative PCR was performed (45 cycles, 95°C for 15 s followed by 60°C for 1 min) using a 7900HT Fast Real-Time PCR System (Thermo) with the primer sets described below and SYBR Green Supermix (Bio-Rad Laboratories). All quantification cycle (Cq) values were normalized to GAPDH and a fibronectin standard was used to analyze absolute RNA expression. Experiments were performed in biological and technical triplicates using the CFX Connect (Bio-Rad) real-time PCR detection system. Human primer sequences were used as follows: *Twist1* (5′-TGCATGCATTCTCAAGAGGT-3′, 5′-CTATGGTTTTGCA-GGCCAGT-3′), *Snail1* (5′-CTAGCGAGTGGTTCTTCTG-3′, 5′-CTGC-TGGAAGGTAAACCTCTG-3′), *Snail2* (5′-ATGAGGAATCTGGCTGC-TGT-3′, 5′-CAGGAGAAAATGCCTTTGGA-3′), *Zeb1* (5′-GCCAATAA-GCAAACGATTCTG-3′, 5′-CTTGTCTTTCATCCTGATTTCC-3′), *Zeb2* (5′-CAGTCCAGACCAGTATTCCT-3′, 5′-GCAATTCTCCCTGAAAT-CCT-3′), *GAPDH* (5′-TCGACAGTCAGCCGCATCTTC-3′, 5′-ACCA-AATCCGTTGACTCCGAC-3′).

Western blotting
Cells were lysed using RIPA buffer (50 mM HEPES, 150 mM NaCl, 1.5 mM $MgCl_2$, 1 mM EDTA, 1% Triton, 10% glycerol, 25 mM sodium deoxycholate, 0.1% SDS) supplemented with Roche Complete Protease Inhibitor (Sigma) and PhosSTOP (Sigma). Total protein was quantified with Pierce BCA Protein Assay Kit (Thermo Fisher Scientific). Cell lysates (20 µg) were loaded and separated in 4-12% Bis-Tris Gels and MES running buffer (50 mM MES, 50 mM Tris base, 1 mM EDTA, 0.1% w/v SDS). Proteins were transferred to nitrocellulose membranes using the iBlot semi-dry transfer system (Invitrogen). Membranes were blocked with 5% Sea Block blocking buffer (Thermo Fisher Scientific) in Tris-buffered saline with Tween (TBS-T, 150 mM NaCl, 15 mM Tris-HCl, 20 mM Tris base, 0.1% Tween) for 1 h. Membranes were then immunoassayed for E-cadherin (1:1000, Cell Signaling, 24E10), N-cadherin (1:1000, Abcam, ab76011) and GAPDH (1:7500, Abcam, ab8245) overnight at 4°C. After washing three times for 5 min in TBS-T, membranes were incubated with Alexa Fluor 680 donkey anti-mouse (1:10,000, Invitrogen, A10038) and Alexa Fluor 790 donkey anti-rabbit (1:10,000, Invitrogen, A11374) for 2 h. Membranes were washed three times for 5 min in TBS-T before imaging. Images were acquired using the LI-COR Odyssey CLx imaging system detection system and Image Studio Lite was used to analyze and quantify the bands. Values for each protein were normalized to the loading control.

Fabrication of polyacrylamide hydrogels
Polyacrylamide hydrogels (PAAGs) were made on No. 1 12 mm and 25 mm glass coverslips that had been methacrylated by first oxidizing the surface through UV/ozone exposure (BioForce Nanosciences) followed by functionalization with 20 mM 3-(trimethoxysilyl)propyl methacrylate (Sigma-Aldrich, cat # 440159) in ethanol. A polymer solution containing either 3%/0.06% acrylamide/bis-acrylamide (Fisher) for 0.48 kPa hydrogels or 8%/0.264% for 20 kPa hydrogels, 1% v/v of 10% ammonium persulfate (Fisher), and 0.1% v/v of N,N,N′,N′-tetramethylethylenediamine (VWR) was prepared. 15 µl for 12 mm coverslips and 30 µl for 25 mm coverslips of hydrogel solution was sandwiched between a functionalized coverslip and a dichlorodimethylsilane-treated glass slide and polymerized for 15 min. Hydrogels were incubated in 0.2 mg/ml sulfo-SANPAH (Fisher, cat # 22589) in sterile 50 mM HEPES pH 8.5, activated with UV light (wavelength 350 nm, intensity 4 mW/cm^2) for 10 min, washed three times in HEPES, and then incubated in 150 µg/ml collagen solution (Corning) overnight at 37°C.

Migration assay
OSCC cells were plated on either 0.48 or 20 kPa PAAGs for 12 h and were then imaged with a Nikon Eclipse Ti-S microscope equipped with a motorized temperature- and CO_2-controlled stage. Cells were imaged at 10× in brightfield at multiple positions every 15 min for 20 h. For long-term conditioning in a soft or stiff niche, cells were cultivated for 5 days in either soft or stiff PAAGs, then trypsinized and plated onto soft and stiff hydrogel to analyze migration as mentioned. For experiments using high-cation medium, 2.5 mM of magnesium chloride was added before image acquisition. For analysis of migration parameters, the nucleus of each migratory cell was used as a reference point to track each cell with the 'Manual Tracking' plugin on ImageJ. Migration was considered to be in single-cell mode when a cell did not touch any other cell during its migration movement. Migration was considered to be in collective-cell mode when cells migrated in a group of two or more cells.

Traction force microscopy
Traction force microscopy was performed as previously described (Holle et al., 2013). Briefly, polyacrylamide hydrogels (2 kPa, 4%/0.1% acrylamide/bis-acrylamide) were fabricated as described above but with the addition of 2% v/v 568/605 fluorescent 0.2 µm FluoSpheres (ThermoFisher) to the polymer solution. This stiffness was selected due to its optimal deformability resulting in improved resolution of traction forces (Holle et al., 2013). After coating with collagen type I as described above, cells were plated and allowed to attach overnight at 37C and 5% CO_2. Images were obtained of single cells followed by the microspheres underneath them with a 60× water immersion objective using a Nikon Eclipse TI-S microscope equipped with a CARV II confocal system (BD Biosciences), motorized stages with a Cool-Snap HQ camera (Photometrics) controlled by Metamorph (Molecular Devices). Cells were

released with 10% Triton X-100 and the same microsphere positions were acquired. Bead displacements were determined by using a particle image velocimetry script in MATLAB (The MathWorks, Natick, MA) and normalized to the cell area − codes will be provided by the corresponding author upon request.

Cell-adhesion strength assay

Glass coverslips (25 mm, Fisher Scientific, St Louis, MO) were sonicated in ethanol and pure water before incubation with 5 mg/cm^2 collagen type I (rat-tail, Corning) for 60 min at room temperature. Cells were allowed to attach for 24 h at 37°C and 5% CO$_2$ in media containing high-cation levels. Coverslips were then mounted on a custom-built spinning-disk device and dipped into temperature-controlled spinning buffer (37°C). The spinning buffer was phosphate-buffered saline [PBS; without Mg^{2+} and Ca^{2+} (Cellgro, Manassas, VA)] supplemented with 4.5 mg/ml dextrose. Once immersed in spinning buffer, coverslips were spun for 5 min at defined angular velocities; cells were fixed with 3.7% formaldehyde immediately after spinning. Quantification of adhesion strength was used according to previous publications (Fuhrmann et al., 2017; Fuhrmann and Engler, 2015). Briefly, coverslips were stained with Hoechst 33342 (Invitrogen, H3570) and imaged at 10× magnification on a Nikon (Melville, NY) Ti-S microscope (∼1000 individual images stitched together with Metamorph 7.6 software and custom macros) and analyzed using a custom-written MATLAB (The MathWorks, Natick, MA) program. Cell densities, as a function of radial position and, subsequently, shear, were stored and combined with other measurements, e.g. those obtained at different RPMs. A sigmoidal decay fit was used to quantify adhesion strength – codes will be provided by the corresponding author upon request.

Immunofluorescence

OSCC cells were directly fixed on the PAAGs (4% paraformaldehyde, 15 min, RT), washed with PBS, permeabilized (0.1% Tween-20, 20 min, RT) and blocked (10% goat serum, 1% BSA, 0.1% Tween-20 and 0.3 M glycine, 30 min, RT). Paxillin (1:250, Abcam, ab32084) primary antibody was incubated overnight at 4°C, washed 3× with blocking buffer, and incubated with Alexa Fluor 488 goat anti-rabbit secondary antibody for 2 h at room temperature (1:500, Invitrogen, A11008). Finally, nuclei were stained with Hoechst 33342 for 15 min at room temperature (1:7500, Invitrogen, H3570), washed with PBS and distilled water. Coverslips were mounted on slides with Fluormount-G (SouthernBiotech) and sealed on the edges using nail polish. Images were obtained by using a LSM780 confocal microscope with a 63× objective and Zeiss software. Images were analyzed using ImageJ analysis software.

OSCC organotypic culture

Rat-tail-derived collagen type I (Corning) was used to produce a 3D matrix with a final concentration of 1.8 mg/ml according to the manufacturer's instructions. Briefly, rat-tail collagen type I was added on ice to 10× DMEM and the pH adjusted with 0.1 M NaOH to 7. 1×10^5 primary fibroblasts were embedded in the matrix, as approved by the Ethical Committee of UFRGS (CAE#59124916.6.0000.5327). On top of the matrix, 5×10^5 of OSCC cells were added. Once cells had reached confluence, the matrix was lifted to create an air–liquid interface. The system was cultivated for 21 days, formalin fixed and paraffin embedded, and then sectioned. Sections were deparafinized and re-hydrated, followed by staining with hematoxylin and eosin. Pictures were taken with an Olympus CX41 microscope coupled to a QColor 5 digital camera (Olympus) at 20× magnification and invasion depth was analyzed using ImageJ software.

Tumors and PicroSirius Red staining

Tumor cells of 29 patients (Table S1) were included in this study, as approved by the Institutional Review Board of the Irmandade da Santa Casa de Misericórdia de Porto Alegre (ISCMPA) under protocol 2.324.217. All patient samples were obtained from the ISCMPA tissue bank and only de-identified patient samples were used. For each sample, only biometric patient information was obtained to create the Kaplan–Meier plot. Formalin-fixed and paraffin embedded 5-μm sections were deparafinized, re-hydrated and followed by staining with PicroSirius Red staining according to

manufacturer's protocol (EasyPath). Polarized microscope (BEL photonics) coupled with a camera device (Bioptika) was used at 4× magnification to acquire images. Per patient sample, ten fields were acquired. The scoring rubric (which was defined prior to blind scoring) was defined as 'organized collagen' in tumors comprising prominent linearized collagens fibers in the margins of the tumors, or as 'disorganized collagen' in tumors comprising either short collagen fibers of a high degree of circularity or low/no PicroSirius Red staining. The total collagen area (mm^2) was measured in the polarized images using ImageJ software.

Statistical analysis

All experiments were performed with at least three biological replicates, *n* indicates the number of technical replicates. Bar graphs represent the mean+ standard deviation (+s.d.). Box and whisker graphs represent the median and extend to the 25% and 75% quartiles. Sample size was determined on the basis of previously published studies in which similar assays were performed (Pickup et al., 2014). We did not exclude any data. No degree of randomization or blind scoring was performed. Statistical differences among two groups were tested using two-tailed Welch's *t*-test, and differences amongst more than two groups were analyzed with one-way analysis of variance (ANOVA) test followed by Tukey's multiple comparison test. To compare survival distributions of two-patient populations, a log-rank (Mantel-Cox) test was used. Statistical analyses were performed using Graphpad Prism software, with the threshold for significance level set at $P<0.05$.

References

Acerbi, I., Cassereau, L., Dean, I., Shi, Q., Au, A., Park, C., Chen, Y. Y., Liphardt, J., Hwang, E. S. and Weaver, V. M. (2015). Human breast cancer invasion and aggression correlates with ECM stiffening and immune cell infiltration. *Integr. Biol.* **7**, 1120-1134.

Angadi, P. V., Patil, P. V., Angadi, V., Mane, D., Shekar, S., Hallikerimath, S., Kale, A. D. and Kardesai, S. G. (2016). Immunoexpression of epithelial mesenchymal transition proteins E-cadherin, β-catenin, and N-cadherin in oral squamous cell carcinoma. *Int. J. Surg. Pathol.* **24**, 696-703.

Bissell, M. J. and Hines, W. C. (2011). Why don't we get more cancer? A proposed role of the microenvironment in restraining cancer progression. *Nat. Med.* **17**, 320-329.

Brown, E. C., Cheng, S., McKenzie, D. K., Butler, J. E., Gandevia, S. C. and Bilston, L. E. (2015). Tongue stiffness is lower in patients with obstructive sleep

apnea during wakefulness compared with matched control subjects. *Sleep* **38**, 537-544.

Calvo, F., Ege, N., Grande-Garcia, A., Hooper, S., Jenkins, R. P., Chaudhry, S. I., Harrington, K., Williamson, P., Moeendarbary, E., Charras, G. et al. (2013). Mechanotransduction and YAP-dependent matrix remodelling is required for the generation and maintenance of cancer-associated fibroblasts. *Nat. Cell Biol.* **15**, 637-646.

Case, L. B. and Waterman, C. M. (2015). Integration of actin dynamics and cell adhesion by a three-dimensional, mechanosensitive molecular clutch. *Nat. Cell Biol.* **17**, 955-963.

Cheng, S., Gandevia, S. C., Green, M., Sinkus, R. and Bilston, L. E. (2011). Viscoelastic properties of the tongue and soft palate using MR elastography. *J. Biomech.* **44**, 450-454.

Colley, H. E., Hearnden, V., Jones, A. V., Weinreb, P. H., Violette, S. M., MacNeil, S., Thornhill, M. H. and Murdoch, C. (2011). Development of tissue-engineered models of oral dysplasia and early invasive oral squamous cell carcinoma. *Br. J. Cancer* **105**, 1582-1592.

Conklin, M. W., Eickhoff, J. C., Riching, K. M., Pehlke, C. A., Eliceiri, K. W., Provenzano, P. P., Friedl, A. and Keely, P. J. (2011). Aligned collagen is a prognostic signature for survival in human breast carcinoma. *Am. J. Pathol.* **178**, 1221-1232.

Curtius, K., Wright, N. A. and Graham, T. A. (2018). An evolutionary perspective on field cancerization. *Nat. Rev. Cancer* **18**, 19-32.

Drifka, C. R., Loeffler, A. G., Mathewson, K., Mehta, G., Keikhosravi, A., Liu, Y., Lemancik, S., Ricke, W. A., Weber, S. M., Kao, W. J. et al. (2016). Comparison of picrosirius red staining with second harmonic generation imaging for the quantification of clinically relevant collagen fiber features in histopathology samples. *J. Histochem. Cytochem.* **64**, 519-529.

Elosegui-Artola, A., Trepat, X. and Roca-Cusachs, P. (2018). Control of mechanotransduction by molecular clutch dynamics. *Trends Cell Biol.* **28**, 356-367.

Engler, A. J., Griffin, M. A., Sen, S., Bonnemann, C. G., Sweeney, H. L. and Discher, D. E. (2004). Myotubes differentiate optimally on substrates with tissue-like stiffness: pathological implications for soft or stiff microenvironments. *J. Cell Biol.* **166**, 877-887.

Fan, C. C., Wang, T. Y., Cheng, Y. A., Jiang, S. S., Cheng, C.-W., Lee, A. Y.-L. and Kao, T.-Y. (2013). Expression of E-cadherin, Twist, and p53 and their prognostic value in patients with oral squamous cell carcinoma. *J. Cancer Res. Clin. Oncol.* **139**, 1735-1744.

Flores, A. P. C., Dias, K. B., Hildebrand, L. C., Oliveira, M. G., Lamers, M. L. and Sant'ana Filho, M. (2018). Focal adhesion kinases in head and neck squamous cell carcinoma. *J. Oral Pathol. Med.* **47**, 246-252.

Friedl, P. and Alexander, S. (2011). Cancer invasion and the microenvironment: plasticity and reciprocity. *Cell* **147**, 992-1009.

Fuhrmann, A. and Engler, A. J. (2015). The cytoskeleton regulates cell attachment strength. *Biophys. J.* **109**, 57-65.

Fuhrmann, A., Banisadr, A., Beri, P., Tlsty, T. D. and Engler, A. J. (2017). Metastatic state of cancer cells may be indicated by adhesion strength. *Biophys. J.* **112**, 736-745.

Greaves, M. and Maley, C. C. (2012). Clonal evolution in cancer. *Nature* **481**, 306-313.

Hanahan, D. and Coussens, L. M. (2012). Accessories to the crime: functions of cells recruited to the tumor microenvironment. *Cancer Cell.* **21**, 309-322.

Hanley, C. J., Noble, F., Ward, M., Bullock, M., Drifka, C., Mellone, M., Manousopoulou, A., Johnston, H. E., Hayden, A., Thirdborough, S. et al. (2016). A subset of myofibroblastic cancer-associated fibroblasts regulate collagen fiber elongation, which is prognostic in multiple cancers. *Oncotarget* **7**, 6159-6174.

Hao, L., Ha, J. R., Kuzel, P., Garcia, E. and Persad, S. (2012). Cadherin switch from E- to N-cadherin in melanoma progression is regulated by the PI3K/PTEN pathway through Twist and Snail. *Br. J. Dermatol.* **166**, 1184-1197.

Holle, A. W. and Engler, A. J. (2011). More than a feeling: discovering, understanding, and influencing mechanosensing pathways. *Curr. Opin. Biotechnol.* **22**, 648-654.

Holle, A. W., Tang, X., Vijayraghavan, D., Vincent, L. G., Fuhrmann, A., Choi, Y. S., Del Álamo, J. C. and Engler, A. J. (2013). In situ mechanotransduction via vinculin regulates stem cell differentiation. *Stem Cells* **31**, 2467-2477.

Hoshino, D., Jourquin, J., Emmons, S. W., Miller, T., Goldgof, M., Costello, K., Tyson, D. R., Brown, B., Lu, Y., Prasad, N. K. et al. (2012). Network analysis of the focal adhesion to invadopodia transition identifies a PI3K-PKCα invasive signaling axis. *Sci. Signal.* **5**, ra66.

Kong, Y. H., Syed Zanaruddin, S. N., Lau, S. H., Ramanathan, A., Kallarakkal, T. G., Vincent-Chong, V. K., Wan Mustafa, W. M., Abraham, M. T., Abdul Rahman, Z. A., Zain, R. B. et al. (2015). Co-expression of TWIST1 and ZEB2 in oral squamous cell carcinoma is associated with poor survival. *PLoS ONE* **10**, e0134045.

Lamouille, S., Xu, J. and Derynck, R. (2014). Molecular mechanisms of epithelial-mesenchymal transition. *Nat. Rev. Mol. Cell Biol.* **15**, 178-196.

Leemans, C. R., Snijders, P. J. F. and Brakenhoff, R. H. (2018). The molecular landscape of head and neck cancer. *Nat. Rev. Cancer* **18**, 269-282.

Levental, K. R., Yu, H. M., Kass, L., Lakins, J. N., Egeblad, M., Erler, J. T., Fong, S. F. T., Csiszar, K., Giaccia, A., Weninger, W. et al. (2009). Matrix crosslinking forces tumor progression by enhancing integrin signaling. *Cell* **139**, 891-906.

Lintz, M., Muñoz, A. and Reinhart-King, C. A. (2017). The mechanics of single cell and collective migration of tumor cells. *J. Biomech. Eng.* **139**.

Liu, C.-H., Chen, H.-J., Wang, P.-C., Chen, H.-S. and Chang, Y.-L. (2013). Patterns of recurrence and second primary tumors in oral squamous cell carcinoma treated with surgery alone. *Kaohsiung J. Med. Sci.* **29**, 554-559.

Lydiatt, W. M., Patel, S. G., O'sullivan, B., Brandwein, M. S., Ridge, J. A., Migliacci, J. C., Loomis, A. M. and Shah, J. P. (2017). Head and Neck cancers-major changes in the American Joint Committee on cancer eighth edition cancer staging manual. *CA Cancer J. Clin.* **67**, 122-137.

Markopoulos, A. K. (2012). Current aspects on oral squamous cell carcinoma. *Open Dent. J.* **6**, 126-130.

Mckenzie, A. J., Hicks, S. R., Svec, K. V., Naughton, H., Edmunds, Z. L. and Howe, A. K. (2018). The mechanical microenvironment regulates ovarian cancer cell morphology, migration, and spheroid disaggregation. *Sci. Rep.* **8**, 7228.

Mekhdjian, A. H., Kai, F., Rubashkin, M. G., Prahl, L. S., Przybyla, L. M., Mcgregor, A. L., Bell, E. S., Barnes, J. M., Dufort, C. C., Ou, G. et al. (2017). Integrin-mediated traction force enhances paxillin molecular associations and adhesion dynamics that increase the invasiveness of tumor cells into a three-dimensional extracellular matrix. *Mol. Biol. Cell* **28**, 1467-1488.

Moazzem Hossain, M., Wang, X., Bergan, R. C. and Jin, J.-P. (2014). Diminished expression of h2-calponin in prostate cancer cells promotes cell proliferation, migration and the dependence of cell adhesion on substrate stiffness. *FEBS Open Biol.* **4**, 627-636.

Montenegro, C. F., Casali, B. C., Lino, R. L. B., Pachane, B. C., Santos, P. K., Horwitz, A. R., Selistre-De-Araujo, H. S. and Lamers, M. L. (2017). Inhibition of αvβ3 integrin induces loss of cell directionality of oral squamous carcinoma cells (OSCC). *PLoS ONE* **12**, e0176226.

Munevar, S., Wang, Y.-L. and Dembo, M. (2001). Traction force microscopy of migrating normal and H-ras transformed 3T3 fibroblasts. *Biophys. J.* **80**, 1744-1757.

Nardone, G., Oliver-De La Cruz, J., Vrbsky, J., Martini, C., Pribyl, J., Skládal, P., Pešl, M., Caluori, G., Pagliari, S., Martino, F. et al. (2017). YAP regulates cell mechanics by controlling focal adhesion assembly. *Nat. Commun.* **8**, 15321.

Nasrollahi, S., Walter, C., Loza, A. J., Schimizzi, G. V., Longmore, G. D. and Pathak, A. (2017). Past matrix stiffness primes epithelial cells and regulates their future collective migration through a mechanical memory. *Biomaterials* **146**, 146-155.

Navin, N., Kendall, J., Troge, J., Andrews, P., Rodgers, L., Mcindoo, J., Cook, K., Stepansky, A., Levy, D., Esposito, D. et al. (2011). Tumour evolution inferred by single-cell sequencing. *Nature* **472**, 90-94.

Nguyen-Ngoc, K.-V., Cheung, K. J., Brenot, A., Shamir, E. R., Gray, R. S., Hines, W. C., Yaswen, P., Werb, Z. and Ewald, A. J. (2012). ECM microenvironment regulates collective migration and local dissemination in normal and malignant mammary epithelium. *Proc. Natl. Acad. Sci. USA* **109**, E2595-E2604.

Nieto, M. A., Huang, R. Y.-J., Jackson, R. A. and Thiery, J. P. (2016). EMT: 2016. *Cell* **166**, 21-45.

Pankova, D., Chen, Y., Terajima, M., Schliekelman, M. J., Baird, B. N., Fahrenholtz, M., Sun, L., Gill, B. J., Vadakkan, T. J., Kim, M. P. et al. (2016). Cancer-associated fibroblasts induce a collagen cross-link switch in tumor stroma. *Mol. Cancer Res.* **14**, 287-295.

Paszek, M. J., Zahir, N., Johnson, K. R., Lakins, J. N., Rozenberg, G. I., Gefen, A., Reinhart-King, C. A., Margulies, S. S., Dembo, M., Boettiger, D. et al. (2005). Tensional homeostasis and the malignant phenotype. *Cancer Cell.* **8**, 241-254.

Pickup, M. W., Mouw, J. K. and Weaver, V. M. (2014). The extracellular matrix modulates the hallmarks of cancer. *EMBO Rep.* **15**, 1243-1253.

Provenzano, P. P., Inman, D. R., Eliceiri, K. W. and Keely, P. J. (2009). Matrix density-induced mechanoregulation of breast cell phenotype, signaling and gene expression through a FAK-ERK linkage. *Oncogene* **28**, 4326-4343.

Quail, D. F. and Joyce, J. A. (2013). Microenvironmental regulation of tumor progression and metastasis. *Nat. Med.* **19**, 1423-1437.

Ramos Gde, O., Bernardi, L., Lauxen, I., Sant'ana Filho, M., Horwitz, A. R. and Lamers, M. L. (2016). Fibronectin modulates cell adhesion and signaling to promote single cell migration of highly invasive oral squamous cell carcinoma. *PLoS ONE* **11**, e0151338.

Scully, C. and Porter, S. (2001). Oral cancer. *West J. Med.* **174**, 348-351.

Seltzer, M. H., Rosato, F. E. and Fletcher, M. J. (1970). Serum and tissue calcium in human breast carcinoma. *Cancer Res.* **30**, 615-616.

Smith, A., Teknos, T. N. and Pan, Q. (2013). Epithelial to mesenchymal transition in head and neck squamous cell carcinoma. *Oral Oncol.* **49**, 287-292.

Sunyer, R., Conte, V., Escribano, J., Elosegui-Artola, A., Labernadie, A., Valon, L., Navajas, D., Garcia-Aznar, J. M., Munoz, J. J., Roca-Cusachs, P. et al. (2016). Collective cell durotaxis emerges from long-range intercellular force transmission. *Science* **353**, 1157-1161.

Taubenberger, A. V., Bray, L. J., Haller, B., Shaposhnykov, A., Binner, M., Freudenberg, U., Guck, J. and Werner, C. (2016). 3D extracellular matrix

interactions modulate tumour cell growth, invasion and angiogenesis in engineered tumour microenvironments. *Acta Biomater.* **36**, 73-85.

Tilghman, R. W., Cowan, C. R., Mih, J. D., Koryakina, Y., Gioeli, D., Slack-Davis, J. K., Blackman, B. R., Tschumperlin, D. J. and Parsons, J. T. (2010). Matrix rigidity regulates cancer cell growth and cellular phenotype. *PLoS ONE* **5**, e12905.

Wei, S. C., Fattet, L., Tsai, J. H., Guo, Y., Pai, V. H., Majeski, H. E., Chen, A. C., Sah, R. L., Taylor, S. S., Engler, A. J. et al. (2015). Matrix stiffness drives epithelial mesenchymal transition and tumour metastasis through a TWIST1-G3BP2 mechanotransduction pathway. *Nat. Cell Biol.* **17**, U678-U306.

Xi, W., Sonam, S., Beng Saw, T., Ladoux, B. and Teck Lim, C. (2017). Emergent patterns of collective cell migration under tubular confinement. *Nat. Commun.* **8**, 1517.

Yangben, Y., Wang, H., Zhong, L., Chiang, M. Y., Tan, Q., Singh, G. K., Li, S., Yang, L. et al. (2013). Relative rigidity of cell-substrate effects on hepatic and hepatocellular carcinoma cell migration. *J. Biomater. Sci. Polym. Ed.* **24**, 148-157.

Yao, X., Sun, S., Zhou, X., Zhang, Q., Guo, W. and Zhang, L. (2017). Clinicopathological significance of ZEB-1 and E-cadherin proteins in patients with oral cavity squamous cell carcinoma. *Onco Targets Ther.* **10**, 781-790.
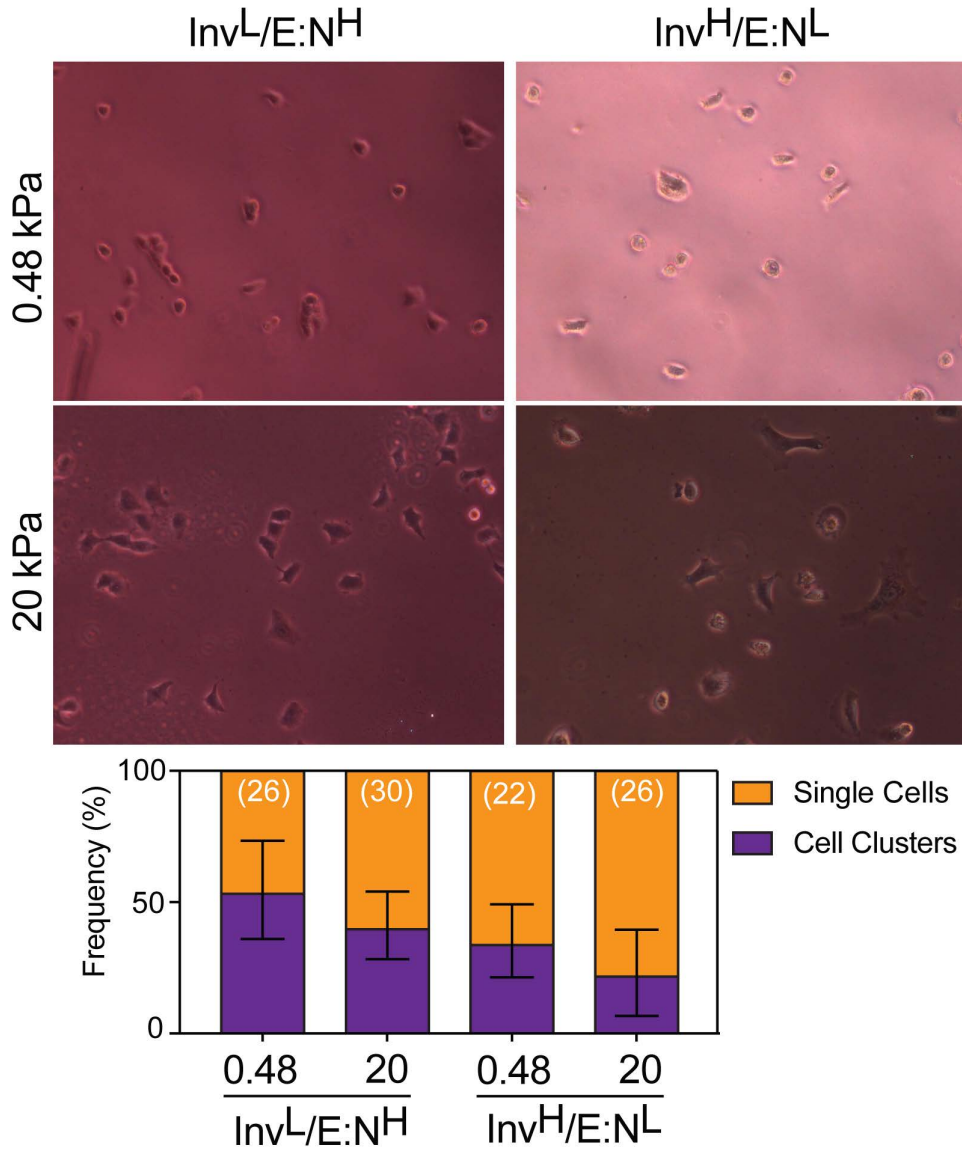
Figure S1. Inv^L/E:N^H cells preferentially exhibit collective, epithelial migration compared to Inv^H/E:N^L, especially on soft substrates. (top) Brightfield microscopy demonstrating cell morphology for Inv^L/E:N^H and Inv^H/E:N^L cells after being cultured on soft and stiff substrates for two days. (bottom) Plot indicates the frequency of single cell or clustered migration. Numbers in parentheses indicate the number of cells in each analysis.
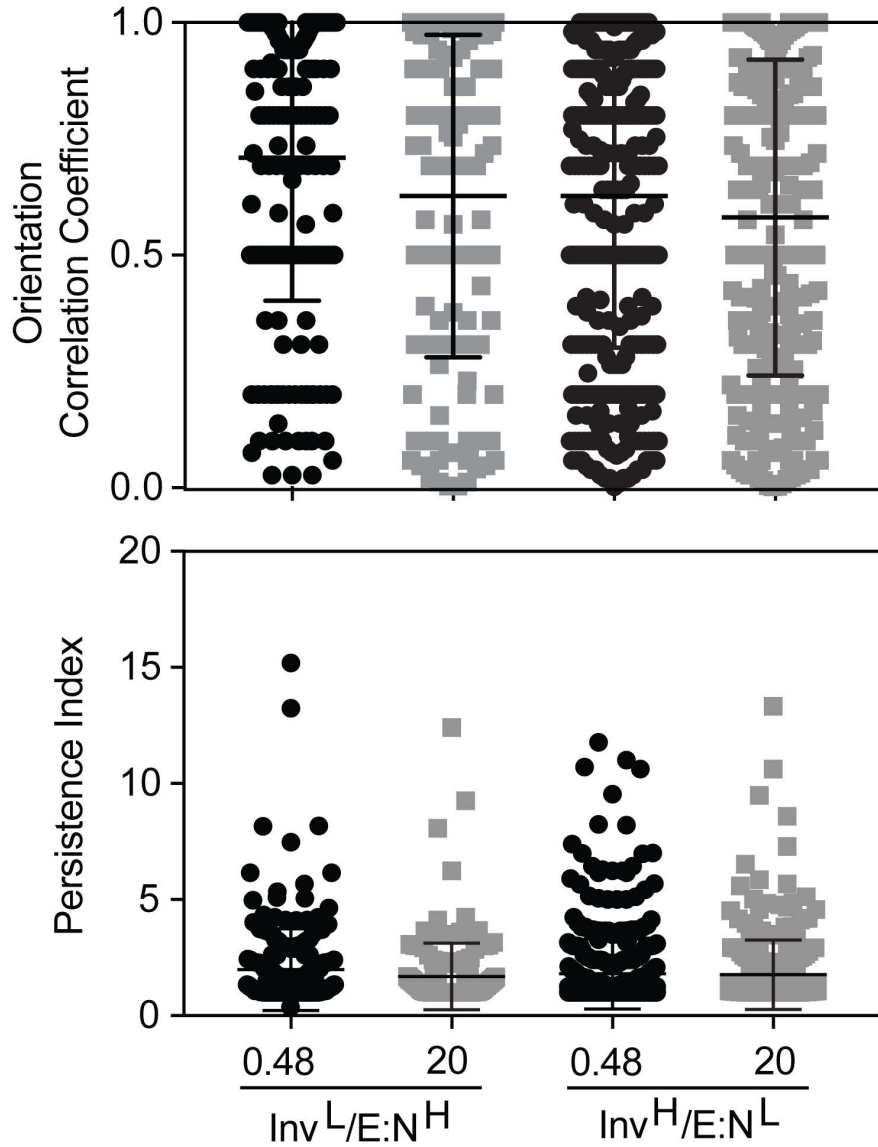
Figure S2. Migration Analyses. (top) Orientation correlation coefficient, i.e. 0.5*(cos (2θ) +1), is plotted for Inv^L/E:N^H and Inv^H/E:N^L single cells migrating on the indicated substrates using a time step of 1 hour between cell vectors. n = 207, 135, 442, and 284 for each group (left to right) counting individual angles over triplicate experiments. (bottom) Plot indicates migration persistence via a ratio of total migration path length divided by total displacement. Data is shown for Inv^L/E:N^H and Inv^H/E:N^L single cells migrating on the indicated substrates. n = 207, 135, 442, and 284 paths analyzed for each group.

Table S1: Patient Demographic Information

Patient data is shown for all tumors examined in Figure 6. Dates are shown in the MM/DD/YY format. Note that patient data was retrieved on 08/01/18. Cancer stage is classified according to the Eight Edition Cancer Staging Manual of the American Joint Committee on Cancer. Cancer stage is classified according to clinical and pathologic characteristics of the tumor (T) and lymph nodes metastasis (N)[61]. The first number corresponds to the tumor stage and second to the lymph node. Note that for the latter number, zero denotes no metastases detected in the node.

Patient ID	Sex	Date of birth	Tumor Resection Date	Tumor Recurrence or End of Clinical Records Date	Cancer Stage
A601746	F	7/4/34	01/09/12	04/05/18	T2N0
A608766	F	6/24/26	03/06/12	12/12/13	T2N0
A609290	M	8/19/65	03/09/12	03/15/13	T2N0
A611141	F	1/28/28	03/23/12	07/24/12	T3N2b
A615386	M	6/24/71	04/25/12	10/25/12	T3N0
A621413	F	6/21/48	06/09/12	08/01/18	T2N0
A623667	F	3/9/44	06/26/12	02/15/18	T3N0
A625701	F	8/25/51	07/10/12	08/04/15	T1N0
A629186	F	4/6/47	08/03/12	07/20/18	T2N0
A632028	F	6/15/43	08/23/12	08/01/18	T3N0
A634944	M	8/20/50	09/14/12	07/19/17	T3N0
A643839	F	8/19/55	11/22/12	01/25/13	T3N0
A650695	M	1/4/52	01/21/13	08/01/18	T2N0
A655663	M	12/13/65	03/02/13	11/01/13	T3N3b
A656900	M	11/13/50	03/12/13	07/05/13	T3N0
A682347	M	11/2/59	09/11/13	01/17/17	T1N0
A683808	F	11/15/58	09/23/13	04/08/14	T3N2b
A696349	F	6/25/33	12/17/13	03/07/18	T2N0
A704061	M	4/21/59	02/21/14	03/22/18	T2N0
A705137	F	1/7/55	03/05/14	03/22/15	T3N0
A705225	F	9/24/58	03/05/14	09/16/14	T3N2b
A 729110	M	8/8/51	08/19/14	11/01/14	T3N0
A731358	M	11/29/55	09/03/14	04/27/18	T3N1
A731691	M	7/20/43	09/05/14	07/05/18	T1N0
A744266	M	1/30/59	11/26/14	08/01/18	T1N2b
A745066	F	11/23/35	12/02/14	06/18/18	T2N0
A664542	M	8/26/60	05/07/13	03/23/16	T1N0
A667482	F	6/15/37	05/28/13	11/19/13	T3N2b
A711885	M	12/24/41	04/22/14	06/26/14	T3N0

3.4 Artigo científico 4:

Artigo científico publicado no periódico Nature Reviews Materials (ISSN 2058-8437, Fator de Impacto: 51,94, DOI: 10.1038/s41578-018-0051-6)

As características físicas do microambiente tumoral tem sido cada vez mais estudadas nos últimos anos devido a sua contribuição na progressão tumoral conforme explanado nos artigos científicos anteriores. Para melhor entender os efeitos destas características, cientistas modulam estas a partir de biomateriais. Este artigo científico realizou uma revisão da literatura sobre os principais biomateriais, de origem natural e sintética, que podem ser utilizados como base para estudo das características físicas do microambiente tumoral. Além disso, biomateriais também vem sendo estudados com aplicações inovadoras de diagnóstico e tratamento do câncer. Portanto, o campo da bioengenharia nos tumores está sendo cada vez mais ampliado, buscando soluções que auxiliem na pesquisa, diagnóstico e tratamento do câncer.

Biomaterials to model and measure epithelial cancers

Pranjali Beri[1], Bibiana F. Matte[1,2], Laurent Fattet[3,4], Daehwan Kim[3,4], Jing Yang[3,4] and Adam J. Engler [ID][1,4,5] *

Abstract | The use of biomaterials has substantially contributed to both our understanding of tumorigenesis and our ability to identify and capture tumour cells in vitro and in vivo. Natural and synthetic biomaterials can be applied as models to recapitulate key features of the tumour microenvironment in vitro, including architectural, mechanical and biological functions. Engineered biomaterials can further mimic the spatial and temporal properties of the surrounding tumour niche to investigate the specific effects of the environment on disease progression, offering an alternative to animal models for the testing of cancer cell behaviour. Biomaterials can also be used to capture and detect cancer cells in vitro and in vivo to monitor tumour progression. In this Review, we discuss the natural and synthetic biomaterials that can be used to recreate specific features of tumour microenvironments. We examine how biomaterials can be applied to capture circulating tumour cells in blood samples for the early detection of metastasis. We highlight biomaterial-based strategies to investigate local regions adjacent to the tumour and survey potential applications of biomaterial-based devices for diagnosis and prognosis, such as the detection of cellular deformability and the non-invasive surveillance of tumour-adjacent stroma.

[1]Department of Bioengineering, University of California, San Diego, La Jolla, CA, USA.

[2]Department of Oral Pathology, Federal University of Rio Grande do Sul, Porto Alegre, Brazil.

[3]Department of Pharmacology, University of California, San Diego, La Jolla, CA, USA.

[4]Moores Cancer Center, University of California, San Diego, La Jolla, CA, USA.

[5]Sanford Consortium for Regenerative Medicine, La Jolla, CA, USA.

*e-mail: aengler@ucsd.edu

Tumours are complex and heterogeneous structures. Understanding tumour progression and cancer metastasis requires the investigation of not only the tumour itself but also of the dynamic and reciprocal interactions between cancer cells and the adjacent tumour stroma, that is, the tumour microenvironment (or niche). This microenvironment is very heterogeneous but generally contains certain cell types (for example, cancer-associated fibroblasts (CAFs)), extracellular matrix (ECM) proteins and signalling molecules, which change as tumours grow and metastasize throughout the body (BOX 1). The tumour microenvironment properties are modulated, in part, as a result of alterations to the 3D fibrillar ECM that surrounds tumour tissue and to the 2D basement membrane that underlies epithelia. For example, the ECM can be modified by CAFs[1,2] and tumour cells alike, causing the matrix to become stiffer[3], more dense[4], crosslinked[5], aligned[3] and less porous[5]. In the case of larger breast tumours, patients can actually feel the stiffened tumour stroma.

Animal models are powerful systems to study the dynamic stromal properties of tumours, but it is difficult to dissect the specific contributions of individual microenvironmental cues to tumour development and progression[6]. However, reducing the in vivo niche to its major biochemical and biophysical components offers a possibility to model the tumour microenvironment in vitro. Identifying and recreating specific aspects of the tumour stroma, for example, stiffness, topography or nutrient exchange, using biomaterials allows for the fabrication of reductionist in vitro systems to study basic mechanisms that regulate cancer cell plasticity, dissemination and repopulation of the niche (BOX 2).

Biomaterials have been used to study tumour biology since the early 1980s, when scientists questioned whether signals from the extracellular compartment could regulate cell behaviour in a distinct and/or similar way as to how genetics can dictate cell fate. In particular, seminal work demonstrating that changes to the extracellular milieu could affect gene expression in mammary glands[7] has triggered unprecedented interest in how the ECM regulates cell behaviour in development. Pioneering work by the group of Mina Bissell established a 'dynamic reciprocity' between the cell and its microenvironment, showing that components of the ECM, such as collagen or fibronectin, associate with the plasma membrane and connect to the intracellular cytoskeleton through specific structures (later identified as focal adhesions). Signals from the ECM are then relayed to the nucleus to affect gene expression and to regulate the expression of ECM molecules or their modification through the expression of ECM-modifying enzymes. However, the detailed mechanisms of cell–ECM interactions are

REVIEWS

Box 1 | **Cancer and metastasis**

Squamous and ductal carcinoma share basic stages of cancer metastasis. These cancers originate from epithelial cells, which line surfaces and vessels of the body.

Primary tumour
The mutation of a single cell leads to uncontrolled division, resulting in an excess of abnormal cells. As the mass grows, the cells can acquire additional mutations and remodel the surrounding tissue, forming a primary tumour. Tumours are heterogeneous and often lack the polarity and cellular organization of the original tissue.

Epithelial-to-mesenchymal transition
Epithelial-to-mesenchymal transition (EMT) is a cellular programme that causes cells within a primary tumour to lose characteristic cell–cell adhesions, to break the basement membrane associated with an epithelial phenotype, to transition to a mesenchymal phenotype that lacks cell polarity and to upregulate and/or activate specific transcription factors, such as Twist family bHLH transcription factor 1 (TWIST1). The EMT programme enables cells of the primary tumour to locally invade the surrounding stroma and is characterized by a shape change of the cells in the primary tumour.

Intravasation
Intravasation is the migration of cancer cells from tumour-adjacent stroma into a blood or lymphatic vessel. This is a multistep process, during which metastatic tumour cells migrate through the extracellular matrix and between cells in the vessel as well as through the water-tight junctions between endothelial cells to reach the fluid in the lumen of the vessel.

Extravasation
Extravasation is the exit of cancer cells from a blood or lymphatic vessel through the endothelial cell layer lining the vessel and into a secondary site distant from the primary tumour. This is also a multistep process, during which circulating tumour cells slow down and stop along the vessel wall through adhesion to endothelial cells. Cells break through the water-tight junctions between endothelial cells and the matrix within the vessel to invade new tissue.

Secondary tumour
A malignant tumour that grows in a secondary organ from cells originating from a primary tumour.

CAF, cancer-associated fibroblast.
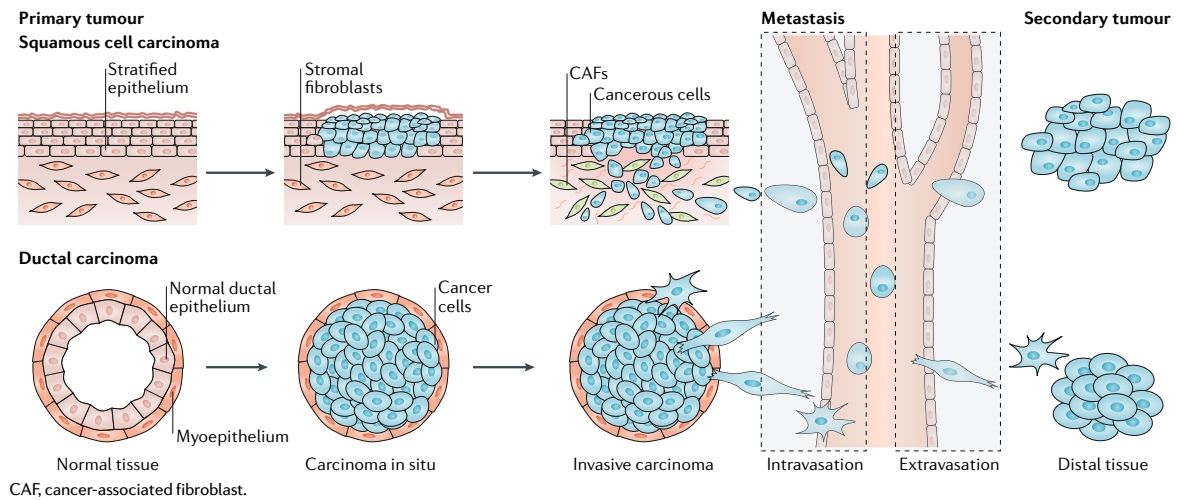
still under intense investigation, and much remains to be understood.

In this Review, we discuss how biomaterials can be applied to model tumours and their microenvironments in vitro. We examine different materials that can be used to capture and measure cancer cells for diagnostics and prognostics and investigate biomaterials for their potential to be used for cancer treatment in vivo.

First attempts to model the tumour ECM
Matrigel
The discovery of dynamic reciprocity was made possible, in part, through the use of tissue-derived biomaterials, which mimic an in vivo microenvironment for in vitro studies of cell–ECM interactions. Matrigel is a solubilized, gelatinous protein mixture composed of reconstituted basement membrane, which was originally isolated from Engelbreth–Holm–Swarm (EHS) mouse sarcoma cells[8,9] and is still routinely used to support the formation of epithelial structures. Matrigel mainly consists of assorted ECM proteins such as

laminin, type IV collagen, heparin sulfate proteoglycans and entactin. However, Matrigel also contains growth factors that can potentially interfere with cell signalling events and thus affect the interpretation of results[10]. Therefore, growth factor-reduced versions of Matrigel have been developed to enable 3D cell culture characterization that focuses on the material properties alone. The use of Matrigel partly allows for the in vitro recreation of the architectural and biochemical complexity of an in vivo cell microenvironment. For example, the first 3D culture of primary mammary epithelial cells (MECs) was achieved using Matrigel, demonstrating that the basement membrane plays a crucial role for the 3D organization of MECs and for the generation of stable and functional hollow-lumen acinar structures[11]. 3D culture of MECs using Matrigel allows the cells to aggregate, remodel the ECM and self-organize into a layer of polarized cells — often with a hollow lumen — through the establishment of epithelial junctions and polarity. This approach enabled the first in vitro differentiated functional alveolar organoid, paving the

Box 2 | **Key aspects of biomaterials for cancer biology**

Biomaterial
A natural or synthetic substance that is compatible with biological systems. It can be engineered for research, diagnostic or therapeutic purposes.

Hydrogel
A polymer gel in which natural or synthetic hydrophilic polymers can be physically or chemically crosslinked to produce a hydrogel that contains different volume fractions of water. The physical and chemical properties of hydrogels can be modulated, for example, by altering the crosslink density or bulk polymer concentration to increase stiffness or by adding peptides or degradation enzymes.

Stiffness
The resistance of a material to deflection or deformation in response to an applied force. Stiffness is a term synonymously used in the biological literature for Young's modulus or elasticity. The stiffness of tumour tissue is higher than that of healthy stromal tissue, leading to alterations of mechanosignalling pathways in cancer cells. Therefore, it is important to model the correct stiffness of tumour tissue in vitro to recreate relevant biomaterial-based cancer models. The stiffness of tissue culture plastic (GPa) is orders of magnitude higher than that of human tissues (kPa), and the stiffness of tumours and of their adjacent stroma is usually an order of magnitude higher than that of healthy tissues; for example, the stiffness of mammary tumours is ~5 kPa, and the stiffness of adjacent stroma is ~0.1 kPa (REF.[3]).

Topography
A parameter that corresponds to the shape and features of the surface of materials. The topography changes with the architecture of the extracellular matrix (ECM). For example, hydrogels and fibrillar matrices have generally smooth and rough topographies, respectively. Increasing collagen deposition increases migration and invasion of tumour cells up to the point at which pore size becomes the limiting factor.

Porosity
Porous or empty spaces within a material are formed as a result of polymer crosslinking. In hydrogels and fibrillar matrices, pores are filled with fluid, and tumour cells can migrate through them to invade the material. The minimum size limitation for cells to pass through pores is <5 μm² (REF.[23]); however, cancer cells can release matrix-cleaving enzymes to degrade the ECM and make room to migrate, which can be recreated in biomaterials using enzyme-degradable peptides as crosslinkers.

way for morphogenesis and developmental studies in vitro using biomaterials. These recombinant basement membrane-derived systems have also been used to assess differences in gene expression profiles between cell lines[12]. The use of Matrigel in combination with collagen further enabled the identification of cellular differences between normal and malignant cells in 3D[13].

The seed and soil hypothesis of metastasis

Originally, biomaterials were mainly used to understand how the adjacent tumour ECM regulates tumorigenesis. An equally important aspect — albeit less well studied — is the cellular and ECM composition of the microenvironment at distant sites of metastasis. The distant microenvironment was described by Stephen Paget as the 'soil' in his 'seed and soil hypothesis'[14]. On the basis of the analysis of the data of a large cohort of patients with breast cancer, he hypothesized that the microenvironment plays a crucial role in regulating the seeding and growing of secondary tumours. Similar to disease progression-associated changes of the tumour ECM, Paget suggested that unique features of the soil can cause cancer cells to metastasize to specific locations. Stromal and immune cells are also part of the soil, migrating to distal sites prior to the arrival of tumour seeds[15]. Extracted stromal ECM components can further promote or prevent tumour progression[16,17], demonstrating

that the ECM plays a role in seed implantation and can remodel tumour stroma[18]. Both in the tumour microenvironment and at distant sites of metastasis, a complex network of ECM proteins contributes to tumour progression and impacts cancer cell behaviour. Natural biomaterials can be applied to recreate these microenvironments, incorporating different stromal and ECM features to improve in vitro disease models and to develop new generations of therapeutics and diagnostics. However, there is a veritable balance between preserving the native ECM structure and composition to precisely resemble the in vivo architecture and the removal of cellular and antigenic material, such as nucleic acids, membrane lipids and cytosolic proteins, to be able to reproducibly use these biomaterials in vitro. These caveats have led to the development of new natural matrices as well as synthetic hydrogels that are more reductionist than these initially used natural biomaterials.

Engineering the tumour microenvironment
Natural biomaterials
Mimicking the microenvironment of tumours requires the use of 3D rather than 2D architectures to enable morphogenesis. Collagen gels were first used as 3D scaffolds to demonstrate how normal murine MECs form lumens in 3D as opposed to monolayers on 2D substrates[7], emphasizing the importance of 3D materials to recreate in vivo cell morphologies in vitro. The first ECM-specific behaviour observed using 3D biomaterials was cancer cell dissemination from tumour cell aggregates. In collagen gels, mammary carcinoma cells migrate as single cells with larger protrusions and higher local dissemination than cells embedded in Matrigel, in which cells migrate in a collective pattern[19]. These data indicate that protein composition of the matrix is an important property of neoplastic cell invasion. Unlike invasive carcinomas, malignant cells establish a vasculogenic network when embedded in collagen matrices with small pores and short fibres; tumours that feature such a tumour-adjacent matrix are correlated with poor prognosis. Such a short fibre-based network is not established if cells are exposed to increasing amounts of recombinant basement membrane[20], and thus the vasculogenic network is not formed. This effect can be titrated, and increasing collagen concentration restores vascular network formation[21].

Natural matrices containing collagen and/or recombinant basement membrane can be crosslinked or fabricated at different concentrations to modulate their stiffness and thus enable the assessment of the influence of stiffness in concert with specific genetic alterations. For example, MECs respond to increasing collagen matrix stiffness, which is achieved through adding collagen proteins, by breaking the acinar structure and invading into the ECM. If the genome of the MECs contains specific cancer-driving oncogenes, for example, receptor tyrosine-protein kinase ERBB2 (REF.[5]), they display an even more aggressive phenotype when interacting with a stiff matrix. MicroRNAs also play a role in regulating the expression of genes that favour tumour progression and are implicated in the increased stiffness sensitivity of MECs[22]. In addition to stiffness, ECM porosity further plays a central role in cancer cell migration and tumour

growth. Small pore sizes reduce the migration speed of cells in natural ECMs, such as collagen, by acting as barriers for nuclei deformation. A similar behaviour has been observed using synthetic materials[23]. However, in contrast to synthetic materials, cells can use matrix metalloproteinases (MMPs) to degrade natural ECM and increase the pore size to migrate through dense collagen gels[24]. Beyond a specific pore size threshold, myosin-mediated traction forces can propel the nucleus forward and allow migration through a dense ECM[25,26]. These data indicate that ECM fibre assembly, porosity and composition affect ECM architecture and material properties and, consequently, cancer cell migration and dissemination. However, in a natural matrix, the biochemical and biophysical parameters of the ECM cannot be decoupled; that is, individual matrix properties can only be varied relative to each other. This makes it challenging to accurately predict the impact of individual effects of natural ECMs on cell migration[27,28]. For example, altering ECM stiffness by adding more matrix protein also affects the adhesive properties of the matrix[29]. Moreover, batch-to-batch variations can influence the reproducibility of experiments; even in commercial products, such as Matrigel, variation in matrix protein composition, for example, fibronectin, can drive differences in cell behaviour[30]. Therefore, although natural ECM mimics the microenvironment of native tissue very well, coupled variation of ECM parameters and inconsistent composition are valid concerns.

Given these issues, a clear consensus on the relationship of migration and ECM parameters has not yet been achieved. For example, the concentration of specific ECM components has been shown to have either biphasic[31] or direct[32] effects on cancer cell migration. Cell contractility is also required for migration along a matrix, but how specific ECM properties guide cell contractility is still under debate. In collagen matrices, the forces generated by mammary carcinoma cells are independent of collagen concentration and matrix stiffness[33]. However, invasive cancer cells, which transition to a more mesenchymal phenotype with a spindle-like morphology, exhibit more processive or directed migration, making them more invasive with increasing collagen concentration[34].

These (sometimes controversial) observations have also been made using pristine natural matrices made from recombinant or animal-derived proteins. A better suitable ECM model is matrix exposed to clinically relevant doses of radiation. Irradiated matrices exhibit altered structures that substantially reduce metastatic cancer cell adhesion, spreading and migration[35]. In addition to the interest in using more relevant and reductionist materials, there is an equal interest in moving from common cell lines to their primary human tumour cell counterparts owing to their different and potentially more relevant behaviours. Together, this has created the push to move to mainly synthetic material systems.

Synthetic biomaterials

Natural materials have been key for initial investigations of ECM and cancer, but owing to their above-mentioned disadvantages, synthetic materials are increasingly used to mimic tumour ECM (FIG. 1). Synthetic materials have the advantage that parameters can be decoupled[36]; tuning one parameter, such as substrate stiffness, does not affect other parameters, such as fibre architecture or pore size[37] (BOX 2). They can also serve as a platform for cell adhesion by providing different ECM proteins or peptides, such as arginine–glycine–aspartic acid (RGD), glycine–phenylalanine–hydroxyproline–glycine–glutamate–arginine (GFOGER) or isoleucine–lysine–valine–alanine–valine (IKVAV), to understand how specific ECM components regulate tumorigenesis (FIG. 1a). For example, polyethylene glycol chains decorated with peptides of laminin 1 and type I collagen, but not of fibronectin, support invasive behaviours of metastatic prostate cancer cells, which is not observed for non-metastatic cancer cell lines[38]. Therefore, such systems can be potentially used to separate neoplastic cells from a mixed cell population. Synthetic materials can be easily functionalized with not only adhesive ligands but also a variety of other signalling proteins and peptides; for example, materials can be crosslinked with protease-degradable linkers, thus allowing the cells to control local matrix properties in a similar way as in natural matrices[39]. However, synthetic materials enable variation and individual control of ECM properties, although the combination of specific properties or proteins does not necessarily result in a linear cell response[30,40]. For example, cancer cells show different sensitivity to combinations of matrix proteins than to the individual proteins[41] and can be more or less responsive to specific matrix properties if they adhere to more or less permissive matrix proteins[30].

Modulating matrix stiffness. A breast tumour mass is routinely identified by manual palpation; the patient or doctor identifies a stiff lump relative to the compliant surrounding tissue. In epithelial tumours, a direct correlation between stiffness and metastatic potential has been reported[3,5,42–45]; however, this correlation has not been observed in all animal models[46]. To tune stiffness in natural ECMs, matrix concentration is increased, which also affects porosity and ligand density[3]. By contrast, in synthetic materials, changing crosslink density or bulk polymer concentration allows for the variation of stiffness by several orders of magnitude without modifying adhesion ligand density[47] (FIG. 1b). Most epithelial tumour models use a combination of naturally derived or natural and synthetic matrices in 3D[48,49]. These approaches using materials with increasing stiffness have been applied to study the mechano sensitivity of mammary epithelia during their transition to a mesenchymal phenotype, that is, the epithelial-to-mesenchymal transition (EMT). A stiff matrix triggers focal adhesion assembly through stress-induced elastic deformation, which in combination with cell contractility activates extracellular signal-regulated kinase (ERK) and the RHO family of GTPases, driving MECs towards EMT[3] (FIG. 2). Increasing matrix stiffness also triggers the release of the EMT transcription factor Twist family bHLH transcription factor 1 (TWIST1) from its cytoplasmic binding partner RAS GTPase-activating protein-binding protein 2 (G3BP2), its translocation to the nucleus and initiation of an EMT transcription programme[45].
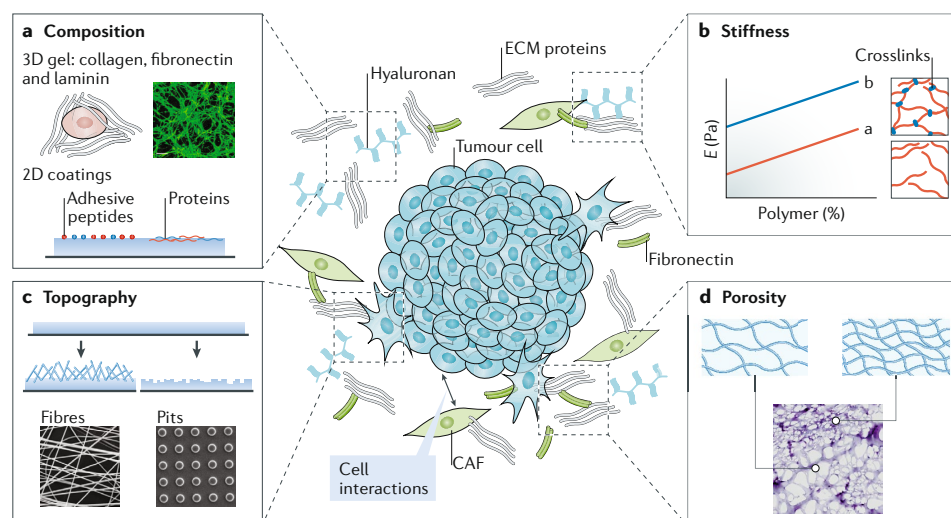
Fig. 1 | **Modelling the tumour microenvironment.** The tumour microenvironment constitutes the niche that surrounds a tumour, including extracellular matrix (ECM), cells and signalling molecules. The niche is characterized by specific dynamic ECM properties. **a |** The composition of the ECM can vary in terms of both ligand type and ligand presentation. 3D hydrogels made of ECM proteins or 2D materials can be used to recreate a specific ECM composition. The ligand type[41] and concentration[3] affect cell behaviour and can induce an epithelial-to-mesenchymal transition (EMT). **b |** Stiffness, that is, the Young's modulus, can also impact EMT[3,45]. The Young's modulus (E) of a material can be modified by changing chain entanglements (line a) or crosslinking (line b). The stiffness is measured as the force per cross-sectional area of the material. **c |** Topographical features of the niche can be recreated by spinning polymers into fibres and depositing them as a thin layer on a surface, to which a cell can adhere. Alternatively, a material can be etched to create specific nanotopographical or microtopographical features, such as pits. Such topographies can be used to induce cell transformations[58–62] or to capture cancer cells[82,85,86]. **d |** The pore size and pore connectivity of the tumour microenvironment can be modelled by modulating bulk polymer density or droplet size in emulsions. Non-malignant cells are highly sensitive to pore size[63,64]; materials with small pores can inhibit migration and proliferation, and large pores are felt by the cells as 2D surfaces. CAF, cancer-associated fibroblast.

Additional evidence suggests that hydrogel stiffness regulates not only malignant transformation but also dissemination and migration of invading cancer cells[50]. Metastatic cells have tumour-specific stiffness preferences; at an optimal stiffness, corresponding to the stiffness of a specific tumour type, they express markers consistent with highly migratory cells and migrate faster than at sub-optimal stiffness[51].

Synthetic materials can also be designed as dynamic systems, in which crosslinking can be gradually[52,53] changed or modified on demand[44,54,55], thus better mimicking slow disease progression. Collective cancer cell behaviours can be substantially different in materials that stiffen following polarization than in materials with static stiffness[56]. Controlled degradation[57] can also provide a strategy to examine cell behaviour in response to an environment that becomes increasingly softer and to identify mechanotransduction pathways that can slow tumorigenesis. Therefore, matrix stiffness and the timing of its presentation are important ECM properties that influence neoplastic cell behaviour.

Fibre architecture, topography and porosity. The architecture and topography of ECM fibres also affect the behaviour of neoplastic cells. Cancer cells can sense whether the surface is atomically flat or has a roughened topography (FIG. 1c), which can induce invasion and

metastasis. For example, fibrillar matrix structures can be synthetically recreated using electrospun fibres, such as silk, to support 3D cell migration of both malignant and non-malignant cell lines[58,59]. Alternatively, poly-dimethylsiloxane (PDMS) is a commonly used polymer for topographical studies. Using patterned PDMS substrates, it has been shown that neoplastic cells are less sensitive to geometrical cues than non-malignant cells[60,61]. On micrografted surfaces, MECs enter a dormant state, whereas their neoplastic counterparts continue to proliferate through a RHO–RHO-associated protein kinase (ROCK)–myosin-dependent pathway[62]. This principle also extends to other roughened surfaces, on which malignant cells appear less sensitive and continue to grow and migrate independent of roughness[60,62].

Similarly, ECM porosity, which dictates cell spreading, can differentially affect non-malignant and metastatic cells (FIG. 1d). For example, metastatic cells can migrate through PDMS channels that are smaller than the diameter of their nuclei by breaking and reforming their nuclear envelope[23]. 3D material systems containing collagen and agarose can be used to independently modulate stiffness, porosity and ligand density. If the porosity of the material is decreased independent of other properties, glioblastoma cell migration is sterically hindered[63]. Conversely, non-malignant cells sense porosity together with other properties, such as stiffness;
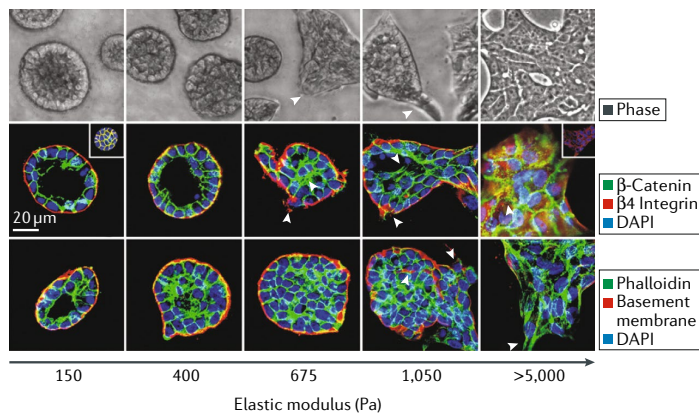
Fig. 2 | **Matrix stiffness regulates the epithelial-to-mesenchymal transition.** Phase contrast and fluorescent images of mammary epithelial cell colonies on polyacrylamide hydrogels of indicated stiffness (150–5,000 Pa) with Matrigel overlay are shown. Microscopy images show colony morphology after 20 days. The fluorescent images show β-catenin (green) before and after (inset) triton extraction, β4 integrin (red), epithelial cadherin (E-cadherin) (red; inset) and nuclei (blue). In the bottom images, actin (green), laminin 5 (basement membrane; red) and nuclei (blue) are shown. DAPI, 4′,6-diamidi-no-2-phenylindole. Figure is reproduced with permission from REF.[3], Elsevier.

for example, in channels of decreasing width, the migration speed of non-malignant cells increases with stiffer channel walls[64]. These data suggest complex and often coupled interactions and therefore do not yet allow an overarching conclusion or propose the ideal material for modelling the tumour microenvironment. However, individual ECM properties have already been identified that can be modulated using biomaterials to study their effects on cancer cells (TABLE 1).

Model requirements beyond materials

Tumours are often described as organs that contain different cell types, including CAFs[65], endothelial cells, pericytes and immune inflammatory cells[66]. The vast majority of biomaterial-based models are incomplete because they do not incorporate these important cell types that modify the microenvironment. Cancer cells secrete soluble factors that activate CAFs, leading to a change in CAF protein expression and an increase in MMP secretion and CAF contractility[67–69]. CAF-generated forces promote angiogenesis[70] and generate holes in the matrix to facilitate cell invasion[69]. CAFs can also directly bind to cancer cells through heterotypic epithelial cadherin (E-cadherin; also known as CDH1) and neural cadherin (N-cadherin; also known as CDH2) junctions and pull cancer cells away from the tumour[71]. CAF contractility further promotes the nuclear translocation of Yes-associated protein YAP65 homologue (YAP1), which in turn results in matrix stiffening, angiogenesis and cancer cell invasion. This positive feedback loop drives tumour progression[72]. However, most current biomaterial approaches to the niche lack these important interactions and signalling events.

Metastasis of cancer cells further depends on the ability of cancer cells to migrate through the stroma, intravasate blood vessels, survive in the circulation and extravasate into new matrix to colonize distant tissues

(BOX 1). Although no hydrogel system to date mimics all these stages, materials-based microphysiological systems have been explored to mimic specific steps in this process, such as extravasation, in which cancer cells pass through the endothelium; for example, microphysiological systems can be fabricated using PDMS to engineer a perfusable microvascular network with hydrogel regions and media channels. Such systems are thin and composed of neo-vessels, allowing imaging analysis to study transendothelial migration[73]. By applying this in vitro approach, it has been shown that tumour necrosis factor (TNF)-α increases endothelial cell permeability, facilitates tumour cell intravasation[74] and modulates extravasation[75,76]. Microphysiological systems can also be used to investigate metastasis of certain cancer cells to specific secondary sites. For example, a microenvironment containing osteoblasts can be used to elucidate why breast cancer cells preferentially metastasize to bone. A higher number of breast cancer cells extravasate into the bone cell-conditioned microenvironment than into a collagen matrix, suggesting that bone-secreted chemokines such as CXC-chemokine ligand 5 (CXCL5) play a role in the chemotactic migration of breast cancer cells[77]. These systems enable the investigation of the contribution of specific families of cell-secreted cytokines to cancer cell metastasis, which is difficult to dissect in animal models. Further development of microfluidic devices and incorporation of various materials will make in vitro models increasingly relevant for cancer biologists as reductionist systems to recreate more steps of the metastatic process within one system.

Capturing cells in blood and stroma

Biomaterials can be applied for diagnostic and prognostic screening of cancer in vivo and ex vivo (FIG. 3). The current standard of care primarily consists of regular screenings, such as mammograms for breast cancer, flexible sigmoidoscopy or faecal occult blood test for colorectal cancer[78] and computed tomography and chest radiography scans for lung cancer[79]. However, by the time the disease is observable, the tumour has often already metastasized. To detect tumours in patients earlier and more accurately, biopsy samples can be taken and genetically tested for prognostic markers, for example, breast cancer markers breast cancer type 1 susceptibility protein (BRCA1) and ERBB2 by using mRNA microarrays[80]. Such assays have dramatically reduced cancer occurrence; however, they do not directly detect disease-causing cells.

Biomaterial-based technologies have primarily focused on capturing circulating tumour cells (CTCs). CTCs are a small fraction of cells that disseminate from primary tumours and are thought to be responsible for the haematogenic spread of cancer to distant sites[81,82]. Increased CTC levels in the blood are correlated with negative prognosis. Therefore, CTC isolation and quantification are essential for the early detection of metastasis and subsequent treatment[82]. However, CTCs are difficult to isolate with high efficiency and purity[81] and thus their unique molecular signatures remain elusive[82]. The most commonly used CTC isolation method relies on increased epithelial cell adhesion molecule (EPCAM)

Table 1 | **Biomaterials for modelling the tumour microenvironment**

Biomaterial	Model	Advantages	Disadvantages	Refs
Synthetic material				
Polydimethylsiloxane (PDMS)	2D micropatterns	Flexible substrate with patterns promoting cancer cell alignment	Uncertain viscoelastic mechanics and protein attachment	37,148
	Microchannels and microfluidics	• Directed cell migration in channels • Cell confinement • Confined fluid flow for controlled application of shear stress to cells	• Curing ratios often create materials that are less flexible • Static substrate	23,114
Polyethylene glycol diacrylate (PEGDA)	3D culture	• Wide stiffness range • Direct conjugation of many types of adhesive ligands • Can be used to identify tumour-specific stiffness	–	51
Polyethylene glycol (PEG)	3D culture	• Wide stiffness range • Direct conjugation of many types of adhesive ligands or degradable linkers • Inert and biocompatible	Backbone is not degradable	39,149,150
Poly(lactide-co-glycolide) acid (PLGA)	3D culture	• Porous scaffold • Biocompatible • Biodegradable	Methyl side groups increase hydrophobicity	151,152
	Implantable material	Recruitment and capture of metastatic cells	Degradation prior to cell capture	93
Poly(ε-caprolactone) (PCL)	Implantable material	Recruitment and capture of metastatic and immune cells	Degradation prior to cell capture	92
Polyacrylamide	Substrate gradients	• Sequential polymerization to create spatial patterns • Indication of metastatic cell 'memory' • Small well polymerization for high-throughput drug screens	Substrate stiffness does not change with time	153–155
	Used with Matrigel overlay for 3D culture	• Wide stiffness range • Conjugation of individual or multiple ligands resulting in nonlinear cell responses	• Cytotoxic prior to polymerization, preventing cell encapsulation • Difficult to measure forces in 3D	3,30,40,45
	Elastic 2D substrate	Measurement of traction forces in cancer cells	• Cytotoxic prior to polymerization, preventing cell encapsulation • Difficult to measure forces in 3D	42
Synthetic–natural hybrid materials				
Polyethylene glycol-heparin	3D culture	• Direct conjugation of adhesive ligands • Enzymatically degradable	Limited degradation control	38
Methacrylated hyaluronic acid (MeHA)	3D culture	• Direct conjugation of adhesive ligands • Enzymatically degradable • Temporal gradients through sequential crosslinking	• Radical polymerization limits in vivo application • Can induce DNA damage • Modifications can reduce bioactivity	44,54,55
Natural materials				
Matrigel	3D culture	• Established fibrillar model system • Temperature-based polymerization • Easy encapsulation methods • Growth factor-reduced version • 3D organization of acinar structures	• Batch-to-batch variation • Difficult to independently modulate parameters • Tumour-derived (inductive composition) • Temperature sensitive	8,9,11,30
Alginate	3D culture	• Stiffness can be modulated independently of architecture • Time-dependent stiffening with calcium crosslinking • Enables mammary epithelial cells to polarize before EMT	Calcium-dependent covalent bonds	56,156
Type I collagen	3D culture	• Fibrillar • Adhesion of multiple cell types • Facilitates cell invasion • Shows same radiation damage as tumours	• Transglutaminases and oxidases can crosslink with limited range Harsh organics are more common crosslinkers with a wider range • Limited stiffness range of ~1–1,000 Pa	23,35,69,157
	Matrigel-impregnated	Migration is biphasic and directly dependent on concentration	• Pore size changes with Matrigel concentration • Limited ligand presentation	31,32
	Agarose-impregnated	• Stiffness can be modulated independently of ligand density • Restricted invasion of glioma cells	Pore size changes with agarose concentration	63

EMT, epithelial-to-mesenchymal transition.
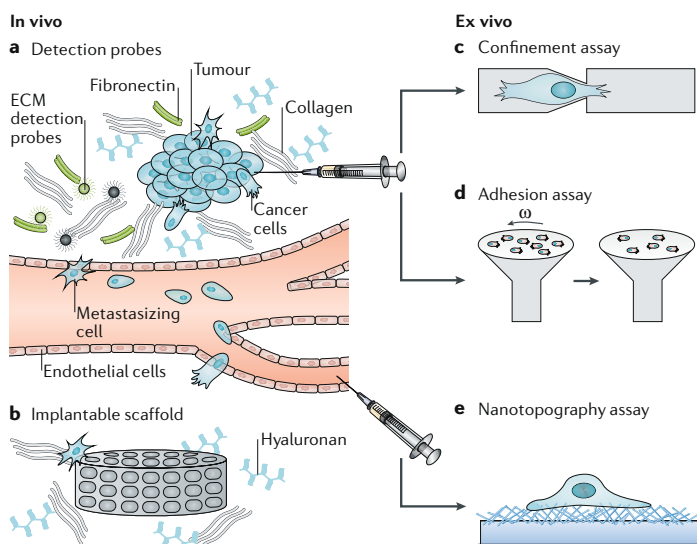
Fig. 3 | Next-generation material-based cancer technologies. The specific interactions between cancer cells and the tumour stroma can be exploited for the detection of cancer cells. **a |** Magnetic resonance imaging (MRI) or positron emission tomography (PET) contrast agents can be conjugated with extracellular matrix (ECM)-affinity peptides to create specific probes to target the dense ECM of the tumour stroma for the detection of mature tumours in vivo. **b |** Implantable scaffolds can be used to recreate a pre-metastatic niche at the implant site, recruiting cells for capture and therapy and at the same time lowering the tumour burden in typical secondary metastasis sites. **c,d |** Confinement assays or adhesion assays can be applied to test cells obtained from tumour biopsy samples for their aggressiveness by measuring cellular deformation or adhesion to specific ECM molecules. Omega (ω) is the angular velocity that defines the shear stress applied to cells. **e |** Circulating tumour cells (CTCs) can be isolated from patient blood samples using nanotopography assays that take advantage of the affinity of CTCs for nano-roughed substrates.

expression on the surface of CTCs[81], which is used by the US Food and Drug Administration (FDA)-approved CellSearch System. However, this system requires a very large sample volume, has low sensitivity and is time consuming[81].

Ex vivo detection using nanotopographies
CTC capture efficiency can be improved by increasing the local concentration of capture substrate or by coupling the substrate with surface-functionalizing molecules, such as antibodies or aptamers. For example, microfluidic chip assays composed of PDMS microposts with a surface coating of anti-EPCAM antibody can concentrate CTCs in smaller sample volumes[79] than systems without antibody coating. Silicon nanopillars further improve CTC capture by clustering antibodies through binding to streptavidin or gold[83]. Aptamer-functionalized gold nanopillar arrays show efficient cell release through cleavage of the sulfur–gold bonds between the aptamers and the gold nanopillars[84].

CTC purification and capture can also be achieved using artificial nanoscale topographies, mimicking structural features and dimensions of ECM[81]. Cancer cells preferentially adhere to nanostructured rough substrates compared with smooth substrates, even in the absence of surface functionalization with antibodies[82]. For example,

fractal nanostructures have an uneven topography and a crystalline structure, which increase cancer cell binding to the surface[85,86]. Fractal nanostructures can be generated from synthetic materials, such as TiO$_2$, with inverse opal photonic crystals to mimic cellular components or natural materials, such as hydroxyapatite nanostructures of seashells[86,87]. Alternatively, rough nanoscale substrates can be fabricated with an anti-EPCAM antibody-coated, mesh-like silicon nanowire substrate and overlaid with a PDMS-based chaotic mixer[88,89]. These systems show a >95% capture efficiency of EPCAM-positive MCF7 breast cancer cells, which is more than 20-fold higher than EPCAM antibody-coated smooth substrates[90,91]. The addition of electrospun thermoresponsive nanofibres enables an even higher capture efficiency and allows on-demand release and single-CTC analysis, for example, for next-generation sequencing[88]. Cell release can also be achieved by using degradable zinc-phosphate nanosubstrates[92].

Nanostructured surfaces enable high capture efficiency but cannot provide high cell purity owing to nonspecific cell adhesion. Dual-functional lipid coating can be applied to improve the capture specificity of nanopillars owing to the higher concentration of antibody on the surface and inhibition of nonspecific cell adhesion[93]. Poly(carboxybetaine methacrylate) brushes also decrease nonspecific cell adhesion, and the active carboxyl groups capture CTC-specific biomolecules[94]. These nanostructure-based methods enable ex vivo detection of CTCs, demonstrating how specific ECM properties, such as topography, can be exploited to increase capture efficiency and provide a strategy for proactive disease monitoring. It has been suggested that CTC detection probability scales with patient mortality[79] and, thus, technologies for the continuous detection of CTCs could provide a strategy to detect cancer cell metastasis early enough to substantially increase patient survival.

In vivo cell detection using implantable materials
Biomaterials can also be implanted to monitor tumour progression in vivo[95,96]. According to Paget's seed and soil hypothesis, secondary metastases do not occur randomly[14]. Specific microenvironments are primed for tumour cell colonization through the presence of tumour-supportive fibroblasts, endothelial progenitor cells, immune cell-secreted factors and ECM-remodelling events[95–97]. Current imaging techniques are limited in their ability to detect micrometastases that form at distal sites[95–97], which reduces their prognostic capabilities and offers an area of opportunity for biomaterial-based solutions.

For example, microporous scaffolds such as poly(lactide-co-glycolide) acid (PLGA) can be implanted to recruit and capture metastasized cells. Breast cancer cells that have metastasized to the brain can be injected into the fat pads of mice and entrapped in an implanted PLGA scaffold. Mice with scaffolds implanted to capture circulating cells develop fewer lung tumours[96] than animals without any implanted material, indicating that the scaffolds reduce secondary metastases formation. Poly(ε-caprolactone) (PCL) has similar physical properties to PLGA but degrades more slowly[95]. PCL scaffolds

can also be used to recruit tumour and immune cells, which are implicated in establishing a pre-metastatic niche, and to decrease the number of detectable tumour cells in common secondary sites[95,98–100]. Additional modifications, such as graphene oxide (GO) functionalization, can further increase cancer cell adhesion compared with non-functionalized scaffolds[101]. GO addition to the scaffold can also enable photothermal ablation of cancer cells within the scaffold owing to the near-infrared absorbance of GO[101,102], demonstrating how implantable scaffolds can be used for both cancer cell capture and therapy. Besides chemical modifications, scaffolds can also be coated with ECM proteins, including fibronectin and type IV collagen, to improve scaffold capture efficiency. Each tumour type is characterized by specific ECM combinations and thus scaffolds can be coated with a tumour-specific ECM that supports metastases[41] to improve cancer cell recruitment. For example, coating with decellularized lung or liver matrix of metastatic tumours substantially increases capture efficiency[97].

Matrix is not the only niche component that can be used to improve cell capture. Cancer cell-secreted exosomes or haptoglobin can also be incorporated into synthetic scaffolds to create a bioengineered niche that captures metastatic cells more effectively than tissues to which cells commonly metastasize and increases survival in animals implanted with these scaffolds[103,104]. Natural materials such as silk can also be functionalized with proteins, such as bone morphogenetic protein 2 (BMP2), to mimic a bone marrow microenvironment. This material can serve as a surrogate for a pre-metastatic niche and recruit metastasizing cancer cells that would normally home to bone marrow[105]. In particular, BMP2 increases the adhesion of metastatic prostate and breast cancer cell lines to the scaffold[105,106]. Such scaffolds can be implanted to capture tumour cells, reduce the tumour burden on standard metastatic organs and prevent the local remodelling of tissue into a pre-metastatic niche, making them potent therapeutic tools to detect, capture and ablate metastasized cancer cells. However, these scaffolds do not have an inherent proclivity to capture specific cell types.

Ex vivo cell detection using physical properties
Cells migrate through the stromal ECM through confined pores, which can be smaller than the nucleus of the cell. To achieve this, cells can either degrade adjacent matrix using MMPs[24] or physically deform it[107]. Increased MMP expression and decreased nuclear size[108,109] are associated with aggressive cancers and thus cell deformability is emerging as a marker for the invasive potential of cancer cells[110]. Assays for the investigation of cellular deformability exploit the variable pore size in the ECM to shed light on the relationship between the degree of deformation and the corresponding invasive and metastatic potential. The most common strategy is to micro-fabricate channels — for example, in PDMS — with defined geometries and track cellular movement. Cells with low expression of nuclear lamina proteins, which contribute to nuclear stiffness, pass more quickly through narrow regions[107] than cells with high lamin A and/or lamin C expression and stiff nuclei.

Specific deformation tolerances can be assessed using funnel-shaped constrictions in series[111] or in parallel to analyse cell transition effects[112]. Metastatic cells modulate their morphology, as they are forced into confined spaces more than their non-metastatic counterparts, resulting in faster and larger deformation events[112]. Highly metastatic cells can even rupture and reassemble their nuclear envelops when they encounter transit constrictions[23]. Intravasation constitutes one of the most restrictive parts of the journey of a metastasizing cell. Microfluidic devices with cell and nutrient chambers separated by microchannels of varying width can be used to determine the minimum gap that cancer cells can migrate through in confined environments. Such a device has been applied to demonstrate that the nucleus is a crucial limiting factor for a cell to be able to traverse confined environments[113].

Constrictive devices rely on cell-generated forces; alternatively, external hydrodynamic forces can be applied to deform cells. Opposing flows, that is, hydrodynamic stretching, can uniformly deform cells, and the degree of deformation can be controlled by simply changing the flow rate[114] or through pinched-flow stretching in a single inlet[115]. The latter design forces cells to flow in the centre of the channel, siphons fluid on the sides of the channel away from the cells and then compresses the cells when the fluid is added back to the channel[115]. These assays can be applied to analyse cell deformability of single cells or populations of cells using pressure-driven microfiltration systems. Using these systems, it has been observed that induction of EMT or drug resistance leads to an increase in cell deformability[116]. Such microfiltration devices enable high-throughput assessment of transit time and deformability[117] to investigate a population of cells from a tumour. These assays, applying forces either internally or externally, measure internal features of the cytoskeleton that are found in metastatic but not in non-metastatic cells. Therefore, microchannel assays can be useful as diagnostic tools to assess the aggressiveness of cells isolated from tumour biopsy samples and to observe the effect of cancer therapies on cell deformability and thus disease progression.

Adhesion properties and mechanisms provide another physical metric to determine the metastatic potential of cancer cells. Assays that apply negative pressure to detach cells[118], to assess binding efficiencies to ECMs[119] or to analyse adhesion turnover[120] have demonstrated that adhesion is modulated differentially in metastatic cancer cells compared with in non-metastatic cells. For example, metastatic cancer cells can move rapidly through tissue through increased cation sensitivity that leads to more rapid formation and disassembly of focal adhesions than in their non-metastatic counterparts[121]. Cell–matrix adhesions are directly modulated by magnesium, manganese and calcium cations, which increase integrin affinities for matrix proteins in proportion to their concentration. The concentration of cations is tenfold lower in the stroma than in the tumour[122,123]. Thus, once metastatic cells reach the stroma, only cells with labile adhesions can migrate. Indeed, cancer cell adhesion strength to fibronectin and type I collagen at low cation conditions correlates with metastatic potential;

within a highly metastatic cell population, the subset of cells with high adhesion strength is less migratory and invasive than malignant and non-cancerous epithelial cells or strongly adherent metastatic cells[121]. Analysing the weakly adherent cell fraction enables the determination of the metastatic potential of a tumour in situ. Each of the above-discussed assays yields valuable information about the metastatic potential of cancer cells, which could make such devices useful diagnostic tools for prognostic assessment and for determining a course of treatment.

Non-invasive surveillance of tumour-adjacent stroma
Interaction with the surrounding matrix is an important regulator of cell dissemination, and various matrix properties can act as markers to detect and/or capture highly invasive cells that are predisposed towards tumour formation. Exploiting the similarities of tumour microenvironments across different cancer types opens up avenues for monitoring the presence and growth of primary tumours. For example, overexpression of integrins, common matrix signatures[41] and overexpression of specific MMPs can act as prognostic indicators of the metastatic potential of tumours in patients with primary breast tumours[124]. Unlike most physical parameters of the ECM, the composition of the tumour-adjacent stroma can be non-invasively monitored, making it an attractive property for the assessment of tumour progression in patients.

In addition to biochemical surveillance, imaging methods are also being explored using material-based probes. For example, a combination of high-affinity fibrin peptides and tracer molecules (that is, radioisotopes) that are detectable by magnetic resonance imaging (MRI) or single photon emission computed tomography (SPECT) are being developed to assess increased fibrin deposition in tumours[125,126]. Antigen-binding fragment (Fab) probes can be combined with a radioisotope to image fibrin clots in the tumour microenvironment[127]. Such probes also demonstrate low retention times in non-target tissue in vivo[126,128]. Fibronectin is also overexpressed during EMT, making it a prime target for early cancer detection probes[124,129–131]. Similar to MRI contrast agents for fibrin, gadolinium-based MRI contrast agents can be used to target fibronectin–fibrin complexes, demonstrating robust detection of the primary tumour and of >0.5 mm³ micrometastases[129]. Most current strategies target major ECM components; however, probes that target more tumour-specific ECM elements, such as periostin in oesophageal cancer[132], could improve detection specificity, decrease background signalling through rapid clearance of non-bound contrast agents[124] and increase tissue penetration depth owing to their small size. These approaches, which are still being developed, enable us to image tumours with increasing spatial resolution, but they do not provide information about the aggressiveness of tumours.

Perspectives and conclusion
Strategies to understand and detect tumours have greatly improved our ability to recognize and assess specific tumour pathways and cell behaviours that are indicative of disease progression. As the field matures, cancer

diagnosis and treatment will most certainly involve more materials-based approaches to address shortcomings in our ability to model, detect and treat cancer. Despite the development of a variety of dynamic, synthetic biomaterials applicable for the modelling and study of cancer, Matrigel is still most commonly used by cancer biologists for 3D cell culture systems even though it is highly variable, difficult to purify and derived from a mouse tumour. Therefore, the field of material science must continue to evolve and incorporate tuneable synthetic materials to help understand the cell behaviours induced by these increasingly complex materials.

As the biomaterials community, we also aim to clinically translate lessons learned from in vitro models to diagnostic assays. The substantial progress made in our understanding of the tumour as a material and in detecting and capturing cancer cells makes this an exciting time for material-based cancer research. There are great opportunities to improve our basic understanding of cancer and also our detection and treatment capabilities, for example, investigating tumour–stroma interactions in reductionist matrix systems, developing a complete tumour-in-a-dish model (including intravasation and extravasation) and understanding how animal models reflect clinical outcomes. Improvement of detection probes using biomaterials, whether invasive or not, is also a growing research area, which is reflected in the expanding body of literature. For example, during tumour growth, collagen, fibrin and hyaluronan concentrations increase in the surrounding ECM, and the matrix stiffens and is aligned by lysyl oxidases[5,133,134] to facilitate invasion[124,135]. Potential therapeutic avenues include the use of proteases to degrade matrix proteins and decrease stiffness to improve drug penetration. Conversely, hyaluronidase, which degrades the extracellular glycosaminoglycan hyaluronan, can be inhibited to limit tumour growth and metastasis[136,137]. Clinical trials of hyaluronidase delivery have demonstrated its safety[138], and a phase III study is currently being conducted (NCT02715804). Finally, future improvements in treatment options using biomaterials will ultimately impact clinical outcomes. For example, altering ECM structure could improve nanoparticle and drug delivery, resulting in more effective, deeper-penetrating therapies and improved patient outcomes[133,139–142]. In addition to enzymatic strategies, physical disruption of the matrix using high-intensity ultrasound can be used to improve the penetration of nanoparticles into the tumour tissue without damaging surrounding tissues[139]. Thermal strategies with nanotubes[143] or gold nanorods[144] can also be applied to denature the collagen matrix and increase tumour diffusivity.

Using biomaterials for the modelling, detection and treatment of cancer is a promising strategy. Another important contribution of material science in the near future will be to help rectify the differences in disease progression and treatment between humans, animal models and patient-derived xenografts[145]. Biomaterial-based models are reductionist in nature; thus, their application in vivo could improve the reliability of animal models, making them more predictive of patient outcomes[146]. Animal models are considered the standard assay for tumour biology, and material-based

in vivo strategies are required to understand the differences between humans and animal models. For example, recombinant, chemically defined natural[147] or synthetic[45] biomaterials could be used that can actively modify tissue properties[5]. Such materials have already enabled the identification of cancer stem cells and mechanotransduction mechanisms and have demonstrated how material properties can drive tumorigenesis, making future applications in vivo promising.

The examples discussed in this Review demonstrate that biomaterials can serve as powerful tools to replicate mechanisms of disease and the response to treatments in vitro. The materials-based strategies that have enabled these discoveries should be broadly applied in the future to further improve our understanding of cancer biology and to begin to impact clinical outcomes.

Published online: 06 September 2018

1. Affo, S., Yu, L. X. & Schwabe, R. F. The role of cancer-associated fibroblasts and fibrosis in liver cancer. *Annu. Rev. Pathol.* **12**, 153–186 (2017).
2. Pankova, D. et al. Cancer-associated fibroblasts induce a collagen cross-link switch in tumor stroma. *Mol. Cancer Res.* **14**, 287–295 (2016).
3. Paszek, M. J. et al. Tensional homeostasis and the malignant phenotype. *Cancer Cell* **8**, 241–254 (2005).
   This paper uses a hydrogel–Matrigel sandwich culture system to show that initial matrix stiffness can drive loss of mammary epithelial polarity.
4. Pickup, M. W., Mouw, J. K. & Weaver, V. M. The extracellular matrix modulates the hallmarks of cancer. *EMBO Rep.* **15**, 1243–1253 (2014).
5. Levental, K. R. et al. Matrix crosslinking forces tumor progression by enhancing integrin signaling. *Cell* **139**, 891–906 (2009).
   This paper demonstrates that stiffer tissues can drive tumour growth and metastasis in vivo.
6. Mak, I. W., Evaniew, N. & Ghert, M. Lost in translation: animal models and clinical trials in cancer treatment. *Am. J. Transl Res.* **6**, 114–118 (2014).
7. Bissell, M. J., Hall, H. G. & Parry, G. How does the extracellular matrix direct gene expression? *J. Theor. Biol.* **99**, 31–68 (1982).
8. Kleinman, H. K. et al. Isolation and characterization of type IV procollagen, laminin, and heparan sulfate proteoglycan from the EHS sarcoma. *Biochemistry* **21**, 6188–6193 (1982).
9. Orkin, R. W. et al. A murine tumor producing a matrix of basement membrane. *J. Exp. Med.* **145**, 204–220 (1977).
10. Vukicevic, S. et al. Identification of multiple active growth factors in basement membrane Matrigel suggests caution in interpretation of cellular activity related to extracellular matrix components. *Exp. Cell Res.* **202**, 1–8 (1992).
11. Barcellos-Hoff, M. H., Aggeler, J., Ram, T. G. & Bissell, M. J. Functional differentiation and alveolar morphogenesis of primary mammary cultures on reconstituted basement membrane. *Development* **105**, 223–235 (1989).
12. Kenny, P. A. et al. The morphologies of breast cancer cell lines in three-dimensional assays correlate with their profiles of gene expression. *Mol. Oncol.* **1**, 84–96 (2007).
13. Petersen, O. W., Ronnovjessen, L., Howlett, A. R. & Bissell, M. J. Interaction with basement membrane serves to rapidly distinguish growth and differentiation pattern of normal and malignant human breast epithelial cells. *Proc. Natl Acad. Sci. USA* **89**, 9064–9068 (1992).
14. Paget, S. The distribution of secondary growths in cancer of the breast. *Lancet* **133**, 571–573 (1889).
15. Kalluri, R. & Zeisberg, M. Fibroblasts in cancer. *Nat. Rev. Cancer* **6**, 392–401 (2006).
16. Ozdemir, B. C. et al. Depletion of carcinoma-associated fibroblasts and fibrosis induces immunosuppression and accelerates pancreas cancer with reduced survival. *Cancer Cell* **25**, 719–734 (2014).
17. Rhim, A. D. et al. Stromal elements act to restrain, rather than support, pancreatic ductal adenocarcinoma. *Cancer Cell* **25**, 735–747 (2014).
18. Vennin, C. et al. Reshaping the tumor stroma for treatment of pancreatic cancer. *Gastroenterology* **54**, 820–838 (2018).
19. Nguyen-Ngoc, K. V. et al. ECM microenvironment regulates collective migration and local dissemination in normal and malignant mammary epithelium. *Proc. Natl Acad. Sci. USA* **109**, E2595–E2604 (2012).
20. Velez, D. O. et al. 3D collagen architecture induces a conserved migratory and transcriptional response linked to vasculogenic mimicry. *Nat. Commun.* **8**, 1651 (2017).

21. Guzman, A., Ziperstein, M. J. & Kaufman, L. J. The effect of fibrillar matrix architecture on tumor cell invasion of physically challenging environments. *Biomaterials* **35**, 6954–6963 (2014).
22. Mouw, J. K. et al. Tissue mechanics modulate microRNA-dependent PTEN expression to regulate malignant progression. *Nat. Med.* **20**, 360–367 (2014).
23. Denais, C. M. et al. Nuclear envelope rupture and repair during cancer cell migration. *Science* **352**, 353–358 (2016).
   This manuscript is the first to describe the mechanisms that enable cancer cells to migrate through pores in matrix that are smaller than the diameter of the nucleus.
24. Sodek, K. L., Brown, T. J. & Ringuette, M. J. Collagen I but not Matrigel matrices provide an MMP-dependent barrier to ovarian cancer cell penetration. *BMC Cancer* **8**, 223 (2008).
25. Wolf, K. et al. Physical limits of cell migration: control by ECM space and nuclear deformation and tuning by proteolysis and traction force. *J. Cell Biol.* **201**, 1069–1084 (2013).
26. Carey, S. P., Martin, K. E. & Reinhart-King, C. A. Three-dimensional collagen matrix induces a mechanosensitive invasive epithelial phenotype. *Sci. Rep.* **7**, 42088 (2017).
27. Friedl, P. & Wolf, K. Plasticity of cell migration: a multiscale tuning model. *J. Cell Biol.* **188**, 11–19 (2009).
28. Zaman, M. H. et al. Migration of tumor cells in 3D matrices is governed by matrix stiffness along with cell-matrix adhesion and proteolysis. *Proc. Natl Acad. Sci. USA* **103**, 10889–10894 (2006).
29. Mason, B. N., Starchenko, A., Williams, R. M., Bonassar, L. J. & Reinhart-King, C. A. Tuning three-dimensional collagen matrix stiffness independently of collagen concentration modulates endothelial cell behavior. *Acta Biomater.* **9**, 4635–4644 (2013).
30. Williams, C. M., Engler, A. J., Slone, R. D., Galante, L. L. & Schwarzbauer, J. E. Fibronectin expression modulates mammary epithelial cell proliferation during acinar differentiation. *Cancer Res.* **68**, 3185–3192 (2008).
31. Fraley, S. I. et al. A distinctive role for focal adhesion proteins in three-dimensional cell motility. *Nat. Cell Biol.* **12**, 598–604 (2010).
32. Anguiano, M. et al. Characterization of three-dimensional cancer cell migration in mixed collagen-Matrigel scaffolds using microfluidics and image analysis. *PLOS One* **12**, e0171417 (2017).
33. Steinwachs, J. et al. Three-dimensional force microscopy of cells in biopolymer networks. *Nat. Methods* **13**, 171–176 (2016).
34. Koch, T. M., Munster, S., Bonakdar, N., Butler, J. P. & Fabry, B. 3D Traction Forces in Cancer Cell Invasion. *PLOS One* **7**, e33476 (2012).
35. Miller, J. P. et al. Clinical doses of radiation reduce collagen matrix stiffness. *APL Bioeng.* **2**, 031901 (2018).
36. Beck, J. N., Singh, A., Rothenberg, A. R., Elisseeff, J. H. & Ewald, A. J. The independent roles of mechanical, structural and adhesion characteristics of 3D hydrogels on the regulation of cancer invasion and dissemination. *Biomaterials* **34**, 9486–9495 (2013).
37. Wen, J. H. et al. Interplay of matrix stiffness and protein tethering in stem cell differentiation. *Nat. Mater.* **13**, 979–987 (2014).
38. Taubenberger, A. V. et al. 3D extracellular matrix interactions modulate tumour cell growth, invasion and angiogenesis in engineered tumour microenvironments. *Acta Biomater.* **36**, 73–85 (2016).
39. Loessner, D. et al. Bioengineered 3D platform to explore cell–ECM interactions and drug resistance of epithelial ovarian cancer cells. *Biomaterials* **31**, 8494–8506 (2010).
40. Alcaraz, J. et al. Laminin and biomimetic extracellular elasticity enhance functional differentiation in mammary epithelia. *EMBO J.* **27**, 2829–2838 (2008).
41. Reticker-Flynn, N. E. et al. A combinatorial extracellular matrix platform identifies cell-extracellular matrix interactions that correlate with metastasis. *Nat. Commun.* **3**, 1122 (2012).
   This paper highlights how non-additive matrix properties, specifically the combination of multiple matrix proteins, can drive metastatic behaviour.
42. Kraning-Rush, C. M., Califano, J. P. & Reinhart-King, C. A. Cellular traction stresses increase with increasing metastatic potential. *PLOS One* **7**, e32572 (2012).
43. Leight, J. L., Wozniak, M. A., Chen, S., Lynch, M. L. & Chen, C. S. Matrix rigidity regulates a switch between TGF-β1-induced apoptosis and epithelial-mesenchymal transition. *Mol. Biol. Cell* **23**, 781–791 (2012).
44. Stowers, R. S., Allen, S. C. & Suggs, L. J. Dynamic phototuning of 3D hydrogel stiffness. *Proc. Natl Acad. Sci. USA* **112**, 1953–1958 (2015).
45. Wei, S. C. et al. Matrix stiffness drives epithelial–mesenchymal transition and tumor metastasis through a TWIST1–G3BP2 mechanotransduction pathway. *Nat. Cell Biol.* **17**, 678–688 (2015).
46. Fenner, J. et al. Macroscopic stiffness of breast tumors predicts metastasis. *Sci. Rep.* **4**, 5512 (2014).
47. Tse, J. R. & Engler, A. J. Preparation of hydrogel substrates with tunable mechanical properties. *Curr. Protoc. Cell Biol* **47**, 10.16.1–10.16.16 (2010).
48. Emerman, J. T. & Pitelka, D. R. Maintenance and induction of morphological differentiation in dissociated mammary epithelium on floating collagen membranes. *In Vitro* **13**, 316–328 (1977).
49. Bissell, M. J. The differentiated state of normal and malignant cells or how to define a "normal" cell in culture. *Int. Rev. Cytol.* **70**, 27–100 (1981).
50. Pang, M. F. et al. Tissue stiffness and hypoxia modulate the integrin-linked kinase ILK to control breast cancer stem-like cells. *Cancer Res.* **76**, 5277–5287 (2016).
51. Jabbari, E., Sarvestani, S. K., Daneshian, L. & Moeinzadeh, S. Optimum 3D matrix stiffness for maintenance of cancer stem cells is dependent on tissue origin of cancer cells. *PLOS One* **10**, e0132377 (2015).
52. Shu, X. Z., Ahmad, S., Liu, Y. & Prestwich, G. D. Synthesis and evaluation of injectable, in situ crosslinkable synthetic extracellular matrices for tissue engineering. *J. Biomed. Mater. Res. A* **79**, 902–912 (2006).
53. Young, J. L. & Engler, A. J. Hydrogels with time-dependent material properties enhance cardiomyocyte differentiation in vitro. *Biomaterials* **32**, 1002–1009 (2011).
54. Guvendiren, M. & Burdick, J. A. Stiffening hydrogels to probe short- and long-term cellular responses to dynamic mechanics. *Nat. Commun.* **3**, 792 (2012).
55. Ondeck, M. G. & Engler, A. J. Mechanical characterization of a dynamic and tunable methacrylated hyaluronic acid hydrogel. *J. Biomech. Eng.* **138**, 021003 (2016).
56. Stowers, R. S. et al. Extracellular matrix stiffening induces a malignant phenotypic transition in breast epithelial cells. *Cell. Mol. Bioeng.* **10**, 114–123 (2017).
   Temporal changes in matrix stiffness can modulate mammary epithelial cell responses in a different way than static materials, which when stiff, always induce phenotype transitions.
57. Kloxin, A. M., Kasko, A. M., Salinas, C. N. & Anseth, K. S. Photodegradable hydrogels for dynamic tuning of physical and chemical properties. *Science* **324**, 59–63 (2009).

58. Maghdouri-White, Y., Elmore, L. W., Bowlin, G. L. & Dreau, D. Breast epithelial cell infiltration in enhanced electrospun silk scaffolds. *J. Tissue Eng. Regen Med.* **10**, E121–131 (2016).

59. Chen, Z. et al. Electrospun nanofibers for cancer diagnosis and therapy. *Biomater. Sci.* **4**, 922–932 (2016).

60. Kushiro, K., Yaginuma, T., Ryo, A. & Takai, M. Differences in three-dimensional geometric recognition by non-cancerous and cancerous epithelial cells on microgroove-based topography. *Sci. Rep.* **7**, 4244 (2017).

61. Ning, D. et al. Mechanical and morphological analysis of cancer cells on nanostructured substrates. *Langmuir* **32**, 2718–2723 (2016).

62. Chaudhuri, P. K., Pan, C. Q., Low, B. C. & Lim, C. T. Topography induces differential sensitivity on cancer cell proliferation via Rho-ROCK-Myosin contractility. *Sci. Rep.* **6**, 19672 (2016).

63. Ulrich, T. A., Jaim, A., Tanner, K., MacKay, J. L. & Kumar, S. Probing cellular mechanobiology in three-dimensional culture with collagen-agarose matrices. *Biomaterials* **31**, 1875–1884 (2010).

64. Pathak, A. & Kumar, S. Independent regulation of tumor cell migration by matrix stiffness and confinement. *Proc. Natl Acad. Sci. USA* **109**, 10334–10339 (2012).

65. Attieh, Y. & Vignjevic, D. M. The hallmarks of CAFs in cancer invasion. *Eur. J. Cell Biol.* **95**, 493–502 (2016).

66. Hanahan, D. & Weinberg, R. A. Hallmarks of cancer: the next generation. *Cell* **144**, 646–674 (2011).

67. Gaggioli, C. et al. Fibroblast-led collective invasion of carcinoma cells with differing roles for RhoGTPases in leading and following cells. *Nat. Cell Biol.* **9**, 1392–1400 (2007).

68. Goetz, J. G. et al. Biomechanical remodeling of the microenvironment by stromal caveolin-1 favors tumor invasion and metastasis. *Cell* **146**, 148–163 (2011).

69. Glentis, A. et al. Cancer-associated fibroblasts induce metalloprotease-independent cancer cell invasion of the basement membrane. *Nat. Commun.* **8**, 924 (2017).

70. Wang, K. et al. Stiffening and unfolding of early deposited-fibronectin increase proangiogenic factor secretion by breast cancer-associated stromal cells. *Biomaterials* **54**, 63–71 (2015).

71. Labernadie, A. et al. A mechanically active heterotypic E-cadherin/N-cadherin adhesion enables fibroblasts to drive cancer cell invasion. *Nat. Cell Biol.* **19**, 224–237 (2017).

72. Calvo, F. et al. Mechanotransduction and YAP-dependent matrix remodelling is required for the generation and maintenance of cancer-associated fibroblasts. *Nat. Cell Biol.* **15**, 637–646 (2013).

73. Chen, M. B. et al. On-chip human microvasculature assay for visualization and quantification of tumor cell extravasation dynamics. *Nat. Protoc.* **12**, 865–880 (2017).

74. Lee, H., Park, W., Ryu, H. & Jeon, N. L. A microfluidic platform for quantitative analysis of cancer angiogenesis and intravasation. *Biomicrofluidics* **8**, 054102 (2014).

75. Zervantonakis, I. K. et al. Three-dimensional microfluidic model for tumor cell intravasation and endothelial barrier function. *Proc. Natl Acad. Sci. USA* **109**, 13515–13520 (2012).

76. Chen, M. B., Whisler, J. A., Jeon, J. S. & Kamm, R. D. Mechanisms of tumor cell extravasation in an in vitro microvascular network platform. *Integr. Biol.* **5**, 1262–1271 (2013).

77. Bersini, S. et al. A microfluidic 3D in vitro model for specificity of breast cancer metastasis to bone. *Biomaterials* **35**, 2454–2461 (2014).

78. Saquib, N., Saquib, J. & Ioannidis, J. P. Does screening for disease save lives in asymptomatic adults? Systematic review of meta-analyses and randomized trials. *Int. J. Epidemiol.* **44**, 264–277 (2015).

79. Zhang, Z. et al. Expansion of CTCs from early stage lung cancer patients using a microfluidic co-culture model. *Oncotarget* **5**, 12383–12397 (2014).

80. Mehta, S. et al. Predictive and prognostic molecular markers for cancer medicine. *Ther. Adv. Med. Oncol.* **2**, 125–148 (2010).

81. Qian, W. Y., Zhang, Y. & Chen, W. Q. Capturing cancer: emerging microfluidic technologies for the capture and characterization of circulating tumor cells. *Small* **11**, 3850–3872 (2015).

82. Chen, W. Q. et al. Nanoroughened surfaces for efficient capture of circulating tumor cells without using capture antibodies. *ACS Nano* **7**, 566–575 (2013).

83. Park, G. S. et al. Full surface embedding of gold clusters on silicon nanowires for efficient capture and photothermal therapy of circulating tumor cells *Nano Lett.* **12**, 2176–2176 (2012).

84. Zhai, T. T., Ye, D. K., Zhang, Q. W., Wu, Z. Q. & Xia, X. H. Highly efficient capture and electrochemical release of circulating tumor cells by using aptamers modified gold nanowire arrays. *ACS Appl. Mater. Interfaces* **9**, 34706–34714 (2017).

85. Zhang, W., Zhao, K., Banks, C. E. & Zhang, Y. Antibody-modified hydroxyapatite surfaces for the efficient capture of bladder cancer cells in a patient's urine without recourse to any sample pre-treatment. *J. Mater. Chem. B* **5**, 8125–8132 (2017).

86. Xu, H. W. et al. Three-dimensional inverse opal photonic crystal substrates toward efficient capture of circulating tumor cells. *ACS Appl. Mater. Interfaces* **9**, 30510–30518 (2017).

87. Zhang, J. et al. Surface chemistry induces mitochondria-mediated apoptosis of breast cancer cells via PTEN/PI3K/AKT signaling pathway. *Biochim. Biophys. Acta Mol. Cell Res.* **1865**, 172–185 (2018).

88. Jan, Y. J. et al. NanoVelcro rare-cell assays for detection and characterization of circulating tumor cells. *Adv. Drug Deliv. Rev.* **125**, 78–93 (2018).

89. Wang, L. X., Asghar, W., Demirci, U. & Wan, Y. Nanostructured substrates for isolation of circulating tumor cells. *Nano Today* **8**, 374–387 (2013).

90. Wang, S. T. et al. Three-dimensional nanostructured substrates toward efficient capture of circulating tumor cells. *Angew. Chem. Int. Ed.* **48**, 8970–8973 (2009).

91. Wang, S. T. et al. Highly efficient capture of circulating tumor cells by using nanostructured silicon substrates with integrated chaotic micromixers. *Angew. Chem. Int. Ed.* **50**, 3084–3088 (2011).

92. Guo, S. et al. Degradable zinc-phosphate-based hierarchical nanosubstrates for capture and release of circulating tumor cells. *ACS Appl. Mater. Interfaces* **8**, 15917–15925 (2016).

93. Lou, H. Y. et al. Dual-functional lipid coating for the nanopillar-based capture of circulating tumor cells with high purity and efficiency. *Langmuir* **33**, 1097–1104 (2017).

94. Sun, N. et al. Chitosan nanofibers for specific capture and nondestructive release of CTCs assisted by pCBMA brushes. *Small* **12**, 5090–5097 (2016).

95. Rao, S. S. et al. Enhanced survival with implantable scaffolds that capture metastatic breast cancer cells in vivo. *Cancer Res.* **76**, 5209–5218 (2016).

96. Azarin, S. M. et al. In vivo capture and label-free detection of early metastatic cells. *Nat. Commun.* **6**, 8094 (2015).
This paper describes an implantable hydrogel-based method to capture cells that have intravasated from tumours.

97. Aguado, B. A. et al. Extracellular matrix mediators of metastatic cell colonization characterized using scaffold mimics of the pre-metastatic niche. *Acta Biomater.* **33**, 13–24 (2016).

98. Qian, B. Z. et al. CCL2 recruits inflammatory monocytes to facilitate breast-tumour metastasis. *Nature* **475**, 222–U129 (2011).

99. Kitamura, T., Qian, B. Z. & Pollard, J. W. Immune cell promotion of metastasis. *Nat. Rev. Immunol.* **15**, 73–86 (2015).

100. Hiratsuka, S., Watanabe, A., Aburatani, H. & Maru, Y. Tumour-mediated upregulation of chemoattractants and recruitment of myeloid cells predetermines lung metastasis. *Nat. Cell Biol.* **8**, 1369–U1331 (2006).

101. Mauro, N., Scialabba, C., Pitarresi, G. & Giammona, G. Enhanced adhesion and in situ photothermal ablation of cancer cells in surface-functionalized electrospun microfiber scaffold with graphene oxide. *Int. J. Pharm.* **526**, 167–177 (2017).

102. Ma, H. S. et al. A bifunctional biomaterial with photothermal effect for tumor therapy and bone regeneration. *Adv. Funct. Mater.* **26**, 1197–1208 (2016).

103. Aguado, B. A. et al. Secretome identification of immune cell factors mediating metastatic cell homing. *Sci. Rep.* **5**, 17566 (2015).

104. de la Fuente, A. et al. M-trap: exosome-based capture of tumor cells as a new technology in peritoneal metastasis. *J. Natl Cancer Inst.* **107**, djv184 (2015).

105. Seib, F. P., Berry, J. E., Shiozawa, Y., Taichman, R. S. & Kaplan, D. L. Tissue engineering a surrogate niche for metastatic cancer cells. *Biomaterials* **51**, 313–319 (2015).

106. Aguado, B. A., Bushnell, G. G., Rao, S. S., Jeruss, J. S. & Shea, L. D. Engineering the pre-metastatic niche. *Nat. Biomed. Eng.* **1**, 0077 (2017).

107. Davidson, P. M., Denais, C., Bakshi, M. C. & Lammerding, J. Nuclear deformability constitutes a rate-limiting step during cell migration in 3-D environments. *Cell. Mol. Bioeng.* **7**, 293–306 (2014).

108. Yao, N. et al. Structure and function analysis in circulating tumor cells: using nanotechnology to study nuclear size in prostate cancer. *Am. J. Clin. Exp. Urol.* **6**, 43–54 (2018).

109. Chen, J. F. et al. Subclassification of prostate cancer circulating tumor cells by nuclear size reveals very small nuclear circulating tumor cells in patients with visceral metastases. *Cancer* **121**, 3240–3251 (2015).

110. Alibert, C., Goud, B. & Manneville, J. B. Are cancer cells really softer than normal cells? *Biol. Cell* **109**, 167–189 (2017).

111. Guo, Q., Park, S. & Ma, H. S. Microfluidic micropipette aspiration for measuring the deformability of single cells. *Lab. Chip* **12**, 2687–2695 (2012).

112. Mak, M. & Erickson, D. A serial micropipette microfluidic device with applications to cancer cell repeated deformation studies. *Integr. Biol.* **5**, 1374–1384 (2013).

113. Malboubi, M., Jayo, A., Parsons, M. & Charras, G. An open access microfluidic device for the study of the physical limits of cancer cell deformation during migration in confined environments. *Microelectron. Eng.* **144**, 42–45 (2015).

114. Gossett, D. R. et al. Hydrodynamic stretching of single cells for large population mechanical phenotyping. *Proc. Natl Acad. Sci. USA* **109**, 7630–7635 (2012).
This paper demonstrates a high-throughput single cell microfluidic-based deformability cytometry assay showing that mechanical properties of cells can be used to separate populations with different metastatic potentials.

115. Dudani, J. S., Gossett, D. R., Tse, H. T. K. & Di Carlo, D. Pinched-flow hydrodynamic stretching of single-cells. *Lab. Chip* **13**, 3728–3734 (2013).

116. Qi, D. et al. Screening cell mechanotype by parallel microfiltration. *Sci. Rep.* **5**, 17595 (2015).

117. Nyberg, K. D. et al. The physical origins of transit time measurements for rapid, single cell mechanotyping. *Lab. Chip* **16**, 3330–3339 (2016).

118. Palmer, C. P. et al. Single cell adhesion measuring apparatus (SCAMA): application to cancer cell lines of different metastatic potential and voltage-gated Na⁺ channel expression. *Eur. Biophys. J.* **37**, 359–368 (2008).

119. Veiseh, M. et al. Cellular heterogeneity profiling by hyaluronan probes reveals an invasive but slow-growing breast tumor subset. *Proc. Natl Acad. Sci. USA* **111**, E1731–E1739 (2014).

120. Bijian, K. et al. Targeting focal adhesion turnover in invasive breast cancer cells by the purine derivative reversine. *Br. J. Cancer* **109**, 2810–2818 (2013).

121. Fuhrmann, A., Banisadr, A., Beri, P., Tlsty, T. D. & Engler, A. J. Metastatic state of cancer cells may be indicated by adhesion strength. *Biophys. J.* **112**, 736–745 (2017).

122. Seltzer, M. H., Rosato, F. E. & Fletcher, M. J. Serum and tissue magnesium levels in human breast carcinoma. *J. Surg. Res.* **10**, 159–162 (1970).

123. Seltzer, M. H., Rosato, F. E. & Fletcher, M. J. Serum and tissue calcium in human breast carcinoma. *Cancer Res.* **30**, 615–616 (1970).

124. Zhou, Z. X. & Lu, Z. R. Molecular imaging of the tumor microenvironment. *Adv. Drug Deliv. Rev.* **113**, 24–48 (2017).

125. Chaabane, L. et al. In vivo MR imaging of fibrin in a neuroblastoma tumor model by means of a targeting Gd-containing peptide. *Mol. Imag. Biol.* **17**, 819–828 (2015).

126. Starmans, L. W. E. et al. Noninvasive visualization of tumoral fibrin deposition using a peptidic fibrin-binding single photon emission computed tomography tracer. *Mol. Pharm.* **12**, 1921–1928 (2015).

127. Obonai, T. et al. Tumour imaging by the detection of fibrin clots in tumour stroma using an anti-fibrin Fab fragment. *Sci. Rep.* **6**, 23613 (2016).

128. van Mourik, T. R., Claesener, M., Nicolay, K. & Grull, H. Development of a novel, fibrin-specific PET tracer. *J. Labelled Comp. Radiopharm.* **60**, 286–293 (2017).

129. Zhou, Z. X. et al. MRI detection of breast cancer micrometastases with a fibronectin-targeting contrast agent. *Nat. Commun.* **6**, 7984 (2015).

130. Li, C. L. et al. Fibronectin induces epithelial-mesenchymal transition in human breast cancer MCF-7 cells via activation of calpain. *Oncol. Lett.* **13**, 3889–3895 (2017).

131. Han, Z. & Lu, Z. R. Targeting fibronectin for cancer imaging and therapy. *J. Mater. Chem. B* **5**, 639–654 (2017).
132. Heidari, P. et al. Imaging of secreted extracellular periostin, an important marker of invasion in the tumor microenvironment in esophageal cancer. *J. Nuclear Med.* **56**, 1246–1251 (2015).
133. Khawar, I. A., Kim, J. H. & Kuh, H. J. Improving drug delivery to solid tumors: priming the tumor microenvironment. *J. Control. Release* **201**, 78–89 (2015).
134. Grossman, M. et al. Tumor cell invasion can be blocked by modulators of collagen fibril alignment that control assembly of the extracellular matrix. *Cancer Res.* **76**, 4249–4258 (2016).
135. Theocharis, A. D., Skandalis, S. S., Gialeli, C. & Karamanos, N. K. Extracellular matrix structure. *Adv. Drug Deliv. Rev.* **97**, 4–27 (2016).
136. Provenzano, P. P. et al. Enzymatic targeting of the stroma ablates physical barriers to treatment of pancreatic ductal adenocarcinoma. *Cancer Cell* **21**, 418–429 (2012).
137. Jacobetz, M. A. et al. Hyaluronan impairs vascular function and drug delivery in a mouse model of pancreatic cancer. *Gut* **62**, 112–120 (2013).
138. Hingorani, S. R. et al. Phase Ib study of PEGylated recombinant human hyaluronidase and gemcitabine in patients with advanced pancreatic cancer. *Clin. Cancer Res.* **22**, 2848–2854 (2016).
139. Lee, S. et al. Extracellular matrix remodeling in vivo for enhancing tumor-targeting efficiency of nanoparticle drug carriers using the pulsed high intensity focused ultrasound. *J. Control. Release* **263**, 68–78 (2017).
140. Baronzio, G., Parmar, G. & Baronzio, M. Overview of methods for overcoming hindrance to drug delivery to tumors, with special attention to tumor interstitial fluid. *Front. Oncol.* **5**, 165 (2015).

141. Yhee, J. Y. et al. Effects of tumor microenvironments on targeted delivery of glycol chitosan nanoparticles. *J. Control. Release* **267**, 223–231 (2017).
142. Nicolas-Boluda, A., Silva, A. K. A., Fournel, S. & Gazeau, F. Physical oncology: new targets for nanomedicine. *Biomaterials* **150**, 87–99 (2018).
143. Marangon, I. et al. Tumor stiffening, a key determinant of tumor progression, is reversed by nanomaterial-induced photothermal therapy. *Theranostics* **7**, 329–343 (2017).
144. Raeesi, V. & Chan, W. C. W. Improving nanoparticle diffusion through tumor collagen matrix by photo-thermal gold nanorods. *Nanoscale* **8**, 12524–12530 (2016).
145. Schuh, J. C. Trials, tribulations, and trends in tumor modeling in mice. *Toxicol. Pathol.* **32**, 53–66 (2004).
146. Day, C. P., Merlino, G. & Van Dyke, T. Preclinical mouse cancer models: a maze of opportunities and challenges. *Cell* **163**, 39–53 (2015).
147. Quintana, E. et al. Efficient tumour formation by single human melanoma cells. *Nature* **456**, 593–598 (2008).
148. Tzvetkova-Chevolleau, T. et al. The motility of normal and cancer cells in response to the combined influence of the substrate rigidity and anisotropic microstructure. *Biomaterials* **29**, 1541–1551 (2008).
149. Zhu, J. Bioactive modification of poly(ethylene glycol) hydrogels for tissue engineering. *Biomaterials* **31**, 4639–4656 (2010).
150. Lewis, K. J. R. et al. Epithelial-mesenchymal crosstalk influences cellular behavior in a 3D alveolus-fibroblast model system. *Biomaterials* **155**, 124–134 (2018).
151. Fischbach, C. et al. Engineering tumors with 3D scaffolds. *Nat. Methods* **4**, 855–860 (2007).
152. Makadia, H. K. & Siegel, S. J. Poly lactic-co-glycolic acid (PLGA) as biodegradable controlled drug delivery carrier. *Polymers* **3**, 1377–1397 (2011).

153. Choi, Y. S. et al. The alignment and fusion assembly of adipose-derived stem cells on mechanically patterned matrices. *Biomaterials* **33**, 6943–6951 (2012).
154. Nasrollahi, S. et al. Past matrix stiffness primes epithelial cells and regulates their future collective migration through a mechanical memory. *Biomaterials* **146**, 146–155 (2017).
155. Zustiak, S., Nossal, R. & Sackett, D. L. Multiwell stiffness assay for the study of cell responsiveness to cytotoxic drugs. *Biotechnol. Bioeng.* **111**, 396–403 (2014).
156. Chaudhuri, O. et al. Extracellular matrix stiffness and composition jointly regulate the induction of malignant phenotypes in mammary epithelium. *Nat. Mater.* **13**, 970–978 (2014).
157. Fang, J. Y., Tan, S. J., Yang, Z., Tayag, C. & Han, B. Tumor bioengineering using a transglutaminase crosslinked hydrogel. *PLOS One* **9**, e105616 (2014).

Author contributions
P.B., J.Y. and A.J.E. organized the manuscript content. The manuscript was written by all authors.

Competing interests
The authors declare no competing interests.

Publisher's note
Springer Nature remains neutral with regard to jurisdictional claims in published maps and institutional affiliations.

4. CONSIDERAÇÕES FINAIS

A relação das células tumorais com os diversos fatores do microambiente tumoral leva a diferenças na expressão gênica e no fenótipo dessas células. Como consequência, observa-se que as células tumorais apresentam diferenças entre si, assim como a região do tumor influencia no fenótipo das células. Dentre os fatores que influenciam o comportamento das células tumorais, foi observado que a rigidez da matriz extracelular tem efeito sobre elas em relação a sua expressão gênica e comportamento migratório. Neste sentido de estudar as características físicas do microambiente tumoral, também foi visto que existe uma gama de biomateriais disponíveis que estão permitindo uma melhor compreensão dos efeitos das características físicas do microambiente tumoral sobre a progressão da doença. Portanto, compreender estes efeitos é essencial para buscar por opções inovadoras de diagnóstico e tratamento do câncer.

A presente tese demonstrou que:

- Os estudos que realizam reação da transcriptase reversa com reação em cadeia da polimerase em tempo real em carcinoma espinocelular oral utilizam principalmente GAPDH e β-actina como genes de referência;

- Existe variabilidade da expressão gênica, mesmo de genes de referência, entre as linhagens de células o que demonstra a importância de verificar qual gene de referência é o mais estável dentro das condições experimentais;

- O perfil de expressão gênica, observada via transcriptograma, das regiões do carcinoma espinocelular de cabeça e pescoço apresentam diferenças as quais também foram observadas entre os tecidos sadios o que aponta para a variabilidade existente dentre dos nossos organismos;

- A rigidez do microambiente tumoral é capaz de alterar a expressão gênica e determinar alterações no comportamento das células tumorais;

- Presença de estroma com colágeno organizado em espécimes de carcinoma espinocelular oral de pacientes está correlacionado a um pior prognóstico para os pacientes;
- Diversos biomateriais estão disponíveis para o estudo dos aspectos físicos do microambiente tumoral, sendo que cada um possui vantagens e desvantagens;
- A utilização de biomateriais para detecção de células tumorais, avaliação de prognóstico e potenciais tratamentos vem crescendo como campo de estudo.

5. PERSPECTIVAS

Nas últimas décadas, a capacidade de análise dos tumores passou de um ou alguns genes por vez para sequenciamento de todo o genoma. A ampliação do conhecimento sobre a iniciação e progressão tumoral permite o levantamento de novos questionamentos, novos modelos de estudo e novos conhecimentos. Com o crescente número de evidências sobre a variabilidade dos tumores e maior acesso ao sequenciamento genético, são importantes as iniciativas em coletar e analisar estes dados para permitir identificação de padrões. A criação de bancos de dados com informações biológicas e clínicas, permitirá com que o tratamento do câncer possa fazer parte da Quarta Revolução Industrial, ou Indústria 4.0, que vivenciamos em outras áreas do conhecimento. Ou seja, a identificação de padrões utilizando *big data* e *machine learning* nos dados dos tumores podem levar a uma terapia individualizada para cada padrão. Contudo, devido a essa grande variabilidade existente nos tumores, apenas com um grande número de informações é possível criar estes padrões e, muito provavelmente, dentro de um mesmo grupo de tumores, existem diversos padrões. Ainda assim, o levantamento e análise destes dados podem trazer informações extremamente relevantes em relação ao diagnóstico e prognóstico da doença.

Outro ponto a ser observado é em relação ao avanço de metodologias laboratoriais capazes de mimetizar os microambiente tumorais. Neste sentido, o uso de biomateriais e culturas tridimensionais de células estão se tornando ferramentais importantes para avaliar as células tumorais e do microambiente tumoral bem como para desenvolver novas modalidades de tratamento. A importância de bons modelos para o desenvolvimento de novas terapias é fundamental para reduzir o tempo e o custo deste desenvolvimento, assim tornando as pesquisas *in vitro* cada vez mais reprodutíveis ao que acontece *in vivo*. Dentro destes modelos de estudos utilizando biomateriais, é observada a influência que a rigidez do ambiente exerce no fenótipo das células tumorais, modulando inclusive sua expressão gênica. Como é observado o endurecimento dos tecidos tumorais e peritumorais em diversos tipos de neoplasias, esta é uma característica que também pode ser alvo de terapias que complementem o

tratamento dos tumores. Além disso, a influência da rigidez dos tecidos pode ser fundamental em outras patologias, como em doenças cardiovasculares.

Além de permitir estudos de mecanismos tumorais, o estudo dos biomateriais vem crescendo recentemente pelo potencial de utilização no diagnóstico, avaliação de prognóstico e tratamento das doenças. Por exemplo, utilizar biomateriais como ferramenta de avaliação das características das células tumorais para auxiliar na decisão de tratamento e prognóstico da doença. Dessa maneira, cada vez mais nos aproximamos de desenvolver terapias individuais, seguindo a ideia de medicina personalizada, para melhorarmos o prognóstico de pacientes diagnosticados com câncer. Portanto, acredita-se que diversos avanços estão sendo feitos com o intuito de expandir o conhecimento, mas concomitantemente com o objetivo de cruzar estas informações para qualificar nosso conhecimento e poder alcançar a prática clínica.

REFERÊNCIAS

ALVES, A. M.; DIEL, L. F.; LAMERS, M. L. Macrophages and prognosis of oral squamous cell carcinoma: A systematic review. **J Oral Pathol Med,** v. 47, n. 5, p. 460-467, May 2018. ISSN 1600-0714. Disponível em: < https://www.ncbi.nlm.nih.gov/pubmed/28940738 >.

ANDERSEN, C. L.; JENSEN, J. L.; ØRNTOFT, T. F. Normalization of real-time quantitative reverse transcription-PCR data: a model-based variance estimation approach to identify genes suited for normalization, applied to bladder and colon cancer data sets. **Cancer Res,** v. 64, n. 15, p. 5245-50, Aug 2004. ISSN 0008-5472. Disponível em: < https://www.ncbi.nlm.nih.gov/pubmed/15289330 >.

ATTIEH, Y.; VIGNJEVIC, D. M. The hallmarks of CAFs in cancer invasion. **Eur J Cell Biol,** v. 95, n. 11, p. 493-502, Nov 2016. ISSN 1618-1298. Disponível em: < https://www.ncbi.nlm.nih.gov/pubmed/27575401 >.

BECELLI, R. et al. Intracellular and extracellular tumor pH measurement in a series of patients with oral cancer. **J Craniofac Surg,** v. 18, n. 5, p. 1051-4, Sep 2007. ISSN 1049-2275. Disponível em: < https://www.ncbi.nlm.nih.gov/pubmed/17912080 >.

BENTON, G. et al. Matrigel: from discovery and ECM mimicry to assays and models for cancer research. **Adv Drug Deliv Rev,** v. 79-80, p. 3-18, Dec 2014. ISSN 1872-8294. Disponível em: < https://www.ncbi.nlm.nih.gov/pubmed/24997339 >.

BERTOUT, J. A.; PATEL, S. A.; SIMON, M. C. The impact of O2 availability on human cancer. **Nat Rev Cancer,** v. 8, n. 12, p. 967-75, Dec 2008. ISSN 1474-1768. Disponível em: < https://www.ncbi.nlm.nih.gov/pubmed/18987634 >.

BIASOLI, É. et al. Lip Cancer: A Clinicopathological Study and Treatment Outcomes in a 25-Year Experience. **J Oral Maxillofac Surg,** v. 74, n. 7, p. 1360-7, Jul 2016. ISSN 1531-5053. Disponível em: < https://www.ncbi.nlm.nih.gov/pubmed/26917204 >.

BISSELL, M. J.; HALL, H. G.; PARRY, G. How does the extracellular matrix direct gene expression? **J Theor Biol,** v. 99, n. 1, p. 31-68, Nov 1982. ISSN 0022-5193. Disponível em: < https://www.ncbi.nlm.nih.gov/pubmed/6892044 >.

BISWAS, S. K.; ALLAVENA, P.; MANTOVANI, A. Tumor-associated macrophages: functional diversity, clinical significance, and open questions. **Semin Immunopathol,** v. 35, n. 5, p. 585-600, Sep 2013. ISSN 1863-2300. Disponível em: < https://www.ncbi.nlm.nih.gov/pubmed/23657835 >.

BONNANS, C.; CHOU, J.; WERB, Z. Remodelling the extracellular matrix in development and disease. **Nat Rev Mol Cell Biol,** v. 15, n. 12, p. 786-801, Dec 2014. ISSN 1471-0080. Disponível em: < https://www.ncbi.nlm.nih.gov/pubmed/25415508 >.

BOTA, J. P.; LYONS, A. B.; CARROLL, B. T. Squamous Cell Carcinoma of the Lip-A Review of Squamous Cell Carcinogenesis of the Mucosal and Cutaneous Junction. **Dermatol Surg,** v. 43, n. 4, p. 494-506, Apr 2017. ISSN 1524-4725. Disponível em: < https://www.ncbi.nlm.nih.gov/pubmed/28157733 >.

BUSTIN, S. A. Quantification of mRNA using real-time reverse transcription PCR (RT-PCR): trends and problems. **J Mol Endocrinol,** v. 29, n. 1, p. 23-39, Aug 2002. ISSN 0952-5041. Disponível em: < https://www.ncbi.nlm.nih.gov/pubmed/12200227 >.

BUSTIN, S. A. et al. The MIQE guidelines: minimum information for publication of quantitative real-time PCR experiments. **Clin Chem,** v. 55, n. 4, p. 611-22, Apr

2009. ISSN 1530-8561. Disponível em: < https://www.ncbi.nlm.nih.gov/pubmed/19246619 >.

CAO, Z. et al. Angiocrine factors deployed by tumor vascular niche induce B cell lymphoma invasiveness and chemoresistance. **Cancer Cell,** v. 25, n. 3, p. 350-65, Mar 2014. ISSN 1878-3686. Disponível em: < https://www.ncbi.nlm.nih.gov/pubmed/24651014 >.

CHAPMAN, J. R.; WALDENSTRÖM, J. With Reference to Reference Genes: A Systematic Review of Endogenous Controls in Gene Expression Studies. **PLoS One,** v. 10, n. 11, p. e0141853, 2015. ISSN 1932-6203. Disponível em: < https://www.ncbi.nlm.nih.gov/pubmed/26555275 >.

CHAUDHURI, P. K. et al. Topography induces differential sensitivity on cancer cell proliferation via Rho-ROCK-Myosin contractility. **Sci Rep,** v. 6, p. 19672, Jan 2016. ISSN 2045-2322. Disponível em: < https://www.ncbi.nlm.nih.gov/pubmed/26795068 >.

CHOUDHARY, M. M. et al. Interleukin-6 role in head and neck squamous cell carcinoma progression. **World J Otorhinolaryngol Head Neck Surg,** v. 2, n. 2, p. 90-97, Jun 2016. ISSN 2095-8811. Disponível em: < https://www.ncbi.nlm.nih.gov/pubmed/29204553 >.

COLLEY, H. E. et al. Development of tissue-engineered models of oral dysplasia and early invasive oral squamous cell carcinoma. **Br J Cancer,** v. 105, n. 10, p. 1582-92, Nov 2011. ISSN 1532-1827. Disponível em: < https://www.ncbi.nlm.nih.gov/pubmed/21989184 >.

COOPER, J. S. et al. National Cancer Database report on cancer of the head and neck: 10-year update. **Head Neck,** v. 31, n. 6, p. 748-58, Jun 2009. ISSN 1097-0347. Disponível em: < https://www.ncbi.nlm.nih.gov/pubmed/19189340 >.

CORBET, C.; FERON, O. Tumour acidosis: from the passenger to the driver's seat. **Nat Rev Cancer,** v. 17, n. 10, p. 577-593, 10 2017. ISSN 1474-1768. Disponível em: < https://www.ncbi.nlm.nih.gov/pubmed/28912578 >.

COX, T. R.; ERLER, J. T. Remodeling and homeostasis of the extracellular matrix: implications for fibrotic diseases and cancer. **Dis Model Mech,** v. 4, n. 2, p. 165-78, Mar 2011. ISSN 1754-8411. Disponível em: < https://www.ncbi.nlm.nih.gov/pubmed/21324931 >.

DA SILVA, S. D. et al. Advances and applications of oral cancer basic research. **Oral Oncol,** v. 47, n. 9, p. 783-91, Sep 2011. ISSN 1879-0593. Disponível em: < https://www.ncbi.nlm.nih.gov/pubmed/21802978 >.

DA SILVA, V. P. et al. Effects of extracellular acidity on resistance to chemotherapy treatment: a systematic review. **Med Oncol,** v. 35, n. 12, p. 161, Oct 2018. ISSN 1559-131X. Disponível em: < https://www.ncbi.nlm.nih.gov/pubmed/30377828 >.

DAGOGO-JACK, I.; SHAW, A. T. Tumour heterogeneity and resistance to cancer therapies. **Nat Rev Clin Oncol,** v. 15, n. 2, p. 81-94, Feb 2018. ISSN 1759-4782. Disponível em: < https://www.ncbi.nlm.nih.gov/pubmed/29115304 >.

DE ALMEIDA, R. M. et al. Transcriptome analysis reveals manifold mechanisms of cyst development in ADPKD. **Hum Genomics,** v. 10, n. 1, p. 37, 11 2016. ISSN 1479-7364. Disponível em: < https://www.ncbi.nlm.nih.gov/pubmed/27871310 >.

DE JONGE, H. J. et al. Evidence based selection of housekeeping genes. **PLoS One,** v. 2, n. 9, p. e898, Sep 2007. ISSN 1932-6203. Disponível em: < https://www.ncbi.nlm.nih.gov/pubmed/17878933 >.

DE PALMA, M.; BIZIATO, D.; PETROVA, T. V. Microenvironmental regulation of tumour angiogenesis. **Nat Rev Cancer,** v. 17, n. 8, p. 457-474, 08 2017. ISSN 1474-1768. Disponível em: < https://www.ncbi.nlm.nih.gov/pubmed/28706266 >.

DENAIS, C. M. et al. Nuclear envelope rupture and repair during cancer cell migration. **Science,** v. 352, n. 6283, p. 353-8, Apr 2016. ISSN 1095-9203. Disponível em: < https://www.ncbi.nlm.nih.gov/pubmed/27013428 >.

DUFFY, S. A. et al. Interleukin-6 predicts recurrence and survival among head and neck cancer patients. **Cancer,** v. 113, n. 4, p. 750-7, Aug 2008. ISSN 0008-543X. Disponível em: < https://www.ncbi.nlm.nih.gov/pubmed/18536030 >.

DUPONT, S. et al. Role of YAP/TAZ in mechanotransduction. **Nature,** v. 474, n. 7350, p. 179-83, Jun 2011. ISSN 1476-4687. Disponível em: < https://www.ncbi.nlm.nih.gov/pubmed/21654799 >.

ELINAV, E. et al. Inflammation-induced cancer: crosstalk between tumours, immune cells and microorganisms. **Nat Rev Cancer,** v. 13, n. 11, p. 759-71, Nov 2013. ISSN 1474-1768. Disponível em: < https://www.ncbi.nlm.nih.gov/pubmed/24154716 >.

ENGLER, A. J. et al. Matrix elasticity directs stem cell lineage specification. **Cell,** v. 126, n. 4, p. 677-89, Aug 2006. ISSN 0092-8674. Disponível em: < https://www.ncbi.nlm.nih.gov/pubmed/16923388 >.

ERDOGAN, B. et al. Cancer-associated fibroblasts promote directional cancer cell migration by aligning fibronectin. **J Cell Biol,** v. 216, n. 11, p. 3799-3816, 11 2017. ISSN 1540-8140. Disponível em: < https://www.ncbi.nlm.nih.gov/pubmed/29021221 >.

ETEMAD-MOGHADAM, S. et al. Evaluation of myofibroblasts in oral epithelial dysplasia and squamous cell carcinoma. **J Oral Pathol Med,** v. 38, n. 8, p. 639-43,   Sep   2009.   ISSN   1600-0714.   Disponível   em: < https://www.ncbi.nlm.nih.gov/pubmed/19473444 >.

FENNER, J. et al. Macroscopic stiffness of breast tumors predicts metastasis. **Sci Rep,** v. 4, p. 5512, Jul 2014. ISSN 2045-2322. Disponível em: < https://www.ncbi.nlm.nih.gov/pubmed/24981707 >.

FRIEDL, P.; ALEXANDER, S. Cancer invasion and the microenvironment: plasticity and reciprocity. **Cell,** v. 147, n. 5, p. 992-1009, Nov 2011. ISSN 1097-4172. Disponível em: < https://www.ncbi.nlm.nih.gov/pubmed/22118458 >.

GAO, G. et al. A novel RT-PCR method for quantification of human papillomavirus transcripts in archived tissues and its application in oropharyngeal cancer prognosis. **Int J Cancer,** v. 132, n. 4, p. 882-90, Feb 2013. ISSN 1097-0215. Disponível em: < https://www.ncbi.nlm.nih.gov/pubmed/22821242 >.

GATTA, G. et al. Prognoses and improvement for head and neck cancers diagnosed in Europe in early 2000s: The EUROCARE-5 population-based study. **Eur J Cancer,** v. 51, n. 15, p. 2130-2143, Oct 2015. ISSN 1879-0852. Disponível em: < https://www.ncbi.nlm.nih.gov/pubmed/26421817 >.

GAUTHIER, J.; YAKOUB-AGHA, I. Chimeric antigen-receptor T-cell therapy for hematological malignancies and solid tumors: Clinical data to date, current limitations and perspectives. **Curr Res Transl Med,** v. 65, n. 3, p. 93-102, 09 2017.   ISSN   2452-3186.   Disponível   em: < https://www.ncbi.nlm.nih.gov/pubmed/28988742 >.

GE, L. et al. Differential mRNA expression profiling of oral squamous cell carcinoma by high-throughput RNA sequencing. **J Biomed Res,** v. 29, Jan 2015.

ISSN 1674-8301. Disponível em: < https://www.ncbi.nlm.nih.gov/pubmed/26273018 >.

GILKES, D. M.; SEMENZA, G. L.; WIRTZ, D. Hypoxia and the extracellular matrix: drivers of tumour metastasis. **Nat Rev Cancer,** v. 14, n. 6, p. 430-9, 06 2014. ISSN 1474-1768. Disponível em: < https://www.ncbi.nlm.nih.gov/pubmed/24827502 >.

GINZINGER, D. G. Gene quantification using real-time quantitative PCR: an emerging technology hits the mainstream. **Exp Hematol,** v. 30, n. 6, p. 503-12, Jun 2002. ISSN 0301-472X. Disponível em: < https://www.ncbi.nlm.nih.gov/pubmed/12063017 >.

GLENTIS, A. et al. Cancer-associated fibroblasts induce metalloprotease-independent cancer cell invasion of the basement membrane. **Nature Communications,** v. 8, p. 13, Oct 2017. ISSN 2041-1723. Disponível em: < <Go to ISI>://WOS:000412871700008 >.

HANAHAN, D.; WEINBERG, R. A. The hallmarks of cancer. **Cell,** v. 100, n. 1, p. 57-70, Jan 2000. ISSN 0092-8674. Disponível em: < https://www.ncbi.nlm.nih.gov/pubmed/10647931 >.

_____. Hallmarks of cancer: the next generation. **Cell,** v. 144, n. 5, p. 646-74, Mar 2011. ISSN 1097-4172. Disponível em: < http://www.ncbi.nlm.nih.gov/pubmed/21376230 >.

HANNA, S.; EL-SIBAI, M. Signaling networks of Rho GTPases in cell motility. **Cell Signal,** v. 25, n. 10, p. 1955-61, Oct 2013. ISSN 1873-3913. Disponível em: < https://www.ncbi.nlm.nih.gov/pubmed/23669310 >.

HUGGETT, J. et al. Real-time RT-PCR normalisation; strategies and considerations. **Genes Immun,** v. 6, n. 4, p. 279-84, Jun 2005. ISSN 1466-4879. Disponível em: < https://www.ncbi.nlm.nih.gov/pubmed/15815687 >.

HUH, K. et al. Human papillomavirus type 16 E7 oncoprotein associates with the cullin 2 ubiquitin ligase complex, which contributes to degradation of the retinoblastoma tumor suppressor. **J Virol,** v. 81, n. 18, p. 9737-47, Sep 2007. ISSN 0022-538X. Disponível em: < https://www.ncbi.nlm.nih.gov/pubmed/17609271 >.

IKEBE, T. et al. Gelatinolytic activity of matrix metalloproteinase in tumor tissues correlates with the invasiveness of oral cancer. **Clin Exp Metastasis,** v. 17, n. 4, p. 315-23, Jun 1999. ISSN 0262-0898. Disponível em: < https://www.ncbi.nlm.nih.gov/pubmed/10545018 >.

JACOB, F. et al. Careful selection of reference genes is required for reliable performance of RT-qPCR in human normal and cancer cell lines. **PLoS One,** v. 8, n. 3, p. e59180, 2013. ISSN 1932-6203. Disponível em: < https://www.ncbi.nlm.nih.gov/pubmed/23554992 >.

JETHWA, A. R.; KHARIWALA, S. S. Tobacco-related carcinogenesis in head and neck cancer. **Cancer Metastasis Rev,** v. 36, n. 3, p. 411-423, 09 2017. ISSN 1573-7233. Disponível em: < https://www.ncbi.nlm.nih.gov/pubmed/28801840 >.

KANG, H.; KIESS, A.; CHUNG, C. H. Emerging biomarkers in head and neck cancer in the era of genomics. **Nat Rev Clin Oncol,** v. 12, n. 1, p. 11-26, Jan 2015. ISSN 1759-4782. Disponível em: < https://www.ncbi.nlm.nih.gov/pubmed/25403939 >.

KOSMEHL, H. et al. Distribution of laminin and fibronectin isoforms in oral mucosa and oral squamous cell carcinoma. **Br J Cancer,** v. 81, n. 6, p. 1071-9, Nov 1999. ISSN 0007-0920. Disponível em: < https://www.ncbi.nlm.nih.gov/pubmed/10576667 >.

KUANG, J. et al. An overview of technical considerations when using quantitative real-time PCR analysis of gene expression in human exercise research. **PLoS One,** v. 13, n. 5, p. e0196438, 2018. ISSN 1932-6203. Disponível em: < https://www.ncbi.nlm.nih.gov/pubmed/29746477 >.

KUSHIRO, K. et al. Differences in Three-Dimensional Geometric Recognition by Non-Cancerous and Cancerous Epithelial Cells on Microgroove-Based Topography. **Sci Rep,** v. 7, n. 1, p. 4244, Jun 2017. ISSN 2045-2322. Disponível em: < https://www.ncbi.nlm.nih.gov/pubmed/28652607 >.

LABERNADIE, A. et al. A mechanically active heterotypic E-cadherin/N-cadherin adhesion enables fibroblasts to drive cancer cell invasion. **Nature Cell Biology,** v. 19, n. 3, p. 224-237, Mar 2017. ISSN 1465-7392. Disponível em: < <Go to ISI>://WOS:000395355500012 >.

LAMOUILLE, S.; XU, J.; DERYNCK, R. Molecular mechanisms of epithelial-mesenchymal transition. **Nat Rev Mol Cell Biol,** v. 15, n. 3, p. 178-96, Mar 2014. ISSN 1471-0080. Disponível em: < https://www.ncbi.nlm.nih.gov/pubmed/24556840 >.

LEE, S. L. et al. Hypoxia-induced pathological angiogenesis mediates tumor cell dissemination, invasion, and metastasis in a zebrafish tumor model. **Proc Natl Acad Sci U S A,** v. 106, n. 46, p. 19485-90, Nov 2009. ISSN 1091-6490. Disponível em: < https://www.ncbi.nlm.nih.gov/pubmed/19887629 >.

LIPPITZ, B. E. Cytokine patterns in patients with cancer: a systematic review. **Lancet Oncol,** v. 14, n. 6, p. e218-28, May 2013. ISSN 1474-5488. Disponível em: < https://www.ncbi.nlm.nih.gov/pubmed/23639322 >.

LIU, L. L. et al. Identification of valid reference genes for the normalization of RT-qPCR expression studies in human breast cancer cell lines treated with and without transient transfection. **PLoS One,** v. 10, n. 1, p. e0117058, 2015. ISSN 1932-6203. Disponível em: < https://www.ncbi.nlm.nih.gov/pubmed/25617865 >.

MAK, I. W.; EVANIEW, N.; GHERT, M. Lost in translation: animal models and clinical trials in cancer treatment. **Am J Transl Res,** v. 6, n. 2, p. 114-8, 2014. ISSN 1943-8141. Disponível em: < https://www.ncbi.nlm.nih.gov/pubmed/24489990 >.

MAMAN, S.; WITZ, I. P. A history of exploring cancer in context. **Nat Rev Cancer,** v. 18, n. 6, p. 359-376, 06 2018. ISSN 1474-1768. Disponível em: < https://www.ncbi.nlm.nih.gov/pubmed/29700396 >.

MCKENZIE, A. J. et al. The mechanical microenvironment regulates ovarian cancer cell morphology, migration, and spheroid disaggregation. **Sci Rep,** v. 8, n. 1, p. 7228, May 2018. ISSN 2045-2322. Disponível em: < https://www.ncbi.nlm.nih.gov/pubmed/29740072 >.

MISHRA, R. Cell cycle-regulatory cyclins and their deregulation in oral cancer. **Oral Oncol,** v. 49, n. 6, p. 475-81, Jun 2013. ISSN 1879-0593. Disponível em: < https://www.ncbi.nlm.nih.gov/pubmed/23434055 >.

MOAZZEM HOSSAIN, M. et al. Diminished expression of h2-calponin in prostate cancer cells promotes cell proliferation, migration and the dependence of cell adhesion on substrate stiffness. **FEBS Open Bio,** v. 4, p. 627-36, 2014.

ISSN 2211-5463. Disponível em: < https://www.ncbi.nlm.nih.gov/pubmed/25161871 >.

MORK, J. et al. Human papillomavirus infection as a risk factor for squamous-cell carcinoma of the head and neck. **N Engl J Med,** v. 344, n. 15, p. 1125-31, Apr 2001. ISSN 0028-4793. Disponível em: < https://www.ncbi.nlm.nih.gov/pubmed/11297703 >.

MÜCKE, T. et al. Quality of life after different oncologic interventions in head and neck cancer patients. **J Craniomaxillofac Surg,** v. 43, n. 9, p. 1895-8, Nov 2015. ISSN 1878-4119. Disponível em: < https://www.ncbi.nlm.nih.gov/pubmed/26421469 >.

NARDONE, G. et al. YAP regulates cell mechanics by controlling focal adhesion assembly. **Nat Commun,** v. 8, p. 15321, May 2017. ISSN 2041-1723. Disponível em: < https://www.ncbi.nlm.nih.gov/pubmed/28504269 >.

NASROLLAHI, S. et al. Past matrix stiffness primes epithelial cells and regulates their future collective migration through a mechanical memory. **Biomaterials,** v. 146, p. 146-155, Nov 2017. ISSN 1878-5905. Disponível em: < https://www.ncbi.nlm.nih.gov/pubmed/28918264 >.

NETWORK, C. G. A. Comprehensive genomic characterization of head and neck squamous cell carcinomas. **Nature,** v. 517, n. 7536, p. 576-82, Jan 2015. ISSN 1476-4687. Disponível em: < https://www.ncbi.nlm.nih.gov/pubmed/25631445 >.

NGUYEN-NGOC, K. V. et al. ECM microenvironment regulates collective migration and local dissemination in normal and malignant mammary epithelium. **Proceedings of the National Academy of Sciences of the United States of America,** v. 109, n. 39, p. E2595-E2604, Sep 2012. ISSN 0027-8424. Disponível em: < <Go to ISI>://WOS:000309604500005 >.

NIETO, M. A. et al. EMT: 2016. **Cell,** v. 166, n. 1, p. 21-45, Jun 2016. ISSN 1097-4172. Disponível em: < https://www.ncbi.nlm.nih.gov/pubmed/27368099 >.

OTTO, T.; SICINSKI, P. Cell cycle proteins as promising targets in cancer therapy. **Nat Rev Cancer,** v. 17, n. 2, p. 93-115, 01 2017. ISSN 1474-1768. Disponível em: < https://www.ncbi.nlm.nih.gov/pubmed/28127048 >.

PAGET, S. The distribution of secondary growths in cancer of the breast. 1889. **Cancer Metastasis Rev,** v. 8, n. 2, p. 98-101, Aug 1989. ISSN 0167-7659. Disponível em: < https://www.ncbi.nlm.nih.gov/pubmed/2673568 >.

PANKOVA, D. et al. Cancer-Associated Fibroblasts Induce a Collagen Cross-link Switch in Tumor Stroma. **Mol Cancer Res,** v. 14, n. 3, p. 287-95, Mar 2016. ISSN 1557-3125. Disponível em: < https://www.ncbi.nlm.nih.gov/pubmed/26631572 >.

PARK, J.; SCHWARZBAUER, J. E. Mammary epithelial cell interactions with fibronectin stimulate epithelial-mesenchymal transition. **Oncogene,** v. 33, n. 13, p. 1649-57, Mar 2014. ISSN 1476-5594. Disponível em: < https://www.ncbi.nlm.nih.gov/pubmed/23624917 >.

PASZEK, M. J. et al. Tensional homeostasis and the malignant phenotype. **Cancer Cell,** v. 8, n. 3, p. 241-254, Sep 2005. ISSN 1535-6108. Disponível em: < <Go to ISI>://WOS:000232199900010 >.

PENG, X.; MCCORMICK, D. L. Identification of reliable reference genes for quantitative gene expression studies in oral squamous cell carcinomas compared to adjacent normal tissues in the F344 rat model. **Oncol Rep,** v. 36, n. 2, p. 1076-84, Aug 2016. ISSN 1791-2431. Disponível em: < https://www.ncbi.nlm.nih.gov/pubmed/27375172 >.

PEPPICELLI, S.; BIANCHINI, F.; CALORINI, L. Extracellular acidity, a "reappreciated" trait of tumor environment driving malignancy: perspectives in diagnosis and therapy. **Cancer Metastasis Rev,** v. 33, n. 2-3, p. 823-32, Sep 2014. ISSN 1573-7233. Disponível em: < https://www.ncbi.nlm.nih.gov/pubmed/24984804 >.

PFAFFL, M. W. et al. Determination of stable housekeeping genes, differentially regulated target genes and sample integrity: BestKeeper--Excel-based tool using pair-wise correlations. **Biotechnol Lett,** v. 26, n. 6, p. 509-15, Mar 2004. ISSN 0141-5492. Disponível em: < https://www.ncbi.nlm.nih.gov/pubmed/15127793 >.

PLUMMER, M. et al. Global burden of cancers attributable to infections in 2012: a synthetic analysis. **Lancet Glob Health,** v. 4, n. 9, p. e609-16, 09 2016. ISSN 2214-109X. Disponível em: < https://www.ncbi.nlm.nih.gov/pubmed/27470177 >.

POHL, J.; RADLER-POHL, A.; SCHIRRMACHER, V. A model to account for the effects of oncogenes, TPA, and retinoic acid on the regulation of genes involved in metastasis. **Cancer Metastasis Rev,** v. 7, n. 4, p. 347-56, Dec 1988. ISSN 0167-7659. Disponível em: < https://www.ncbi.nlm.nih.gov/pubmed/3061678 >.

POTENTE, M.; GERHARDT, H.; CARMELIET, P. Basic and therapeutic aspects of angiogenesis. **Cell,** v. 146, n. 6, p. 873-87, Sep 2011. ISSN 1097-4172. Disponível em: < https://www.ncbi.nlm.nih.gov/pubmed/21925313 >.

PURAM, S. V. et al. Single-Cell Transcriptomic Analysis of Primary and Metastatic Tumor Ecosystems in Head and Neck Cancer. **Cell,** v. 171, n. 7, p. 1611-1624.e24, Dec 2017. ISSN 1097-4172. Disponível em: < https://www.ncbi.nlm.nih.gov/pubmed/29198524 >.

QI, L. et al. Yes-associated protein promotes cell migration via activating Wiskott-Aldrich syndrome protein family member 1 in oral squamous cell carcinoma. **J Oral Pathol Med,** v. 48, n. 4, p. 290-298, Apr 2019. ISSN 1600-0714. Disponível em: < https://www.ncbi.nlm.nih.gov/pubmed/30697796 >.

RAMOS, G. E. O. et al. Fibronectin Modulates Cell Adhesion and Signaling to Promote Single Cell Migration of Highly Invasive Oral Squamous Cell Carcinoma. **PLoS One,** v. 11, n. 3, p. e0151338, 2016. ISSN 1932-6203. Disponível em: < https://www.ncbi.nlm.nih.gov/pubmed/26978651 >.

RODUST, P. M. et al. UV-induced squamous cell carcinoma--a role for antiapoptotic signalling pathways. **Br J Dermatol,** v. 161 Suppl 3, p. 107-15, Nov 2009. ISSN 1365-2133. Disponível em: < https://www.ncbi.nlm.nih.gov/pubmed/19775366 >.

RYBARCZYK-FILHO, J. L. et al. Towards a genome-wide transcriptogram: the Saccharomyces cerevisiae case. **Nucleic Acids Res,** v. 39, n. 8, p. 3005-16, Apr 2011. ISSN 1362-4962. Disponível em: < https://www.ncbi.nlm.nih.gov/pubmed/21169199 >.

SAAD, M. A. et al. Alcohol-dysregulated miR-30a and miR-934 in head and neck squamous cell carcinoma. **Mol Cancer,** v. 14, p. 181, Oct 2015. ISSN 1476-4598. Disponível em: < https://www.ncbi.nlm.nih.gov/pubmed/26472042 >.

SCHEFFNER, M. et al. The E6 oncoprotein encoded by human papillomavirus types 16 and 18 promotes the degradation of p53. **Cell,** v. 63, n. 6, p. 1129-36, Dec 1990. ISSN 0092-8674. Disponível em: < https://www.ncbi.nlm.nih.gov/pubmed/2175676 >.

SCHMIDT, A.; WEBER, O. F. In memoriam of Rudolf virchow: a historical retrospective including aspects of inflammation, infection and neoplasia. **Contrib**

Microbiol, v. 13, p. 1-15, 2006. ISSN 1420-9519. Disponível em: < https://www.ncbi.nlm.nih.gov/pubmed/16627956 >.

SEGRELLES, C.; PARAMIO, J. M.; LORZ, C. The transcriptional co-activator YAP: A new player in head and neck cancer. **Oral Oncol,** v. 86, p. 25-32, Nov 2018. ISSN 1879-0593. Disponível em: < https://www.ncbi.nlm.nih.gov/pubmed/30409308 >.

SIEGEL, R. L.; MILLER, K. D.; JEMAL, A. Cancer statistics, 2019. **CA Cancer J Clin,** v. 69, n. 1, p. 7-34, Jan 2019. ISSN 1542-4863. Disponível em: < https://www.ncbi.nlm.nih.gov/pubmed/30620402 >.

SILVER, N. et al. Selection of housekeeping genes for gene expression studies in human reticulocytes using real-time PCR. **BMC Mol Biol,** v. 7, p. 33, Oct 2006. ISSN 1471-2199. Disponível em: < https://www.ncbi.nlm.nih.gov/pubmed/17026756 >.

SMITH, A.; TEKNOS, T. N.; PAN, Q. Epithelial to mesenchymal transition in head and neck squamous cell carcinoma. **Oral Oncol,** v. 49, n. 4, p. 287-92, Apr 2013. ISSN 1879-0593. Disponível em: < https://www.ncbi.nlm.nih.gov/pubmed/23182398 >.

SONG, W. et al. Validation of housekeeping genes for the normalization of RT-qPCR expression studies in oral squamous cell carcinoma cell line treated by 5 kinds of chemotherapy drugs. **Cell Mol Biol (Noisy-le-grand),** v. 62, n. 13, p. 29-34, Nov 2016. ISSN 1165-158X. Disponível em: < https://www.ncbi.nlm.nih.gov/pubmed/28040059 >.

SOUZA, A. F. et al. Reference gene for primary culture of prostate cancer cells. **Mol Biol Rep,** v. 40, n. 4, p. 2955-62, Apr 2013. ISSN 1573-4978. Disponível em: < https://www.ncbi.nlm.nih.gov/pubmed/23269617 >.

STANAM, A. et al. Upregulated interleukin-6 expression contributes to erlotinib resistance in head and neck squamous cell carcinoma. **Mol Oncol,** v. 9, n. 7, p. 1371-83, Aug 2015. ISSN 1878-0261. Disponível em: < https://www.ncbi.nlm.nih.gov/pubmed/25888065 >.

STRANSKY, N. et al. The mutational landscape of head and neck squamous cell carcinoma. **Science,** v. 333, n. 6046, p. 1157-60, Aug 2011. ISSN 1095-9203. Disponível em: < https://www.ncbi.nlm.nih.gov/pubmed/21798893 >.

SU, Y. W. et al. IL-6 stabilizes Twist and enhances tumor cell motility in head and neck cancer cells through activation of casein kinase 2. **PLoS One,** v. 6, n. 4, p. e19412, Apr 2011. ISSN 1932-6203. Disponível em: < https://www.ncbi.nlm.nih.gov/pubmed/21559372 >.

SUWANWELA, J.; OSATHANON, T. Inflammation related genes are upregulated in surgical margins of advanced stage oral squamous cell carcinoma. **J Oral Biol Craniofac Res,** v. 7, n. 3, p. 193-197, 2017 Sep-Dec 2017. ISSN 2212-4268. Disponível em: < https://www.ncbi.nlm.nih.gov/pubmed/29123999 >.

TE BOEKHORST, V.; FRIEDL, P. Plasticity of Cancer Cell Invasion-Mechanisms and Implications for Therapy. **Adv Cancer Res,** v. 132, p. 209-64, 2016. ISSN 2162-5557. Disponível em: < https://www.ncbi.nlm.nih.gov/pubmed/27613134 >.

TILGHMAN, R. W. et al. Matrix rigidity regulates cancer cell growth and cellular phenotype. **PLoS One,** v. 5, n. 9, p. e12905, Sep 2010. ISSN 1932-6203. Disponível em: < https://www.ncbi.nlm.nih.gov/pubmed/20886123 >.

TIMPSON, P. et al. Organotypic collagen I assay: a malleable platform to assess cell behaviour in a 3-dimensional context. **J Vis Exp**, n. 56, p. e3089, Oct 2011.

ISSN 1940-087X. Disponível em: < https://www.ncbi.nlm.nih.gov/pubmed/22025017 >.

TRICARICO, C. et al. Quantitative real-time reverse transcription polymerase chain reaction: normalization to rRNA or single housekeeping genes is inappropriate for human tissue biopsies. **Anal Biochem,** v. 309, n. 2, p. 293-300, Oct 2002. ISSN 0003-2697. Disponível em: < https://www.ncbi.nlm.nih.gov/pubmed/12413463 >.

VANDER HEIDEN, M. G.; CANTLEY, L. C.; THOMPSON, C. B. Understanding the Warburg effect: the metabolic requirements of cell proliferation. **Science,** v. 324, n. 5930, p. 1029-33, May 2009. ISSN 1095-9203. Disponível em: < https://www.ncbi.nlm.nih.gov/pubmed/19460998 >.

VANDESOMPELE, J. et al. Accurate normalization of real-time quantitative RT-PCR data by geometric averaging of multiple internal control genes. **Genome Biol,** v. 3, n. 7, p. RESEARCH0034, Jun 2002. ISSN 1474-760X. Disponível em: < https://www.ncbi.nlm.nih.gov/pubmed/12184808 >.

VERMA, G. et al. Characterization of key transcription factors as molecular signatures of HPV-positive and HPV-negative oral cancers. **Cancer Med,** v. 6, n. 3, p. 591-604, 03 2017. ISSN 2045-7634. Disponível em: < https://www.ncbi.nlm.nih.gov/pubmed/28155253 >.

VINCENT-CHONG, V. K. et al. Genome wide profiling in oral squamous cell carcinoma identifies a four genetic marker signature of prognostic significance. **PLoS One,** v. 12, n. 4, p. e0174865, 2017. ISSN 1932-6203. Disponível em: < https://www.ncbi.nlm.nih.gov/pubmed/28384287 >.

VOURA, E. B. et al. Proteolysis during tumor cell extravasation in vitro: metalloproteinase involvement across tumor cell types. **PLoS One,** v. 8, n. 10, p.

e78413, 2013. ISSN 1932-6203. Disponível em: < https://www.ncbi.nlm.nih.gov/pubmed/24194929 >.

WALENTA, S. et al. High lactate levels predict likelihood of metastases, tumor recurrence, and restricted patient survival in human cervical cancers. **Cancer Res,** v. 60, n. 4, p. 916-21, Feb 2000. ISSN 0008-5472. Disponível em: < https://www.ncbi.nlm.nih.gov/pubmed/10706105 >.

WANG, H. et al. DNA damage checkpoint recovery and cancer development. **Exp Cell Res,** v. 334, n. 2, p. 350-8, Jun 2015. ISSN 1090-2422. Disponível em: < https://www.ncbi.nlm.nih.gov/pubmed/25842165 >.

WEAVER, V. M. et al. The importance of the microenvironment in breast cancer progression: recapitulation of mammary tumorigenesis using a unique human mammary epithelial cell model and a three-dimensional culture assay. **Biochem Cell Biol,** v. 74, n. 6, p. 833-51, 1996. ISSN 0829-8211. Disponível em: < https://www.ncbi.nlm.nih.gov/pubmed/9164652 >.

WEI, S. C. et al. Matrix stiffness drives epithelial mesenchymal transition and tumour metastasis through a TWIST1-G3BP2 mechanotransduction pathway. **Nature Cell Biology,** v. 17, n. 5, p. 678-U306, May 2015. ISSN 1465-7392. Disponível em: < <Go to ISI>://WOS:000353771500015 >.

WISE-DRAPER, T. M. et al. Future directions and treatment strategies for head and neck squamous cell carcinomas. **Transl Res,** v. 160, n. 3, p. 167-77, Sep 2012. ISSN 1878-1810. Disponível em: < https://www.ncbi.nlm.nih.gov/pubmed/22683420 >.

XIE, F. et al. miRDeepFinder: a miRNA analysis tool for deep sequencing of plant small RNAs. **Plant Mol Biol**, Jan 2012. ISSN 1573-5028. Disponível em: < https://www.ncbi.nlm.nih.gov/pubmed/22290409 >.

YADAV, A. et al. IL-6 promotes head and neck tumor metastasis by inducing epithelial-mesenchymal transition via the JAK-STAT3-SNAIL signaling pathway. **Mol Cancer Res,** v. 9, n. 12, p. 1658-67, Dec 2011. ISSN 1557-3125. Disponível em: < https://www.ncbi.nlm.nih.gov/pubmed/21976712 >.

YANGBEN, Y. et al. Relative rigidity of cell-substrate effects on hepatic and hepatocellular carcinoma cell migration. **J Biomater Sci Polym Ed,** v. 24, n. 2, p. 148-57, 2013. ISSN 1568-5624. Disponível em: < https://www.ncbi.nlm.nih.gov/pubmed/23565595 >.

ZAHRA, A. et al. Meta-Analysis of miRNAs and Their Involvement as Biomarkers in Oral Cancers. **Biomed Res Int,** v. 2018, p. 8439820, 2018. ISSN 2314-6141. Disponível em: < https://www.ncbi.nlm.nih.gov/pubmed/29516011 >.

ZHOU, B. et al. A role for cancer-associated fibroblasts in inducing the epithelial-to-mesenchymal transition in human tongue squamous cell carcinoma. **J Oral Pathol Med,** v. 43, n. 8, p. 585-92, Sep 2014. ISSN 1600-0714. Disponível em: < https://www.ncbi.nlm.nih.gov/pubmed/24645915 >.

ZHOU, J. et al. Expression of E-cadherin and vimentin in oral squamous cell carcinoma. **Int J Clin Exp Pathol,** v. 8, n. 3, p. 3150-4, 2015. ISSN 1936-2625. Disponível em: < https://www.ncbi.nlm.nih.gov/pubmed/26045832 >.

ZUAZO-GAZTELU, I.; CASANOVAS, O. Unraveling the Role of Angiogenesis in Cancer Ecosystems. **Front Oncol,** v. 8, p. 248, 2018. ISSN 2234-943X. Disponível em: < https://www.ncbi.nlm.nih.gov/pubmed/30013950 >.